Photoniques

N°113

LIGHT AND APPLICATIONS | EOS & SFO JOINT ISSUE

EXPERIMENT SPP imaging | **LABWORK** Quantum entanglement | **BACK TO BASICS** Optical helicity | **BUYER'S GUIDE** Nanopositioner

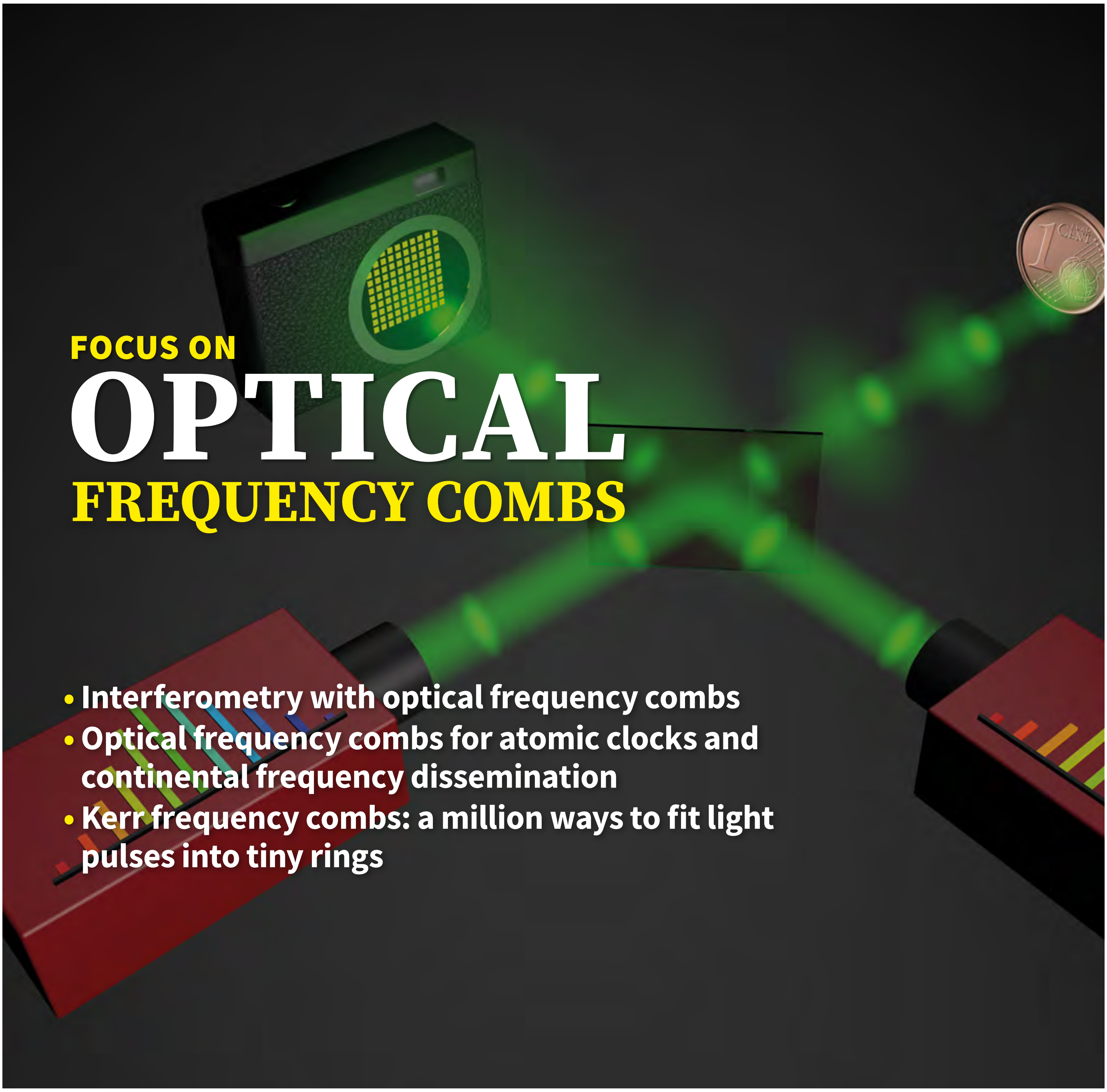

FOCUS ON OPTICAL FREQUENCY COMBS

- Interferometry with optical frequency combs
- Optical frequency combs for atomic clocks and continental frequency dissemination
- Kerr frequency combs: a million ways to fit light pulses into tiny rings

France/EU : 19 € | Rest of the World : 25 €

Photoniques is published
by the French Physical Society.
La Société Française de Physique est une association loi 1901 reconnue d'utilité publique par décret du 15 janvier 1881 et déclarée en préfecture de Paris.

https://www.sfpnet.fr/
33 rue Croulebarbe,
75013 Paris, France
Tel.: +33(0)1 44 08 67 10

CPPAP : 0124 W 93286
ISSN : 1629-4475, e-ISSN : 2269-8418

www.photoniques.com

The contents of Photoniques are elaborated under the scientific supervision of the French Optical Society.
2 avenue Augustin Fresnel
91127 Palaiseau Cedex, France
Florence HADDOUCHE
Secretary General Générale of the SFO
florence.haddouche@institutoptique.fr

Publishing Director
Jean-Paul Duraud, General Secretary of the French Physical Society

Editorial Staff
Editor-in-Chief
Nicolas Bonod
nicolas.bonod@edpsciences.org

Journal Manager
Florence Anglézio
florence.anglezio@edpsciences.org

Editorial secretariat and layout
Agence la Chamade
https://agencelachamade.com/

Advertising
Annie Keller
Cell phone: +33 (0)6 74 89 11 47
Phone/Fax: +33 (0)1 69 28 33 69
annie.keller@edpsciences.org

International Advertising
Bernadette Dufour
Cell phone + 33 7 87 57 07 59
bernadette.dufour@edpsciences.org

Photoniques is hosted and distributed by
EDP Sciences,
17 avenue du Hoggar,
P.A. de Courtaboeuf,
91944 Les Ulis Cedex A, France
Tel.: +33 (0)1 69 18 75 75
RCS: EVRY B 308 392 687

Subscriptions
subscribers@edpsciences.org

Printer
Rotochampagne
Rue des Frères Garnier
ZI Dame Huguenotte
52000 Chaumont
Dépôt légal : May 2022
Routage STAMP (95)

PEFC
10-31-3632
Certifié PEFC
pefc-france.org

Editorial

NICOLAS BONOD
Editor-in-Chief

Photonics, a Science of Precision and Accuracy

The history of science teaches us how numerous scientific breakthroughs were achieved by increased precision and accuracy. It also highlights how pushing forward the limits of precision and accuracy opens the way to novel research fields and applications.

The story of optical frequency combs is the story of an optical spectroscopy method, which was developed to overcome the limits that were reached by conventional methods in atomic spectroscopy. This technique based on phase-locked lasers, initiated in the 1970's, turned out to be a major scientific breakthrough. Its importance was highlighted in 2005 when the Nobel Prize in Physics was awarded to J. L. Hall and T. W. Hänsch "for their contributions to the development of laser-based precision spectroscopy, including the optical frequency comb technique". Articles of this special feature unveil the richness of this method and its huge potential for pushing forward measurement limits in terms of precision and accuracy. The fast development of this technology also benefited from the remarkable work of photonic companies, which managed to implement the most advanced lasers and optical techniques into ergonomic devices providing reliable and commercial sources of optical frequency combs.

Another field associated with excellence and precision is that of optical glass, whose development revolutionized optics. 2022 was declared on May 18th 2021 a United Nations International Year of Glass, and the zoom of this issue is dedicated to this event. Optical glass has deeply broadened our horizons, from the solar system and beyond with the development of telescopes, to the nano/micro world, in the solid state and in life sciences, with the constant progress achieved in optical microscopy. It has also brought communications to a new era by connecting billions of peoples with optical fibers. All these technologies have pushed the efficiency of optical glass to new standards with extremely precise polishing, structuring and transparency. The long and rich history of optical glass is far from being concluded since the soar of micro and nanotechnologies, a science of precision and accuracy, is spurring exciting and original concepts for tailoring light propagation through meta-optics.

This international issue inaugurates the publication of the section "Lab work" devoted to original optical set-ups aimed at learning optics and photonics though experiments. And what better topic than the emblematic experiment on the violation of Bell's inequalities to inaugurate this section? The authors explain how the EPR paradox, long considered a "Gedankenexperiment", has now become a very exciting lab work in order to introduce quantum concepts and related technologies to students.

The preparation of this issue was marked by the invasion of Ukraine by Russia. The international scientific community has been deeply saddened by this attack on a sovereign country, which severely violates international laws. I warmly thank all the scientific societies that clearly and promptly condemned the invasion of Ukraine by Russia, and in particular our partners SFO, SFP, EOS and EDP Sciences.



Table of contents

www.photoniques.com N° 113

03 **NEWS**
Highlights & news
from our 8 partners!

48
Kerr frequency combs:
a million ways to fit light
pulses into tiny rings

60
How to select
a nanopositioner
solution?

Advertisers

SFO forewords

ARIEL LEVENSON
President of the French Optical Society

"Morally as well as physically, the first of human rights is the right to light."
"Au moral comme au physique, le premier des droits de l'homme, est le droit à la lumière"
Proses philosophiques, Victor Hugo

The United Nations International Year of Light in 2015 was a global success in celebrating the many ways that light impacts society. The desire to ensure its legacy led UNESCO to proclaim a permanent annual International Day of Light, and this coming edition in 2022 will also be an occasion to remember our dear friend and colleague Costel Subran who passed away in January. Costel was a passionate organizer of International Day of Light activities in France, and as he would say, Light must go on!

Among the many International Day of Light events in France, I wish to highlight the development of laser teaching kits by the SFO Education Commission intended for outreach, especially at secondary schools. These will be freely distributed to accompany dissemination projects, and please contact the Education Commission for details. Let the light penetrate everywhere!

And...Let the sunshine in! From 4-8 July, the SFO Congress will take place in the Côte d'Azur. OPTIQUE Nice 2022 will bridge the academic and industrial communities, with outstanding plenary speakers including: Alain Aspect, Sophie Brasselet, Rémi Carminati, Jean Dalibard, Frédérique de Fornel, Jérôme Faist, Philippe Goldner, Aurélie Jullien, Sophia Kazamias and Philip Russell. The congress also includes tutorials, SFO Club thematic sessions, and 50 industrial and pedagogical exhibition stands. In addition, to celebrate the International Day of Light several events are planned:

- an exhibition of Low Cost Innovation in Optics organized by the SFO Optics and Physics without Borders Commission, targeted to help promote optics in countries and regions where access to science and technology can be difficult
- a workshop on gender equality organized by the SFO Gender Equality Commission, which aims to develop realistic and efficient actions to address this important issue
- a Scientibus hosted by the SFO Education Commission and the REOD Network, which will showcase a range of exciting experiments to school students

2022 is also the International Year of Glass, and Glass and Light marry well in the SFO Club for Guided Optics (JNOG) that recently joined with the Optical Fibers and Networks Club to better combine the academic and industrial communities in a reinforced JNOG.

In this Photoniques issue celebrating Bell's Inequality experiments, I would like to warmly congratulate our colleague Alain Aspect for his nomination as Honorary Member of OPTICA, a highly deserved and prestigious recognition.

It is a pleasure to share this international edition of Photoniques with the European Optical Society, and I would like here to affirm SFO's full support of EOS's declaration against military intervention in Ukraine. Our thoughts go out to our Ukrainian colleagues and their families, and all whose safety has been jeopardized. They can be assured of our solidarity: нехай вони будуть впевнені в нашій солідарності. At the same time, we know that our many Russian colleagues are equally concerned, and we look forward to the time in the hopefully near future where international science can once again show the way towards peace.

Photoniquement vôtre
Ariel Levenson
Directeur de recherche CNRS
Président de la SFO

The next Laser-Induced Breakdown Spectroscopy France Days, organized by the SFO LIBS Club will take place in Marseille on June 1 and 2, 2022 (France), on the Luminy campus of Aix-Marseille University. The LIBS 2022 Days will be a unique opportunity to bring together the entire chain of specialists in this increasingly developed instrumentation, from academics to manufacturers and instrumentation vendors.

https://www.sfoptique.org/agenda

THE SECOND WAVINAIRE: METASURFACES – JUNE 2022

After the great success of the first edition, the SFO, the GDR Complexe and the GDR Ondes are pleased to announce the second Wavinaire – open questions which will be held on June.
The wavinaires are intended for students, post-docs, engineers and researchers. This second edition is organized around an emblematic publication:

"Light Propagation with Phase Discontinuities: Generalized Laws of Reflection and Refraction", N. Yu, P. Genevet, M. A. Kats, F. Aieta, J.-P. Tetienne, F. Capasso, and Z. Gaburro, Science 334, pp. 333-337 (2011)

An introductory mini course on a basic concept necessary for understanding the article, as well as a brief presentation of its main results, given by a post-doctoral fellow, will be followed by a critical perspective vision proposed by two internationally recognized experts, Pierre Chavel from Institut d'Optique Graduate School and Bernard Kress Director, Optical Engineering - AR hardware - Google, who will discuss the industrial and academic impacts. The Wavinaire will end with questions and a free discussion.

https://www.sfoptique.org/pages/sfo/wavinaire.html

WELCOME TO OPTIQUE NICE 2022

You are cordially invited to participate in the 9th Congress of the French Optical Society SFO, which will take place in Nice, France from July 4 to July 8. This congress provides fertile ground for beneficial exchanges between academic and industrial actors of optics and photonics.

Plenary session : Alain Aspect, Sophie Brasselet, Jean Dalibard, Frédérique De Fornel, Rémi Carminati, Jérôme Faist, Philippe Goldner, Sophie Kazamias, Aurélie Jullien and Philip Russell.

Tutorials sessions will introduce different hot topics: Thermal emission at the nanoscale by Jean-Jacques Greffet and Yannick De Wilde, Single spin detection by Vincent Jacques, Multiphoton microscopy by Emmanuel Beaurepaire, Earth-space telemetry by Clément Courde and we will even go to Mars with Supercam on the Rove Perseverance by Pernelle Bernardi.

OPTIQUE Nice Prizes, to promote optics and photonics research

To recognize excellence, the SFO awards two Scientific Prizes during this congress: Grand Prix SFO Léon Brillouin and the Young researcher Fabry-de Gramont prize. OPTIQUE SFO Congress welcomes for the second time the Jean Jerphagnon Prize, a prestigious award for outstanding scientific contributions with high potential industrial impact.

Women in Optics and Physics commission, to promote parity in Optics

The congress pays a special attention to the number of women working in optics, at all responsibility levels and tends to parity on invited conferences.

PhD students and young researchers are welcome in OPTIQUE Nice

Our goal is to allow all PhD students to participate once in the congress during their thesis. More than 200 students are expected. OPTIQUE Nice 2022 will provide a dedicated and friendly space to initiate a "Youth" action...

Nice hosts the 9th edition of SFO biennial congress

The members of local organizing committee orchestrated by Sébastien Tanzilli do their utmost efforts to accommodate hundreds of participants in a friendly atmosphere. During our networking program you will get to know this exciting city in all its aspects.

United Nations Educational, Scientific and Cultural Organization — International Day of Light

OPTIQUE Nice 2022 is an International Day of Light event
https://www.sfoptique.org/

2ND COLLOQUIUM ON THE PHYSICS AND APPLICATIONS OF METASURFACES

Fortezza da Basso, Florence, Italie, July 18-22, 2022

This 2nd colloquium is organized by the Nanophotonics Club of the French Optical Society (SFO) in collaboration with the Italian Society for Optics and Photonics (SIOF). The attendees will benefit from outstanding international keynote speakers, Andrea Alù (CUNY), Shanui Fan (Stanford University), Federico Capasso (Harvard University), Philippe Lalanne (CNRS Bordeaux), Anatoly Zayats (King's College London) will present the latest developments in all areas of Metasurfaces.
https://www.sfoptique.org/pages/sfo/colloque-metasurface.html

Research in applied optics
at IOGS together with industrial partners

An example of a partnership study between the LCF and industry : Design and implementation of benches for characterizing the optical properties of vials for the pharmaceutical industry (Credit: SGD Pharma)

The Institute of Optics Graduate School (IOGS) has been strengthening its applied research activity with industrial partners, both French and foreign, for a few years now, notably with the creation in early 2019 of a dedicated Industrial Photonics team at the Charles Fabry Laboratory (LCF, CNRS Joint Research Unit 8501) in Palaiseau (Ile de France), headed by Yvan Sortais.

Like any team of a laboratory under the supervision of the CNRS, this one does not aim at competing with private offices, nor to interfere in the competition between companies. It responds to requests from industrials which contain at least one original and innovative point in terms of research, which can be developed in the form of a patent or scientific communication, and when it is free to do so without interfering with the interests of another industrial with whom it is already working on a similar or related subject.

IOGS intends to offer the industry a response adapted to its needs: services, collaboration, supervision of doctoral theses (with industrial funding in particular), and funding applications for shared projects. IOGS status as a higher education and research institution allows industrials to benefit from the Research Tax Credit.

In all cases, whether or not the initial request from the industrial is ultimately translated into a contract, technical exchanges are governed by a confidentiality agreement signed by both parties. When it continues beyond the initial exchanges, the interaction can last from a few weeks for the shortest services, to several years for research projects such as a PhD thesis.

The Industrial Photonics team deals in particular with requests related to the design, prototyping and metrology of optical systems, components or surfaces, in particular freeform optics, or optronic systems, for lighting or imaging. The studies concern many fields (defense, automotive, pharmaceutical, cosmetics, etc.).

The Industrial Photonics team works closely with the French Freeform Optics Association (Freeform Optics - Research and Solutions), of which IOGS is a founding member (see Refs. [1,2]).

It relies on the human and material resources of the LCF: computational resources, modeling (optical, mechanical, photometric, thermal, thin films, radiation, etc.), prototyping (precision optics, mechanics, electronics, 3D printing, etc.), and metrology (deformation and roughness of surfaces, transmission and spectral reflection, radiometric and photometric fluxes, color and visual appearance of materials).

More generally, IOGS offers industry the expertise of the teams from the three laboratories it oversees with the CNRS: the LCF, the Laboratoire de Photonique Numérique et Nanophotonique (LP2N, UMR CNRS 5298) and the Laboratoire Hubert Curien (UMR CNRS 5516). IOGS' response to industrial requests is coordinated by the Innovation and Industrial Relations Department.

Contact: dire@institutoptique.fr.

REFERENCES

[1] R. Geyl, F. Houbre, Y. Cornil, Th. Lépine and Y. Sortais, Optiques freeform : défis et perspectives, Photoniques 106, p. 17 (2021).

[2] Y. Sortais, Th. Lépine, J.-J. Greffet, Des formes libres dans notre champ de vision, La Recherche 568, p. 54 (2022).

Yvan Sortais, Lab. Charles Fabry
Email : yvan.sortais@institutoptique.fr

CONTACT FORMATION CONTINUE INSTITUT D'OPTIQUE GRADUATE SCHOOL:

+33 1 64 53 32 36 - +33 1 64 53 32 15
E-mail : fc@institutoptique.fr
www. fc.institutoptique.fr

AGENDA

Vision Stuttgart
04. - 06. October 2022
Meet us on french pavilion

www.pole-optitec.com

About OPTITEC

OPTITEC's mission on the regional/national level is to foster and promote activities of the photonics and imaging sectors in the south of France and to strengthen the synergies between its stakeholders (research, higher education and industry sectors).

European cluster

At the European level, OPTITEC fosters the participation of its members in various EU research and development programs, notably in Horizon Europe. In order to enhance the visibility and competitiveness of its members it facilitates the interaction with the European partners.

OPTITEC is a cluster dedicated to innovative technologies which harness light to generate, emit, detect, collect, transmit or amplify the flow of photons, from terahertz waves to X rays, applied to five industrial sectors on fast-growing markets : Security/defence & major scientific instruments, Health and life sciences, Industry 4.0, Smart mobility & cities and Digital agriculture.

OPTITEC LAUNCHES PHASE 2 OF ITS EUROPEAN PROJECT SUPPORTING EUROPEAN DUAL-USE SMES

KETs4Dual-Use 2.0 project officially started on 16 September 2021. The project builds on the outcomes of its predecessor EU KETs4Dual-Use, which was carried out as a Phase 1 project between September 2018 and February 2020.

The consortium of partners includes French clusters (pôles de compétitivité) OPTITEC, as the coordinator, Minalogic & SAFE and the defense and security related cluster CenSec (Denmark) as well as the Estonian Defence Industry Association (EDIA).

The project intends to act as a “springboard” for European dual-use companies wishing to access international markets, with the aim of integrating sustainable long-term partnerships. The project will support European dual-use small and medium enterprises (SMEs) accessing markets in Canada, Singapore and the United Arab Emirates (UAE) and generating growth, notably through their participation in international missions.

The main objective is to set up business collaboration and to stimulate demand for European start-ups & SMEs technologies and services in target countries to gain cross-border diversification and sectoral synergies representing both the supplier (technology/service providers) and end-user side.

In order to efficiently support the European companies, notably SMEs, in their conquest of dual-use markets in target countries, various actions are being carried-out:

- Setting-up of focus groups to discuss innovative solutions in the field of dual-use technologies and resilient business models
- Identification of international advisors in target countries
- Training and organisation of international missions
- Providing SMEs with a sustainable lifecycle support following their participation in the missions

In the first 6 months, the consortium has elaborated and carried out a survey acting as the project’s source of market needs as SMEs are required to take a mapping exercise to produce the data that will assist with identifying challenges and advantages of SMEs not only going international, but also collaborating in a cross-sectoral and boundary environment.

Furthermore, a series of four workshops focusing on the role of selected KETs (cyber-security & artificial intelligence) for dual-use and on resilient business models is being organised online between March and June 2022:

- Cyber-security - 24 March 2022
- Artificial Intelligence (AI) - 19 May 2022
- Access to EU funding: European Defence Fund - 2 June 2022
- Procurement processes in target countries - 30 June 2022

Learn more about KETs4Dual-Use project: https://clustercollaboration.eu/content/european-key-enabling-technologies-dual-use-20

LinkedIn profile: https://www.linkedin.com/showcase/eu-kets4dual-use-2-0

THE ALPHA-RLH CLUSTER
AND ITS MEMBERS AT PHOTONICS WEST

After two years of pandemic which slowed down international exchanges, the ALPHA-RLH cluster accompanied its members to the Photonics West exhibition, one of the major photonics and laser events, which finally took place in San Francisco over January 25-27, 2022. Within the French Pavilion organised by Business France, the companies AA Opto-Electronic, ALPhANOV, Femto Easy, First Light Imaging, Fogale Nanotech, GLOphotonics and Spark Lasers had the opportunity to exhibit and promote their technologies. Many other members participated with their own booth and/or visited the trade show. PIMAP+ European project, coordinated by ALPHA-RLH, facilitated the participation as visitors for two members, Polytec and Mathym. ALPHA-RLH also met with its European partners to set-up future internationalisation activities.
The next edition of Photonics West will be held from January 28th to February 2nd, 2023. ALPHA-RLH is planning to attend such a great event!

NewSkin project: application for the second NewSkin Open Call

ALPHA-RLH and the 33 other partners involved in the Horizon 2020 NewSkin project have closed the 1st open call on the 31st of January 2022. This was a great success as 22 applications from SMEs, research organisations and public structures were selected to cooperate with the NewSkin partners in the framework of R&D projects. These services are entirely financed by the NewSkin project and will allow to develop and test new nanotechnological products and processes on prototypes and thus improve the performance of surfaces (including metals, polymers, ceramics, graphene etc.). A second open call will be open from April to July 2022. Do not miss this opportunity to join the Open Innovation Test Bed allowing to evaluate and uptake innovative surface nanotechnologies and connect with a unique innovation ecosystem. Register on the project platform to join the NewSkin community, increase your organisation's visibility, discover the NewSkin service offer and apply for the NewSkin open calls.
Contact: Romain Herault - r.herault@alpha-rlh.com

Available funds from PhotonHub Europe project
to accelerate your cross-border innovation projects

PhotonHub Europe project, whose ALPHA-RLH is one of the partners (linked third party), offers innovation support for European SMEs covering the entire value chain:
- **Prototyping (TRL 3-4):** Highly collaborative co-innovation initiatives between the PhotonHub partner(s) and the company. Max grant: 100 k€.
- **Upscaling (TRL5-6):** Support to optimise an initial prototype for small-series production in a manner which is compatible with full-scale manufacturing (possibility to include third parties). Max grant: 250 k€.
- **Manufacturing (TRL7-8):** Brokerage service, helping companies innovating with photonics to rapidly connect with existing European manufacturers (2 k€ for EPIC to support the company).

Interested companies should fill in the registration form available on the website to be contacted and oriented by the project's team: https://www.photonhub.eu/application-form/

French innovations at CES Las Vegas

The CES Las Vegas, the world's largest event for new technologies, was held over January 5-7, 2022. A French delegation of 140 start-ups was present at the show. Among them, a delegation of 24 start-ups from Nouvelle-Aquitaine, supported by the Nouvelle-Aquitaine Regional Council, the French Tech Bordeaux, the International Chamber of Commerce of Nouvelle-Aquitaine and the ALPHA-RLH cluster. They had the opportunity to present their innovations and benefit from media exposure. We can mention Airudit, a member of the ALPHA-RLH cluster, specialised in the design of voice-controlled human/system interfaces, and MyEli, which won the CES 2022 Innovation Award for its connected jewel that alerts, secures and protects you in case of danger. The exhibition allowed ALPHA-RLH to discover the latest technological innovations and their applications on the markets, particularly in the fields of artificial intelligence, automotive technology, digital health, well-being and smart home. A great experience!

© French Tech Bordeaux

UPCOMING INTERNATIONAL EVENTS

- **Business Mission AISTech 2022**
  May 16-19 in Pittsburgh (USA)
- **Manufacturing World Japan**
  June 22-24 in Tokyo (Japan)
- **Laser World of Photonics China**
  July 13-15 in Shanghai (China)
- **INPHO Venture Summit**
  October 13-14 in Bordeaux (France)

NEW MEMBERS

Welcome to our new members : **Axeclair**, **Cegitek** and **Luzilight** !

The 5th edition of Photonics Online Meetings, a European wide virtual business event dedicated to photonics technologies, will be held on 22 November 2022.

The event will bring together major contractors and suppliers of photonics technologies and services.
An exceptional arrangement of pre-scheduled and relevant meetings between technology suppliers and contractors will make this day a unique event during which partnerships and business opportunities are woven.
In addition, a rich program of plenary conferences, demonstrations and technical presentations led by experts will form pattern of the event.

For further information and to register: https://onlinemeetings.photonics-france.org/

AGENDA

- **Laser world of photonics, Munich, April 26-29, 2022**
- **Business meeting agrifood, Paris, May 24, 2022 [French speaking only]**
- **Journées securite optique et laser (jsol) Bordeaux, November 8-9, 2022**
- **French photonics days Saint-Etienne, October 20-21, 2022 [French speaking only]**
- **Photonics online meetings,** *Online, November 2022*

CONTACT
PHOTONICS FRANCE
contact@photonics-france.org / www.photonics-france.org

BUSINESS MEETING

Photonics for Agrifood industry May 24 in Paris

After many successful editions covering different industries, Photonics France organizes a Business Meeting on May 24, 2022 dedicated to the Agrifood industry. A full day dedicated to business and networking in Paris (Denfert-Rochereau), with conferences and workshops on the needs and projects of major contractors and integrators

For more information and registration : www.billetweb.fr/business-meeting-agroalimentaire
The event is French speaking only;

Call for submissions: optics and laser safety days

JOURNÉES SECURITE OPTIQUE ET LASER (JSOL) November 8-9, 2022 in Bordeaux

The 4th edition of the Optical and Laser Safety Days at Work (Journées Sécurité Optique et Laser au Travail – JSOL), organized by the National Optical Safety Committee (Comité National de Sécurité Optique - CNSO) will take place on November 8 and 9, 2022 in Bordeaux. The objective of this event is to promote a safety and prevention awareness in the field of laser and optical security in companies.

We are looking for speakers to present the risks related to the use of lasers or optical sources, best practices, as well as the evolution of the regulations.

You want to submit a presentation? Send your abstract to cnso@photonics-france.org

Nano-optics & Nanophotonics (NANO-PHOT) Graduate School

An unparalleled 5-year program of excellence

NANO-PHOT (Nano-Optics & Nanophotonics) offers an ambitious 5 years (Master + PhD) education program on the use of light on a nanometer scale. It aims at training the next generations of researchers and professionals at the cutting edge of nanophotonic's sciences and technologies.

Master program (30 ECTS credits/semester)

The NANO-PHOT graduate School offers a rich training program that is 100 % taught in English. It involves more than 20 faculty members, among them 10 external specialist lecturers for about 15 classes.

Semester 1 in Reims: Mathematical and numerical tools for physicists, Wave Optics, Solid state Physics Communication, bibliography, conferences
Foreign Language, Lab Project I (1/day/week)
Semester 2 in Troyes: Classical and quantum light-matter interaction; Materials and devices in optics and optoelectronics; Nano-optics and Nanophotonics; Microscopies & Spectroscopies; Nanofabrication & nanomaterials; Innovative companies: entrepreneurship, economic intelligence, Intellectual properties; Foreign Language; Lab Project II (1 day/week)
Semester 3 in Troyes: Multi-scale characterization; Hot topics in nano-optics & nanophotonics; Quantum Optics and Nano-Optics; Foreign language; Management of research projects; Lab Project III (2 days/week)
Semester 4: 6-month internship in a partner laboratory or company. The master thesis can be based on the previous Lab projects.

PhD program (UTT doctoral school)

- 3-years PhD research project in a Laboratory within the NANO-PHOT network
- Joint international PhDs are possible!
- Science and Technology Training - 60 h - examples of courses: laser use, atomic force microscopy, nano-optics & plasmonics
- Employability-Focused/Human Science training - 60h - example of course: ethics and scientific integrity.

Target skills

- **Basics of the multiscale interaction between light and matter**
- **Knowledge and knowhow in the field of nano-optics and nano-photonics**
- **Knowing the different types of optical materials and their properties**
- **Knowing the behavior of light at the quantum level.**
- **Skills in the use of tools of numerical simulation, nanocharacterization and nano-fabrication.**
- **Getting aware of the potential domain of applications of nanooptics and nanophotonics.**
- **Autonomy in a research laboratory in interaction with a research team.**
- **Setting up and managing national and international research projects.**
- **Understanding the economic and legal environment of innovative companies.**

Training by research

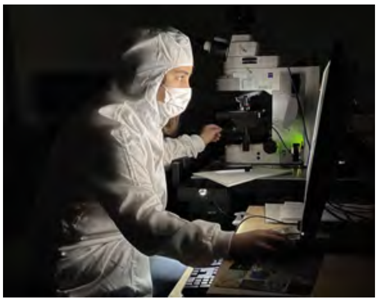

Arousing students' interest in research begins with their involvement in laboratories.
The NANO-PHOT Graduate School allows students to carry out "Lab projects" from the first year of their Master's degree. The NANO-PHOT students may have a complete access of all research facilities after specific trainings. Located on two sites, research facilities are spread among 7 involved laboratories and a 1200 m² platform of technology (including 750 m² of clean rooms).

NEWS

- A Troyes-Berlin-Ohio Nanophotonics Workshop took place in Troyes on 2022, February 24th
https://nano-phot.utt.fr/news/troyes-berlin-ohio-nanophotonics-workshop
- NANO-PHOT has been sponsoring the annual French scanning probe microcopy forum that took place in the beautifull "baie de Somme" in March 2022:
www.sondeslocales.fr/forum2022
- NANO-PHOT is one of the sponsors of the NFO16 conference (The 16th International Conference on Near-Field Optics, Nanophotonics and Related Techniques) that will take place in Victoria, BC, Canada from 29 August to 2 September 2022
https://nfo16.ece.uvic.ca/index.html#clients-j

ECA-iXblue,
a new French naval defense leader

Groupe Gorgé, parent company of robotic specialist ECA-Group, has announced the acquisition of iXblue for 410 million euros. This operation will lead to a world-class player in the fields of maritime, inertial navigation, defense, space and photonics. Long-standing partners, ECA Group and iXblue benefit from strong technological and commercial synergies. With a unique offer ranging from components to complex systems, the group will provide high performance solutions for critical missions in harsh environments.

Photonics Bretagne expands its team

Photonics Bretagne welcomes three new talents who joined the team in 2022 to bring their complementary expertises to the Research and Technology Organisation:

Robin POUYET
Materials Engineer and Polymer Chemist

Stéphane PERRIN
Biophotonics Project Manager

Sébastien CLAUDOT
Technical Manager

AGENDA

■ **Agrophotonics Webinar Québec-Bretagne**
May 11-12, Online

■ **Agrophotonics MorningTech**
"Light technologies at the service of animal production"
June 9, Ploufragan (France)

■ **Photonics Bretagne General Assembly**
June 21, Lannion (France)

Strong attendance of the Photonics Bretagne network at Photonics Europe

Photonics Bretagne and its members (IDIL Fibres Optiques, iXblue, Kerdry, Leukos, Lumibird, Luzilight, mirSense, Optosigma Europe, Oxxius, Silentsys) have exhibited at Photonics Europe in Strasbourg from April 3 to 7 and presented their latest innovations in sensing, imaging, lasers and related components. Photonics Bretagne has put in light its new range of VLMA Yb fibres, draw tower Bragg gratings, and multiple range of PCF (Hollow core, supercontinuum, endlessly singlemode...).
The new Perfos® Polarisation Maintening (PM) Ytterbium doped Very Large Mode Area (VLMA) fibre is particularly suited for the continuously growing ultrafast fibre laser market. The combination of robust single mode behavior in an all-solid glass form factor with 750 µm² fundamental mode area makes this fibre an ideal tool for high-end industrial fibre laser manufacturers.
The fibre Bragg gratings arrays are perfectly suited to be used as thermal or strain sensors. We inscribe them directly during the draw to allow the fibre to preserve its pristine mechanical strength. Our process allows us to inscribe in the fibre as many gratings as requested in a repeatable way.
Photonics Bretagne also showed its very last development on metal coatings that allow optical fibres to handle harsch environment (High temperature, radiative conditions...).

5G ACCELERATION STRATEGY AND NETWORKS OF THE FUTURE: LAUNCH OF SIMBADE PROJECT

The SIMBADE project is one of the seven initiatives selected from the French Government as part of the "5G Acceleration Strategy and Networks of the Future" program, and received funding from Direction Générale des Entreprises (DGE). The partners of the project are Ekinops (project leader), Idil Fibres Optiques, Le Verre Fluoré, Orange, the University Lille 1 - PhLAM laboratory, and Photonics Bretagne. One objective is to develop the telecom infrastructure and transport capabilities to unlock networks of the future. It aims to increase the exploitable bandwidth in DWDM transmission systems through the development of efficient fibre amplifiers in O-E-S telecom bands.

Open platform to explore
new usage scenarios for optic sensors

On April 5th, together with the CEA, Captronic, the Auvergne-Rhône-Alpes region, the IRT Nanoelec and the Auvergne-Rhône-Alpes Entreprises agency, Minalogic presented at the "SystemLab" Regional Digital Campus an open platform for new imaging applications. In particular, STMicroelectronics, Lynred and Prophesee will examine with small enterprises new scenarios for the use of optic sensors by amalgamating data using artificial intelligence. The goal of this activity is to promote closer collaboration between potential users and the R&D actors in optical imaging by exploring, looking ahead to and opening the way for tomorrow's technologies and uses. This morning event involved ten start-ups, small enterprises and micro enterprises and other organizations from the region.

For more information, please go to the IRT Nanoelec web site or contact Florent Bouvier.

AGENDA

- **Minalogic Business Meetings**
  May 31, 2022, in Grenoble
- **Minalogic Annual Day,**
  June 23, 2022, in Grenoble
- **Laser Processing for Industry" talks,**
  June 28-29, 2022, in Saint-Etienne
- **Photonics for Health" week,**
  July 4-8, 2022, in Saint-Etienne
- **Vision trade fair,**
  October 4-6, 2022, in Stuttgart
- **"French Photonics Days", October 20-21, 2022, in Saint-Etienne, as part of the Manufacturing Biennale.**

Contact person:
Florent Bouvier
Photonics Manager in Minalogic
Tel: +33 (0)6 35 03 98 52
florent.bouvier@minalogic.com

All eyes are on the 2022 French Photonics Days in Saint-Etienne

The 4th edition of the French Photonics Days will be held on October 20th and 21st, 2022, in Saint-Etienne. The event is being hosted by Photonics France, SupOptique Alumni, Minalogic and Cluster Lumière, in partnership with Manutech Sleight Graduate School and the Institut d'Optique Graduate School, with support from the Saint-Étienne Urban Area and the Auvergne-Rhône-Alpes Region.

The goal of French Photonics Days is to promote the French field of photonics, to give due credit to the regions' actions and investments in this field, and to highlight the technological advances and market perspectives of local actors.
The topic selected for this 4th year's event is "Photonics for Displays, Lighting and Manufacturing". This topic reflects the skills and experience of the actors in the local networks and enables French Photonics Days to benefit from the label and the dynamics of the Manufacturing Biennale.
Designed for a technical but not specialized audience, the objectives of French Photonics Days are to:
- provide an update on the development of new photonics technologies and present their applications and markets,
- discuss education and training, and future planning for the field of photonics,
- promote new products at the event sponsors' stands,
- offer visits of local companies.

In technical terms, the subjects adopted are: the revolution in free-form optics, photonics and surfaces, and new LEDs and OLEDs for lighting and displays.
This year's event, to be held in the UNESCO city of creative design, will also comprise many occasions for networking, including an evening reception.
Registration can be done on the Minalogic and Photonics France web sites.
Registration is free for members of the sponsoring entities (except for the reception).

LASER WORLD OF PHOTONICS:
A GREAT SUCCESS FOR THIS 2022 EVENT

Minalogic took part in the Laser World of Photonics, the worldwide trade fair for photonics components, systems and applications that was held on April 26-29, in Munich. Our cluster accompanied a regional delegation of 9 members, under the aegis of its International Development Plan, with financial support from the Auvergne-Rhône-Alpes region. Present at the French Pavilion, operated by Business France and coordinated by Photonics France to bring together the French photonics field, 5 members of Minalogic (Data Pixel, Hef Groupe, Qiova, Set Corporation, Teem Photonics) benefited from high visibility and the collective strength of the groups flying the French flag. Alpao, Cedrat Technologies Fibercryst, Edmund Optics and Mathym were present with their own stands.
On site, Florent Bouvier and Damien Cohen, from Minalogic's staff, assisted the members with their R&D and business prospection activities. They also took advantage of the event to promote the regional photonics entities at the international level and to identify relevant contacts. In order to promote networking, conviviality and occasions for meeting people, a reception was held on April 27th at the French Pavilion that brought together the members of the French photonics entities and a number of European partners participating in the Photonics21 platform.
For more information, please refer to the Minalogic web site.

News from the webb

On December 25th 2021, the largest space telescope ever built was launched from Kourou on Ariane 5. After receiving this wonderful Christmas gift, astronomers around the world are now eagerly awaiting the first observations of the Webb telescope.

After receiving this wonderful Christmas gift, astronomers around the world are now eagerly awaiting the first observations of the Webb telescope. However, unlike most of its predecessors, the Webb telescope was not optically operational after its launch. Six months have been planned to bring the Webb into its full scientific capabilities. As of April 1st 2022, no big issues have arisen and all optical parameters that have been checked and tested are performing at the level, or above, of the expectations. Below is a summary of the milestones that have been achieved since the launch:

On Jan 4 2022, the deployment of the five-layered sunshield that protects the telescope from the light and heat of the Sun, Earth, and Moon was successful. This crucial step took 7 days with the unfolding and tensioning of the five thin plastic sheets coated to reduce the solar power received by the telescope by a factor of about one million. The 74 cm secondary mirror was then deployed at 7 m in front of the primary mirror, which was still folded at that time. The telescope was fully deployed on January 8 when the two folded wings of the primary mirror were opened out. The Webb Space Telescope reached its desired orbit, nearly 1.5 million kilometers away from the Earth at the second Sun-Earth Lagrange point on January 24.

While the telescope and instruments were still cooling down, alignment of the telescope started in mid-January and underwent a series of steps to get each individual segment aligned and cophased.

After moving the 7 actuators of each segment of the primary mirror to their flight position, the next step was to identify the 18 images of a star given by each segments using the NIRCam instrument. After repositioning them in a hexagonal pattern (Image 1), each individual image diffracted by a segment is focused by updating the alignment of the secondary mirror and optimizing the positions of the mirror segments using their actuators.

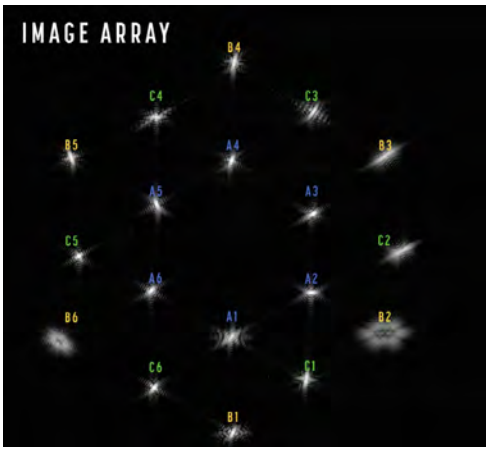

Figure 1: Diffraction image of the same star by each of the 18 segments of the primary mirror. The segments are tilted to create a hexagonal grid on the NIRCam instrument. Each image is labelled with the corresponding mirror segment that captured it. Credits: NASA/STScI/J. DePasquale. https://blogs.nasa.gov/webb/2022/02/18/webb-team-brings-18-dots-of-starlight-into-hexagonal-formation/

After superimposing the 18 images on top of each other, the segments still required to be co-phased with each other by following two steps:

1) Dispersed fringe spectra recorded on NIRCam from 20 separate pairings of mirror segments allow a coarse correction of the vertical displacement (piston difference) between the segments.

2) A fine correction is applied based on the estimation calculated by phase retrieval algorithms using defocused images.

This alignment stage was completed on March 11 with the release of a first image (Image 2) showing the diffraction-limited image of an alignment star and already plenty of small galaxies in the background...

Early April, this was completed with the alignment of other Webb instruments: the Fine Guidance Sensor (FGS), the Near-Infrared Slitless Spectrograph (NIRISS), and the Near-Infrared Spectrometer (NIRSpec). The Mid-Infrared Instrument (MIRI) continues its cooling and should soon reach its cryogenic operating temperature (7K). A second multi-instrument alignment will then be carried out to finalize adjustments of the instruments and mirrors.

The instruments will be tested in their different observation modes, to make sure that they are ready for scientific observations. Before the end of this commissioning phase, a few observations will be made. Once processed, they will provide the very first images available to researchers and public illustrating the capabilities of the James Webb Space Telescope. Where Webb will look first has not yet been disclosed but stay tune... The images will probably be spectacular !

AUTHOR
Pierre Baudoz, LESIA, Observatoire de Paris, Université PSL, CNRS, Sorbonne Université, Université de Paris, France

Figure 2: First diffraction-limited NIRCAM image released. Hundreds of galaxies can already be detected in this image. © Nasa. https://www.nasa.gov/press-release/nasa-s-webb-reaches-alignment-milestone-optics-working-successfully.

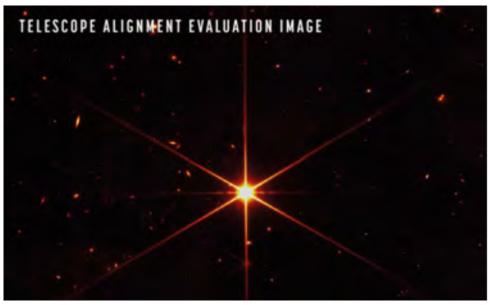

CROSSWORDS
ON OPTICAL FREQUENCY COMBS

By Philippe Adam

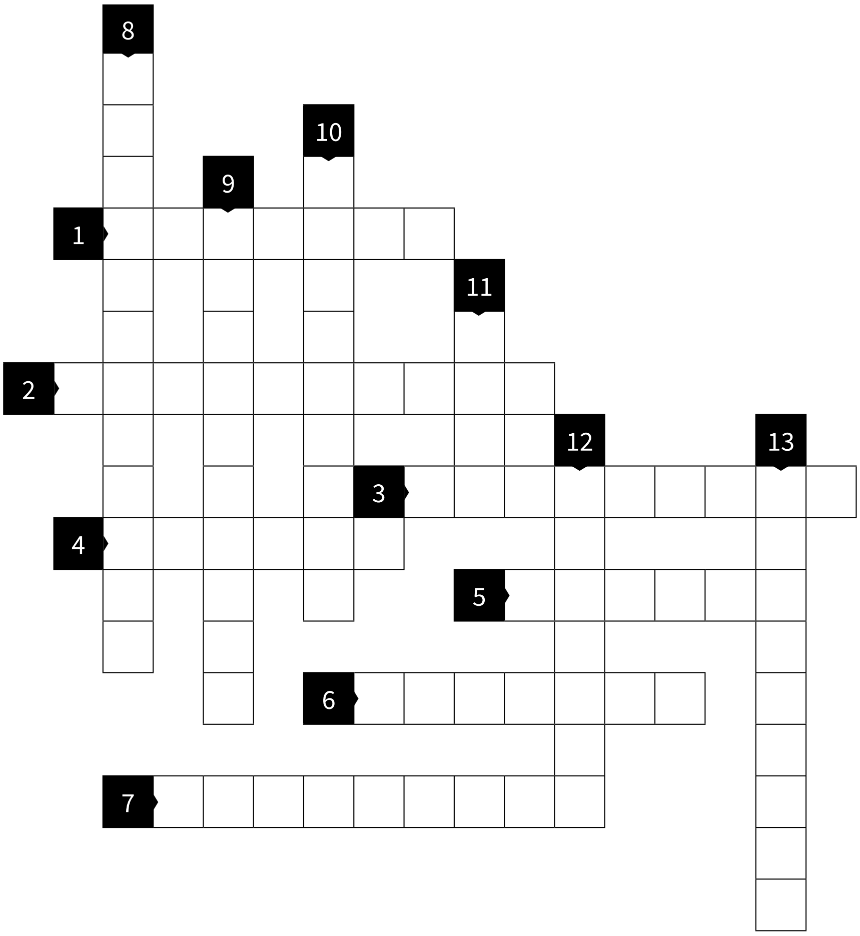

1 Its phase has to be compared with envelope
2 Needed mode to generate frequency combs
3 Interval precisely equal to the repetition rate
4 Spanning music
5 2005 Nobel Prize in Physics
6 Used to measure unknown frequencies
7 Straightforward application of FC
8 Very straightforward application of FC
9 Separation frequency between two modes
10 Long wavelength today produced by photonic chips
11 Nonlinear effect which could induce FC in micro-resonators
12 Efficient (or finesse) factor
13 Transmitted from pulse to pulse

SOLUTION ON
PHOTONIQUES.COM

Electrically driven random lasers

Random lasers (RLs) are intriguing devices that attract the interest of researchers for the varied phenomena they present in areas such as complexity, chaos etc.

But they also have a practical aspect with promising applications as light sources for illumination in microscopy, sensing, super-resolution spectral analysis, or complex network engineering. RLs usually require two material components associated with the amplification (gain) and feedback (light diffusion) processes inherent to lasing. Thus, they have been customarily obtained from optically pumped organic dyes, optical fibers and crystals powders, or electrically pumped semiconductor heterostructures. Semiconductor RLs are usually manufactured by introducing light-diffusing defects in the active layer, something that adds a degree of complexity to the manufacturing process and spoils the ease of realization potentially offered by messy structures. The direct availability of electrically pumped RLs, avoiding an involved and expensive manufacturing process, could crush the principal hurdle to their use in research and technology.

A team of researchers at ICMM (CSIC), in Madrid realized a procedure to manufacture a semiconductor RL from an off-the-shelf laser diode. The fabrication simply uses the high energy pulses from an ablating laser to sculpt the output mirror to create submicrometric roughness. The optical feedback provided by the ablated front mirror in combination with the intact rear mirror results in strong modification of the cavity modes and leads to laser emission with a random multimode spectrum. This in turn lowers the spatial coherence and messes the angular pattern. The speckle, characteristic of highly coherent light sources, is here strongly reduced.

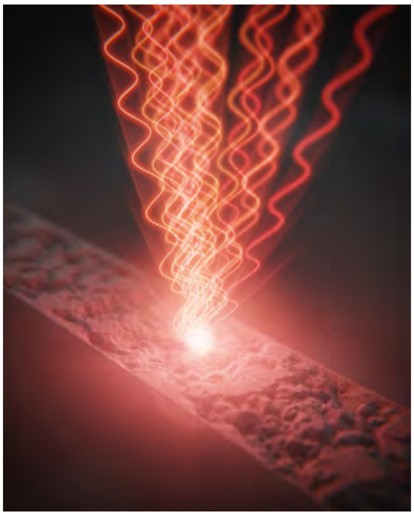

REFERENCE
A. Consoli, N. Caselli, and C. López, "Electrically driven random lasing from a modified Fabry–Pérot laser diode," Nat. Photonics 16, 219–225 (2022).

Brillouin light amplification in silica nanofiber gas cell

Brillouin scattering in optical waveguides draws plenty of attentions since it has been widely exploited for various important applications, such as microwave photonics, highly coherent fibre laser, and distributed fibre sensor. EPFL scientists, in collaboration with FEMTO-ST Institute, have achieved a huge amplification of light over a few centimetre with tapered silica optical fiber surrounding by high pressure gas. The strong Brillouin gain in the evanescent field together with the high tunability offered by the gaz (gaz type and pression), makes the integrated Brillouin amplifier very distinct compared to its solid material counterpart. They research team has demonstrated a 79-times higher peak Brillouin gain coefficient in the nanofibre gas cell with 57 Bar of $C0_2$ compared to that in a standard single-mode fibre.

Yang, F, *et al.* "Large evanescently-induced Brillouin scattering at the surrounding of a nanofibre" Nat. Comm. **13**, 1432 (2022). https://doi.org/10.1038/s41467-022-29051-8

ADVERTORIAL

SEDI-ATI FIBRES OPTIQUES

RELIABLE FIBER-OPTIC HERMETIC FEEDTHROUGHS FOR EXTREME ENVIRONMENTS

FOR PRESSURE, VACUUM, CRYOGENIC, BAKE-OUT, AND RADIATION APPLICATIONS

SEDI-ATI hermetic fiber-optic feedthroughs meet stringent sealing and leak tightness requirements to withstand **extreme environments** in demanding markets such as quantum, space, oil & gas, electric power distribution, and nuclear. Our feedthroughs can achieve hermeticity where pressure is as high as **1000 bars**, vacuum is as low as **10^{-12} mbar**, radiation levels are above **100 M Gray**, temperature exceeds **200 °C** or goes down to **0.5 K**.

BESPOKE DESIGNS TO SUIT MANY APPLICATIONS

SEDI-ATI's great strength is its ability to adapt the feedthrough to the customer's needs. Depending on the application, the design of a feedthrough can be significantly different *i.e.*, **single or multifiber, fixed or reconfigurable, bulkhead or inline, with or without flange...** Also, a wide variety of singlemode, polarization maintaining, and multimode optical fibers can be integrated such as **specialty fibers, solarization resistant fibers, or metal-coated fibers.** Finally, we devote particular attention to both the choice of materials and the choice of the sealing technology: **epoxy, glass-soldering, brazing**.

ABOUT SEDI-ATI FIBRES OPTIQUES

With 50 highly skilled and qualified professionals, a strong R&D team, and ISO 9001 & 13485 certifications, SEDI-ATI has in-house resources required to adapt and integrate an intrinsically fragile material such as the optical fiber to a wide variety of complex and extreme environments. Our essential factory equipment comprises two clean rooms, a pressure test bench, helium leak bench, two evaporation chambers, spectrometers, precision turning machines...

SHARE YOUR DREAMS WITH US!

We are always ready to listen to your needs and offer you optimal solutions to overcome your challenges. So do not hesitate to consult us!

CONTACT
Claire GUYONNET / Sales & Marketing Director
contact@sedi-ati.com
www.sedi-ati.com

INTERVIEW

Michael Mei, Menlo Systems

Menlo Systems recently celebrated its 20th anniversary. *What were your initial motivations for creating a new company in the field of optics and photonics? What have been the main steps in terms of growth and development?*

In the 1990s, Prof. Theodor Hänsch's group at the Max-Planck Institute of Quantum Optics performed precision measurements on the hydrogen atom, but rapidly the possibilities to measure the wavelengths were exhausted. Frequency measurement, on the other hand, was an almost impossible undertaking. This changed with the invention of the optical frequency comb technology: an approach involving the measurement of optical frequencies using the comb spectrum of a mode-locked femtosecond laser.
In 2005, Theodor Hänsch and John Hall were awarded the Nobel Prize in Physics for their contributions to the development of high-precision laser spectroscopy, including frequency comb technology.
Already in 2001, Theodor Hänsch, Ronald Holzwarth and myself had founded Menlo Systems GmbH with the mission to commercialize the frequency comb technology. Today, Menlo Systems is one of the market leaders in high-precision measurement technology and employs over 160 people worldwide.

INNOVATION & TECHNOLOGY

Can you describe the core of your technology? What are the main scientific fields of application of your products?
By means of mode-locked femtosecond lasers, we were able to create frequency combs that could be used like a ruler to directly measure optical frequencies. The progress was enormous: previously, equipment filling a whole laboratory was required to measure a single optical frequency, whereas now we had a setup of approx. 1m^2 with which we could measure any frequency. This was a quantum leap for many applications. The first optical frequency combs were rather sensitive instruments, but over the years the technology has matured, and optical frequency combs nowadays are turn-key fiber-based laser systems designed for 24/7 operation.

Can you comment on the impact of optical frequency combs on science and technology?
The impact of optical frequency combs on science and technology can hardly be overestimated. While some of the early adopters predicted limited applications in traditional high-resolution spectroscopy only, over the course of the last 20 years the field of applications has widened and optical frequency combs are regarded as key enabling tools for many applications from optical clocks, quantum sensing and quantum computing, to detecting exoplanets in astronomy, and offering unmatched accuracies for tasks in industrial metrology.

MARKET & STRATEGY

Are you focusing your sales efforts in Europe or worldwide?
Menlo products all have in common that the optimal use is in applications where precision counts. From the very beginning we had customers from all over the world. From our headquarters in Martinsried, close to Munich, we serve the German and most of the European market, supported by local experts in selected countries like our regional sales engineer located in Bordeaux. In the US, China, and Japan we have sales and service offices, with the aim to be close to the applications and to our customers.

Is Europe a great place for photonics?
Europe has a long tradition in photonics. Many scientific discoveries and inventions have been made by its excellent scientists. The industry benefits from the continuous stream of graduates out of highly-ranked universities. In France, there are around 200 science labs with 13.000 scientists, and about 1000 companies with 50.000 jobs in optics and photonics (according to the French trade association AFOP). In Germany, the situation is excellent as well. So yes, we consider Europe a great place for photonics, with France and Germany both playing an important role.

How do you evaluate the evolution of photonics? How to increase the spread of photonic technologies and strengthen the companies and market?
With new strategic plans for quantum technologies in place we are observing the creation of several new companies and research projects with innovative quantum applications and technologies. In France, Menlo Systems already supports these initiatives by unlocking access to better laser metrology with optical frequency combs, and by providing customizable laser systems for demanding quantum applications. Menlo Systems will keep working closely with French actors of quantum technology to support this ambitious national plan.

VISION & PERSPECTIVES

How do you imagine the next 20 years for your company and for photonics? Have you identified promising scientific areas for photonic technologies?
Taking the optical frequency comb as an example, the evolution of scientific areas has rapidly grown from precision spectroscopy to very diverse fields including precision metrology, optical atomic clocks, astronomy, space applications, and the quantum technologies. We are convinced that we currently only see the tip of the iceberg. By means of integrated optics and chip based optical frequency combs our vision is that advanced spectroscopic tools will become available with any smartphone in 20 years from now.

CONTACT: Dr. Michael Mei
Menlo Systems GmbH
Bunsenstraße 5
82152 Martinsried, Germany
m.mei@menlosystems.com

Data - the deciding factor

TIAMA: THE GLOBAL PROVIDER
OF REAL-TIME DATA AND QUALITY CONTROLS

TIAMA is one of the world leaders in providing inspection and quality control solutions for the glass packaging industry. It offers tools for glassplants to enhance glass production process efficiency and to control the glass container's integrity by detecting defects (visual, non-visible, dimensional, etc.).

Created in 2008 from the complementary know-how of MSC and SGCC firms, Tiama is today a global market player offering a complete range of inspection solutions. Its technical expertise, innovative approach, and market credibility, enable the company to offer solutions that go far beyond the simple control of defects in glass packaging.

In a few figures, Tiama has 91% of export sales, customers in 79 countries over the 5 continents, subsidiaries in China, and the USA, with teams of local technical engineers. Since its creation, it has already installed more than 10,000 online process and quality control solutions around the world.

Tiama provides real-time data and recommendations to help glassmakers to deliver articles with the highest quality and to improve their productivity. To meet all of these needs, Tiama develops its expertise:

- **Intelligence:** Software gathering real-time data across the production line for analysis and management of the plant performances with display of the results on a single platform for a view at-a-glance of the plant productivity.
- **Monitoring:** The modular hot-end monitoring systems provide operators with immediate data and easily applied information (gob specifics, etc.) to help improve productivity.
- **Inspection:** More than 20 years ago, Tiama was paving the way with the Atlas, a camera-based check detection, with automatic settings adapting themselves to the production changes. Since then, Tiama has never stopped improving its various machines with solutions that offer fast adjustments. The next steps, working on Big Data analysis and deep learning features to increase the predictability of glass production.
- **Traceability:** Tiama has launched the first engraving and reading datamatrix code solutions and remains the only company offering you full unitary traceability of each container.
- **Service:** With more than 70 local experts, 2 training academies and a dedicated department focused on customer satisfaction, Tiama offers unrivalled global support services.

Innovation

Innovation, new products, state-of-the-art, solutions are fully part of the Tiama Business model. The company holds today 45 patents and allocates 10 % of its turnover to the R&D department. TIAMA teams have industrialized lighting systems and innovative image processing technics. Some examples:

- **Non-contact detection:** following of collaborative project, we have developed a non-contact and non-destructive measurement system using microfocus X-ray source and CT technics in the XLAB machine. The system generates a full 3D image composed of millions of facets that can be freely rotated. Volume, capacity, vacuity, diameters, and angles can be measured as well as thickness fully mapped.
- **Process monitoring:** for example, in the HOT mass systems, the cameras (located just under the shear cut) take pictures of the free-falling gobs (drops of fused glass) which are then analyzed. These data are used to measure and predict the trajectory of the gobs and regulate the gob weight automatically by controlling the tube and the needles in the feeder system.
- **Thermography:** this technique consists in capturing infrared glass emission with an infrared camera to give information on container glass distribution. The system is synchronized with the individual section machine, so that the images of articles taken are linked to their section and cavity of origin.
- **Prediction with dynamic mask:** for example, in the Argos system, the machine integrates optical devices (using optical fiber) but also dynamic mask allowing an automatic learning process in production, based on a reference mask built with production bottles.

Conclusion

All these projects are just a small part of what we develop, we strive to remain competitive in our field of expertise and always explore all our opportunities for innovation through collaborative projects within our ecosystem for example.

Optical glass:
an interplay of challenges and success

For several hundred years, there has been an impressive interplay between optical design and optical glass development. Step by step, imaging by lenses in microscopes or other optical instruments has almost reached perfection. Simultaneously, optical technologies have broadened their application field by entering, *e.g.*, the area of telecommunication and being even the driver of novel technologies like augmented reality. Remarkably, even with the latter dramatic change in optics, there has been a red thread concerning the desired material properties so far. However, with today´s nanotechnologies, also completely new approaches may contribute to the field of optical materials in future. Who knows?

https://doi.org/10.1051/photon/202111320

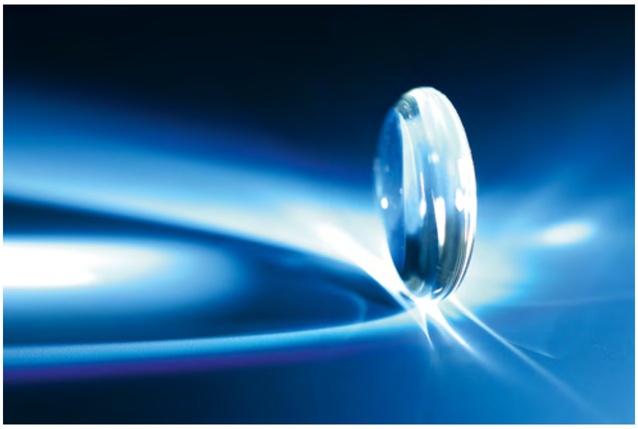

Ulrich FOTHERINGHAM*, Matthias MÜLLER
Schott AG, Hattenbergstraße 10, Mainz, Germany
*ulrich.fotheringham@schott.com

Introduction to Optical Glasses

Optical glass has a long history and has been in use for applications which seem far apart but are not. Who would imagine that the designer of glass for augmented reality has to cope with essentially the same issues as his predecessor working on glass for microscopy 100 years ago? However, there is a red thread connecting all this.

Both the red thread and different applications will be presented. First, the "red thread properties", the transmittancy, the refractive index, and the chromatic dispersion will be introduced. Remarkably, these properties are interrelated due to fundamental physics – not only for glass, but for any optical material (Kramers-Kronig relations [1]). Often, this makes it difficult to simultaneously adjust these properties to desired values.

Transmittancy. Preferably, optical glasses are made from oxides with high bandgaps so that only photons energetically corresponding to a frequency in the ultraviolet (UV) will be absorbed. These are, *e.g.*, SiO_2, B_2O_3, CaO etc. [1]. Low band gap, colouring impurities such as Fe_2O_3 are carefully avoided. With respect to Kramers-Kronig, however, a desired dispersion may require oxides with medium-size band gaps that will move the UV absorption edge close to the lower end of the visible spectrum (400nm) (see Fig. 1).

Chromatic Dispersion. Commonly, optical glasses are categorized in the Abbe diagram [2] according to n_d, the index at the Fraunhofer line d (587.6nm, yellow), and a characteristic figure for the chromatic dispersion, the Abbe number, which is defined by:

$$\boldsymbol{\nu_d} = \frac{n_d - 1}{n_F - n_C} \qquad (1)$$

The Abbe number increases with decreasing difference of the indices at the Fraunhofer lines F (486.1nm, blue) and C (656.3nm, red), *i.e.* with decreasing main dispersion ($n_F - n_C$). It is named after Ernst Abbe who in 1889 founded the Carl Zeiss foundation, the sole shareholder of the two companies Carl Zeiss AG and Schott AG.

Relative Partial Dispersion. As the relation between the refractive index and the wavelength is nonlinear, dispersion characterization requires a quantity which describes the degree of nonlinearity. A suited one is the relative partial dispersion $P_{d,C}$. It is the ratio between the yellow-to-red dispersion $n_d - n_C$ (partial dispersion) and the blue-to-red-dispersion $n_F - n_C$ (main dispersion):

$$\boldsymbol{P_{d,C}} = \frac{n_d - n_C}{n_F - n_C} \qquad (2)$$

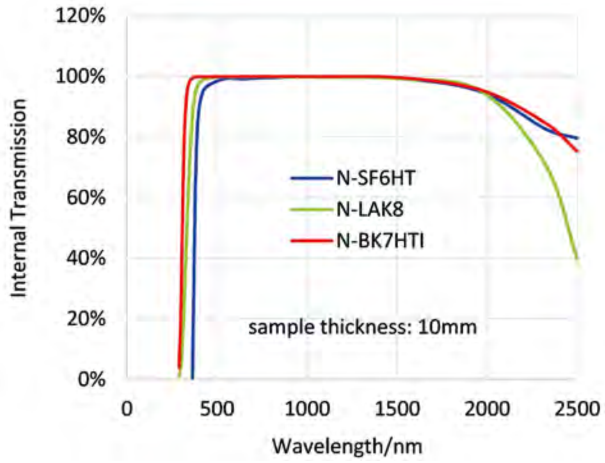

Figure 1: Internal transmission in UV, VIS, NIR for three glasses from SCHOTT AG.

For a linear wavelength dependence of the refractive index, $P_{d,C} = 0.4$ would hold. For real glasses, it is lower. Note that beside $P_{d,C}$, the analogously defined, but differently behaving $P_{g,F}$ is in use. g is the 435.8nm Fraunhofer line.

Refractive Index. Typical refractive index curves of optical glasses are given in Fig. 2. They are as expected from Kramers-Kronig [1]; one observes the following correlations (Figs. 1, 2):

#1. between the refractive index and the UV absorption edge: the higher the average index in the visible spectrum, the closer the UV absorption edge to the visible spectrum;

#2. between the UV absorption edge and main dispersion: the closer the UV absorption edge to the visible spectrum, the bigger the main dispersion;

#3. between the main dispersion and relative partial dispersion $P_{d,C}$: the bigger the main dispersion, the smaller the relative partial dispersion $P_{d,C}$.

The correlations #1-3 are what do make optical materials in the upper left of the Abbe diagram unfeasible! With the above background on optical glass, the challenges from optical design will now be discussed.

Challenges from Conventional Optics and Corresponding Glasses

Clear glass: enabler of optical imaging. Ca. 150 years before the first microscopes and telescopes were assembled in the early 17th century, the first clear glass had been made by Angelo Barovier. However, not knowing how to remove colouring impurities, he titrated the melt with MnO_2 until decolouration was reached [3]. As the absorption spectrum of MnO_2 is complementary to that of, *e.g.*, Fe_2O_3, a light grey absorption and thus an almost clear appearance may be obtained – a tricky, but smart approach. (The first application, however, was tableware.)

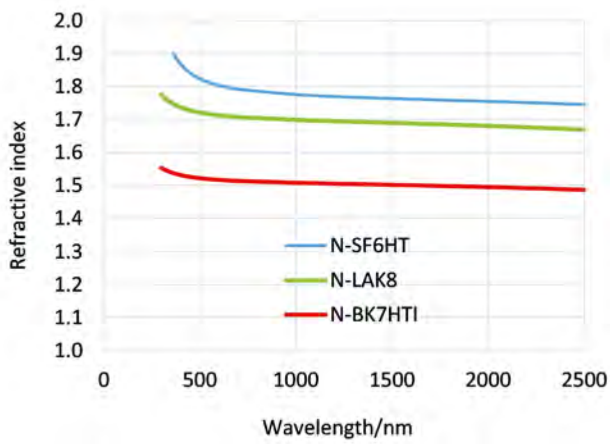

Figure 2: Refractive Index in UV, VIS, NIR for three glasses from SCHOTT AG.

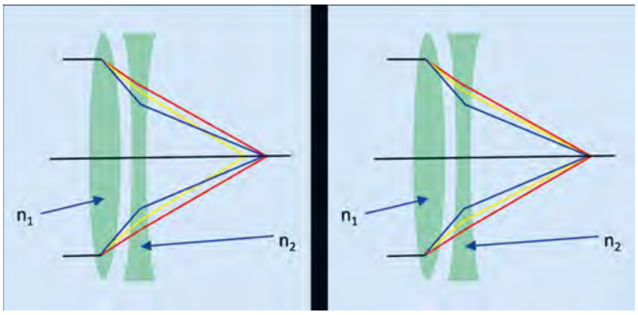

Figure 3: (left) Achromate with residual secondary colour. (Right) Apochromate.

These glasses were soda/potash-lime-silicates, called "crown glasses" after the manufacturing method [3]. The optical position in the Abbe diagram is denoted by "K".

Despite clear glass, the image quality of the early optical instruments was poor. Due to dispersion, "blue" rays are refracted stronger than "red" rays and have another focal length (primary colour). Different colours are imaged to different positions, with different magnifications, which gives rise to undesired colour fringes.

Achromates: solution to primary colour. In the middle of the 17th century, two element lenses were introduced, with the first element being a converging one with strong refractive power (short focal length), but small main dispersion, and the second element being a diverging one with small refractive power, but strong main dispersion.

By means of glass selection and lens element geometry, they are constructed such that (1) the resulting doublet is converging, but that (2) the strong main dispersion of the second element compensates the small main dispersion of the first element. (The dispersion by a converging element spreads colours, the dispersion by a diverging element recombines colours.) So coincidence of the "blue focus" and the "red focus" was reached (achromate, Fig. 3).

Expressed as a formula, the condition for achromatism is [3]:

$$0 = \frac{1}{f_{1,d}\cdot \nu_{1,d}} + \frac{1}{f_{2,d}\cdot \nu_{2,d}} \qquad (3)$$

The total focal length f_d (referring to $n = n_d$) for the doublet follows from the additivity rule for thin lens elements:

$$\frac{1}{f_d} = \frac{1}{f_{1,d}} + \frac{1}{f_{2,d}}. \qquad (4)$$

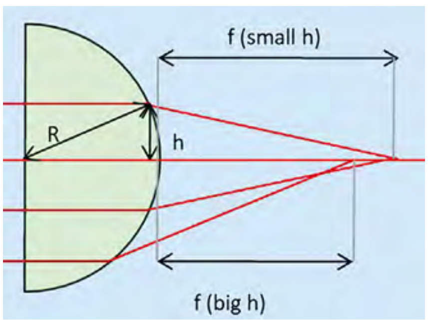

Figure 4: Spherical Aberration

By "$_{1,2}$" reference to the first or second lens element is indicated.

Fortunately, the high dispersion glass required had been invented some time before [3] by George Ravenscroft, who had introduced lead silicate for tableware, with its sparkling due to high chromatic dispersion being a very much desired feature. Consider, for instance, $PbO\cdot 2SiO_2$. Its bandgap is 3.1 eV which corresponds to 400nm [3]. With correlation #2 (the closer the UV absorption edge to the visible, the bigger the main dispersion), a high dispersion glass can be expected. Such low Abbe number glasses are called "flints". Two names are attached to the first achromates: Chester Moore Hall (made the invention), and John Dolland (got the patent and made the money) [3].

Today, lead-free alternatives are often preferred. So beside the lead silicates with the acronym "SF", the lead- and arsenic-free "N-SF"-glasses, situated at the same positions in the upper right of the Abbe diagram, are available.

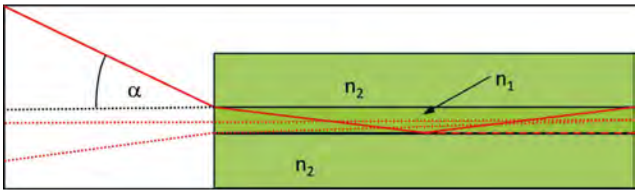

Figure 5: Lightguide

Apochromates: solution to residual secondary colour. In Fig. 3 (right), the yellow focal length is slightly smaller than that for blue and red. This is due to the nonlinear wavelength dependence of the refractive index, because of which the blue-to-yellow-dispersion is much bigger than the yellow-to-red-dispersion. If the spreading of wavelengths caused by the converging element is to be compensated by the diverging element, the ratio of the blue-to-yellow-dispersion to the yellow-to-red-dispersion must be the same for both elements. This is equivalent to equal relative partial dispersions.

However, correlation #3 says that the bigger the main dispersion, the smaller the relative partial dispersion $P_{d,C}$. is. So even if the main dispersion of the second element is strong enough to compensate the main dispersion of the first element, the partial dispersion will not be. This is why the yellow focal length is smaller than the one of red and blue. Therefore an apochromate with all colours in one focus did not yet exist when in the late 19th century, Otto Schott appeared on the scene.

Otto Schott could not override Kramers-Kronig. What he could do was to slightly scale up the index curve by increasing packing density. Thus, the average index and the main dispersion in the visible could be increased with neither moving the UV absorption edge nor affecting relative partial dispersion.

For this purpose, he switched from silicates to borates. $PbO\cdot 2B_2O_3$, for instance, has a bigger band gap and a higher packing density than $PbO\cdot 2SiO_2$ [3]. Starting with $PbO\cdot 2B_2O_3$, he developed the borate flint S7 [3] ($n_D = 1.61$, $\nu_D = 44.3$) that, with

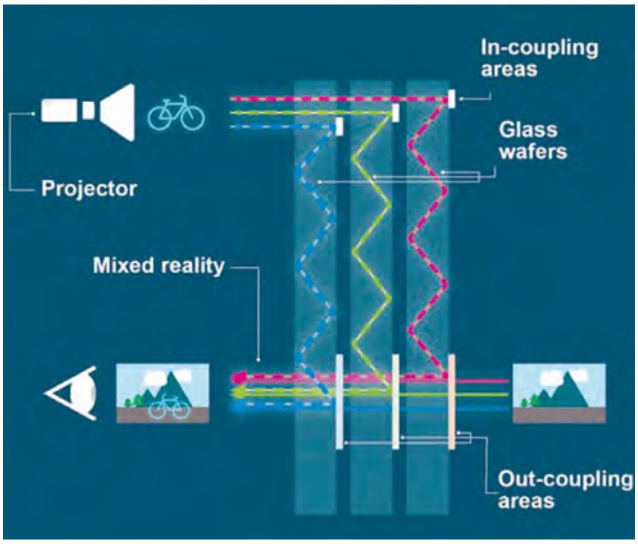

Figure 6: Three layers of glass in a waveguide for augmented reality (AR) glasses. Taken with permission from [6].

respect to relative partial dispersion, perfectly fitted to the high-potassium crown glass O13 [3] ($n_D = 1.52$, $\nu_D = 58$). This and other "special short flints" enabled the first apochromates, Fig. 3 (right). (In Otto Schott´s literature, the Fraunhofer line d is replaced with the nearby line D.)

First, chemical resistivity was an issue both for the borate flints and the high potassium crown glass. One approach by Otto Schott to settle this was to mix the two glass formers B_2O_3 and SiO_2, a pioneering step in glass development. Today, for example, the special short flint N-KZFS11 and the crown glass SCHOTT N-BK7® are borosilicates – such as numerous other optical and technical glasses.

Spherical Aberration: suppression requires high indices. Lens elements can easily be ground and polished by simple rotating devices [1], however, only spherical surfaces can thus be made. With them, the focus depends on the distance between rays and optical axis (longitudinal spherical aberration, Fig. 4). A second order calculation gives [1]:

$$f = \frac{R}{n-1} - \frac{h^2}{2R} \qquad (5)$$

So to suppress spherical aberration while maintaining f, a simultaneous increase of R and n is necessary. Due to Kramers-Kronig (correlation #1), this is especially challenging for low dispersion glasses.

Again Otto Schott was to find the solution, being the first to melt barium-containing glasses in an optical quality. With a band gap of 6eV, much higher than the one of PbO, BaO is well suited for low dispersion glasses. Although Kramers-Kronig prevents an ultra-high index, a moderately high index is achieved by the high packing density of, *e.g.*, glassy sanbornite $BaO{\cdot}2SiO_2$. Thus the barium crowns "BAK" as well as the (very) dense crowns "(S)SK" were launched. A later milestone ● ● ●

Figure 7: FOV in AR glasses with different indices. Left: FOV with binocular vision. Centre: FOV with display glass, n = 1.5. Right: FOV for AR glass with n = 1.6 (smallest FOV) up to n = 2 (largest FOV). Taken with permission from [6].

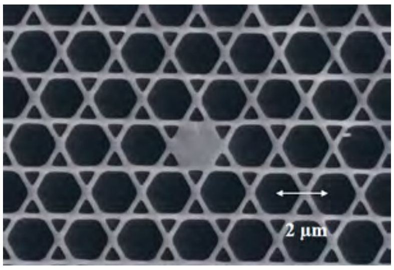

Figure 8: Cross section of a photonic crystal fibre manufactured by Schott AG.

concerning high index and low dispersion was lanthanum glass (George W. Morey, [1]).

Today´s high-end microscopes such as the ZEISS Axio Observer® offer sophisticated features like artificial-intelligence-based sample finders for biological samples to prevent them from the lasting illumination during a lengthy sample inspection by eye. The optical core is a high-end apochromate – with its roots going back to the extremely fruitful cooperation of Ernst Abbe, Carl Zeiss, and Otto Schott.

Novel Optics

"Lightguiding": key to the photonic revolution. Out of the numerous recent optical inventions, the most striking glass-related ones exploit the phenomenon of lightguiding. Already discovered in the 17th century by Johannes Kepler [4], total internal reflection had to wait until the 20th century with its first commercial use for illumination, imaging and communication.

Transmission is crucial. In conventional optics, light has to pass through centimeters of material only. Glass fibres for telecommunication, on the contrary, have to be so free of impurities that one could look through a several kilometer thick plate made of that glass. Manufacturing is by chemical vapour deposition [5]. Index and dispersion also play an important role. The acceptance angle of a lightguide, *i.e.* the maximum angle that is compatible with total reflection, is given by

$$\sin(\alpha) = \sqrt{n_1^2 - n_2^2} \qquad (5)$$

where n_1 is the core index and n_2 is the cladding index (see Fig. 5).

The desired indices depend on the application. For telecommunication, a low acceptance angle is preferred. Light entering at different angles would take different paths and thus cause an unwanted broadening of optical pulses. So no high indices are needed. Core and cladding are usually made from vitreous silica with certain dopants [5].

It is different for lightguiding in augmented reality (AR, [6]), Fig. 6. Here, the acceptance angle determines the field of view (FOV, [6]). The higher the index, the broader the field of view is. So high index glasses are required. Dispersion management is by different layers for different colours.

Photonic Crystals and Meta-Materials: exploiting the wave nature of light. Although the principles of lightguiding can be explained with ray optics, the complex behaviour of, *e.g.*, telecommunication fibres can only be understood considering the guided light as propagating modes, *i.e.* hybrid electromagnetic waves which are propagating along the fibre axis and standing waves in the perpendicular plane.

The wave character becomes particularly important if the confinement of light to the core is caused by interference in the cladding. That may occur at structures with a crystal-like order, so-called photonic crystals (Fig. 8) or at disordered structures, as it is the case for lightguiding with Anderson-localization where lightguiding is due to the interference of scattered light with the scatter centres lying closely together [7].

Photonic crystal fibres offer many different features, among them being special dispersion management for telecommunication, low-loss transport of laser power, and others [7].

Nevertheless, photonic crystal fibres are only a small part of what is generally possible with photonic crystals, *i.e.* ordered structures where periodicities with the magnitude of the wavelength cause special effects. Even more striking effects are possible with sub-wavelength structures with which very peculiar phenomena may be generated, *e.g.*, wave propagation and energy transport in opposite directions which is equivalent to a negative refractive index [7]. With respect to the highly sophisticated nanostructures involved, such materials will certainly not replace classical optical materials, but will offer highly welcome add-ons of the toolbox.

Conclusion

It is a long way from classical optical imaging to today´s optical applications like augmented reality. Nevertheless, glassmakers are all times confronted with similar issues concerning transmission, refractive index, and dispersion. This is due to the fact that said properties are inter-related by fundamental physical laws which prevent "once and for all times" solutions. On the other hand, these constraints are providing an ever-lasting challenge to find the limits of feasibility, employing all modern technologies like, *e.g.*, nanostructuring.

REFERENCES

[1] U. Fotheringham et al., Optical Glass: Challenges From Optical Design, in: Encyclopedia of Materials: Technical Ceramics and Glasses, M. Pomeroy Editor-in-Chief, (Elsevier, Amsterdam, 2021)

[2] https://www.schott.com/de-de/products/optical-glass-p1000267/downloads

[3] U. Fotheringham, Opt. Mat. Express Feature Issue Celebrating Optical Glass - IYOG 2022, in press

[4] Molecular Expressions: Science, Optics and You - Timeline - Johannes Kepler (fsu.edu)

[5] U. Fotheringham, Glastechn. Ber. **62**, 52-55(1989)

[6] R. Sprengard, Inf. Disp. **36**, 30-33 (2020)

[7] Encyclopedia of Modern Optics, 2nd edn., B.D. Guenther, D.G. Steel eds., Elsevier Amsterdam (2018).

LE VERRE FLUORÉ GLASSES AND FIBER OPTICS
KEY TECHNOLOGIES OF THE 21ST CENTURY

Our company

Since its foundation in 1977, after the discovery of fluoride glasses by Poulain Brothers at Rennes University in 1974, Le Verre Fluoré (LVF) has been thriving in the world of fluoride glass technology as an expert and main innovator in this field.

Among LVF outstanding pioneering achievements, we can cite the first commercial fluorozirconate glass fibers (1983), the first single mode fluoride fibers (1988), the first ZBLAN fiber lasers (1989) and the first fluoroindate glass fibers (1992).

Over the years, LVF has developed unique manufacturing processes of glasses and fibers and recently industrial capacity has been increased, with batches now produced on a daily basis.

LVF is today the world leading fluoride and germanate glass manufacturer, offering the world the best fluoride and germanate glasses and optical fibers on the market.

Why LVF fluoride glass fibers are so interesting ?

They offer :

- A high transparency from UV to mid-IR (300 nm – 5500 nm), with best transparency among all fiber technologies in the 2 – 5 µm range.
- Thanks to their high rare earth solubility and low phonon energy, they offer more than 50 rare-earth transitions in the visible, infrared and mid-infrared bands, allowing the manufacturing of visible and mid-IR fiber lasers, and near-IR fiber amplifiers

LVF technology addresses today a multitude of domains

LVF fluoride glass and optical fiber mature technology enables today the realization of innovative solutions that respond to challenges of the 21st century like improving the human health, better monitoring air and water pollution, monitoring our food quality while improving animal welfare, improving telecommunication infrastructures and monitoring quality in industrial processes.

Let cite few examples where LVF products are key enabling technologies.

INDUSTRY & ECOLOGY

- Oil and gas spectroscopy, Urban pollution monitoring, Aircraft exhaust gas monitoring,
- Semiconductors process monitoring (mid-IR OCT (Optical coherence tomography))
- Wet paint thickness measurements, Pyrometry
- Water quality and wastewater monitoring
- Waste recycling
- Smart agriculture (boar taint monitoring, online milk monitoring)

LVF Key components for NIR and MIR spectroscopy

Fiber patch cables, hermetic feedthroughs and flow cells
Fiber combiners for mid-IR laser diodes (ICL/QCL)
Fiber modules for mid IR supercontinuum lasers (up to 5µm and up to 9.5µm)
Targazh industrial sensor

MEDICAL

- Surgery, Ophtalmology, Osteotomy, Dentistry, Dermatology
- 3D living cells bio printing (skin, breast)
- Super-resolution microscopy, Cytometry, Ophtalmology
- DNA sequencing
- Cancer detection

LVF Key components

CW and pulsed 2.9µm laser (using Er doped fiber)
Multiwatts visible lasers and amplifiers
Passive fibers for mid-IR transmission
Er-YAG/Er-YSGG laser delivery (up to 1.5J/pulse)
Rare earth-doped fluoride glass fluorescent dyes

GROUND and SPACE COMMUNICATIONS

- Telescopes coupling
- Ground-to-ground and ground-to-space communication, O-Band and S-band telecom amplifiers
- High bit rate LIFI communications

LVF Key components

Passive ZBLAN fiber sub-systems
Rare earth doped fiber modules
3.9 µm pulsed laser
R G B pulsed fiber lasers

These examples highlight the diversity of our applications and new solutions powered by our fluoride glass technology. All of them are useful to human kind. Create a better future is our leitmotiv!

CONTACT

info@leverrefluore.com, www.leverrefluore.com
Follow us on LinkedIn: https://www.linkedin.com/company/le-verre-fluoré and Twitter https://twitter.com/LeVerreFluore

Quantum entanglement in the lab : an experimental training platform for the second quantum revolution

Benjamin VEST[1], Lionel JACUBOWIEZ[1]
[1]Université Paris-Saclay, Institut d'Optique Graduate School, CNRS, Laboratoire Charles Fabry, 91127 Palaiseau, France
***lionel.jacubowiez@institutoptique.fr, benjamin.vest@institutoptique.fr**

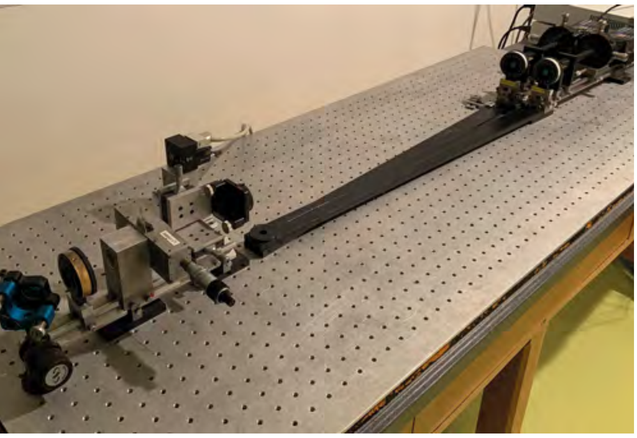

https://doi.org/10.1051/photon/202211326

The recent and rapid progress in the field of quantum technologies stimulates developments of specific courses and experimental training for future engineers and scientists. We describe below the experimental setup developed at Institut d'Optique Graduate School for engineering and Master students. During a labwork session afternoon, students can study a source of polarization entangled state pairs of photons and perform an experimental violation of Bell's inequalities. This emblematic experiment is one of the experiments dedicated to quantum photonics. It was built in 2005 in the LEnsE (the Laboratoire d'Enseignement Experimental) of the *Institut d'Optique Graduate School* and has been perfectly working for almost eighteen years already.

Entangled states represent one of the most strikingly counter-intuitive features of quantum mechanics, and as such, are often held as a great example of what quantum world means. Before the experiments by Alain Aspect and his team at Institut d'Optique reporting Bell's inequalities violation in the early 80s [1], decades of research have led to tremendous results revolutionizing our understanding of light-matter interaction. The first revolution of quantum physics has deep connections with the wave-particle-duality and the description of physical systems using the concept of wave functions. For instance, the process of carrier photogeneration by semiconducting devices is a direct consequence of the ability of quantum mechanics to explain the structure of matter and the optical properties of materials. As a consequence, it is reasonable to consider that many experimental labwork sessions in the LEnsE, dedicated to cameras and light detectors, are true quantum experiments!
However, the term "quantum photonics" usually refers to the concepts that emerged and were popularized after a second quantum revolution. Starting from the Aspect experiments, this second quantum revolution is focused on the most surprising and counter-intuitive predictions of quantum mechanics whose manipulation can lead to the development of a new generation of sensors, quantum

communication schemes, simulators or quantum computing.

A two-photon polarization entangled state

Entangled states are a class of multi-particle states whose existence is predicted by quantum mechanics [2,3]. The state of the polarization entangled pairs of photons that we produce in the labwork experiment can be written as:

$$|\psi_{2ph}\rangle = \frac{1}{\sqrt{2}}\left(|V_I\rangle|V_{II}\rangle + |H_I\rangle|H_{II}\rangle\right)$$

This is a typical polarization entangled state where V and H refer to the vertical and horizontal direction of polarization and I and II refer to each photon of the pair.

Why this entangled polarization state is so extraordinary? So strikingly counter-intuitive?

To explore more in details the features exhibited by this two-photon entangled state in polarization, we will perform measurements on the polarization of each photon of the pair. Figure 1 below describes the classical polarization measurement setup that we use in our experiment.

For the entangled state $|\psi_{2ph}\rangle$, whatever the direction of polarization, α, photon I is detected 50% of the time in state $|V_I^\alpha\rangle$ and is detected 50% of the time in state $|H_I^\alpha\rangle$ (the probabilities are : $P(|V_I^\alpha\rangle) = P(|H_I^\alpha\rangle) = 1/2$). The same result would be obtained for photon II ($P(|V_I^\beta\rangle) = P(|H_I^\beta\rangle) = 1/2$, whatever the direction of projection β is). So, in this entangled state, none of the photons of the pair has initially a defined polarization state and the measurement process attributes randomly the state $|V_I^\alpha\rangle$ or $|H_I^\alpha\rangle$ to the photon I.

A question now arises: what does happen with the other photon of the pair, let us say photon II? The answer is hard to believe: it is not even necessary to measure the state of photon II! Quantum formalism tells us that the polarization state of photon II is identical to the polarization state already measured of photon I. In other words, if the same settings are selected for both channels ($\beta = \alpha$), the second photon is systematically detected in the same state as photon I. The measurement outcomes on both channels I and II are *perfectly correlated*: that is, the conditional probabilities $P(V_{II}^\alpha|V_I^\alpha)$ and $P(H_{II}^\alpha|H_I^\alpha)$ are equal to 1 whatever α is.

So $P(|V_I^\alpha\rangle,\ |H_{II}^\alpha\rangle) = P(|V_I^\alpha\rangle|V_{II}^\alpha\rangle) = 1/2$ and $P(|H_I^\alpha\rangle,\ |V_{II}^\alpha\rangle) = P(|V_I^\alpha\rangle|H_{II}^\alpha\rangle) = 0$

and the degree of correlation of measurements between both channels is in this case : $E = (\alpha, \alpha) = P(|V_I^\alpha\rangle,\ |V_{II}^\alpha\rangle) + P(|H_I^\alpha\rangle,\ |H_{II}^\alpha\rangle) - P(|H_I^\alpha\rangle,\ |V_{II}^\alpha\rangle) - P(|V_I^\alpha\rangle,\ |H_{II}^\alpha\rangle) = 1$

Bell's parameter

More generally, we can choose to rotate the measurement basis on path I with an angle α and on path II by an angle β, different from α. Quantum formalism then predicts that the conditional probability of detection is expressed as:

$$P\left(|V_I^\alpha\rangle \ \middle|\ |V_{II}^\beta\rangle\right) = \cos^2(\alpha - \beta)$$

which is maximal and equal to 1, as we already noticed, as long as $\alpha = \beta$. The degree of correlation of the measurements between both channels is in this case :

$$E(\alpha, \beta) = P\left(|V_I^\alpha\rangle, |V_{II}^\beta\rangle\right) + P\left(|H_I^\alpha\rangle, |H_{II}^\beta\rangle\right) - P\left(|H_I^\alpha\rangle, |V_{II}^\beta\rangle\right) - P\left(|V_I^\alpha\rangle, |H_{II}^\beta\rangle\right)$$

$$E(\alpha, \beta) = \cos^2(\alpha, \beta) - \sin^2(\alpha, \beta) = \frac{1}{2}\cos 2(\alpha, \beta)$$

So, with this experiment setup, we can measure the Bell's parameter which is :

$$S_{\text{Bell}} = E(\alpha, \beta) + E(\alpha', \beta) + E(\alpha', \beta') + E(\alpha, \beta')$$

The maximal value is obtained for $\alpha = 22.5°$, $\alpha' = 45°$, $\beta = 45°$ and $\beta' = 67.5°$ for which the Bell's parameter is $S_{\text{Bell}} = 2\sqrt{2}$.

Non-locality in quantum correlations

We must however stress that the formalism of quantum mechanics has several counterintuitive (maybe ●●●

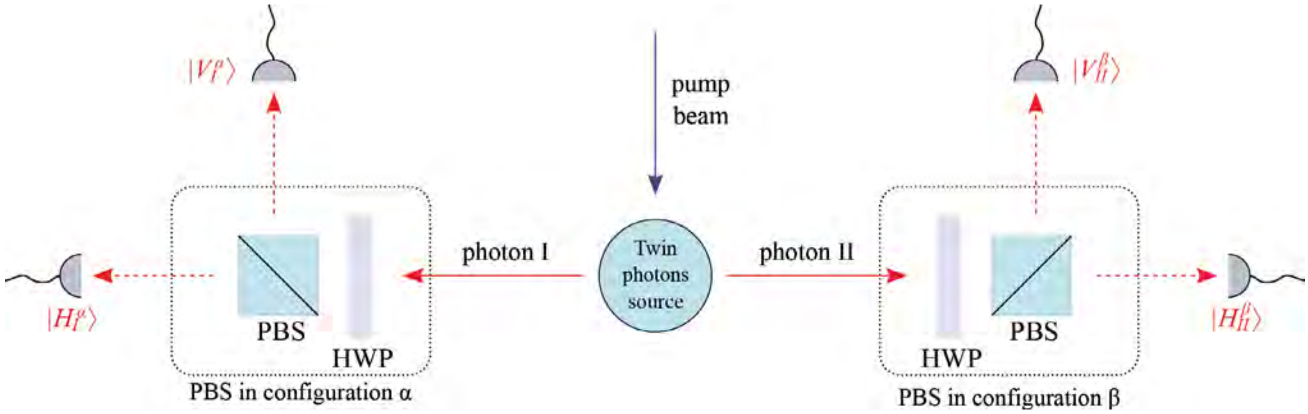

even disturbing!) consequences. Let us recall that the measurement outcomes on photon I are uniformly distributed over states $|V_I^\alpha\rangle$ and $|H_I^\alpha\rangle$, and that this property does not even depend on α. So, when considering the outcome of the first measurement occurring in the setup, one cannot assign any preferred direction to any photon whatsoever. The polarizer settings on both channels can be changed independently until the very last moment. Then, as soon as projection occurred on photon *I*, quantum formalism tells us that the state of photon *II* is also instantaneously projected and known with certainty. There is no need to explicitly perform a measurement on photon *II*: it becomes assigned to a specific state, not defined by a measurement of one of its own features, but via a measurement performed on another particle, *possibly located at the opposite side of the universe*! This instantaneous "spooky action at a distance" disrupts our understanding of "locality".

Figure 1. Classical polarization measurement setup: Each channel is composed of a polarizing beam splitter (PBS) preceded by a half-wave plate (HWP) which allows one to choose the projection basis of the polarization measurements (α and β).

EPR paradox: The completeness of quantum mechanics in question

Entangled states display correlations that seem to involve non-local influence between physically separated, non-interacting systems. This deeply troubled many physicists including Einstein, and led to the famous Einstein-Podolsky-Rosen (EPR) paper published in 1935 [4]. In this article, the authors imagined a similar situation as the one exemplified above in a famous thought experiment ("Gedankenexperiment"). But they also explicitly assumed that such spooky action at a distance was impossible, so that the quantum

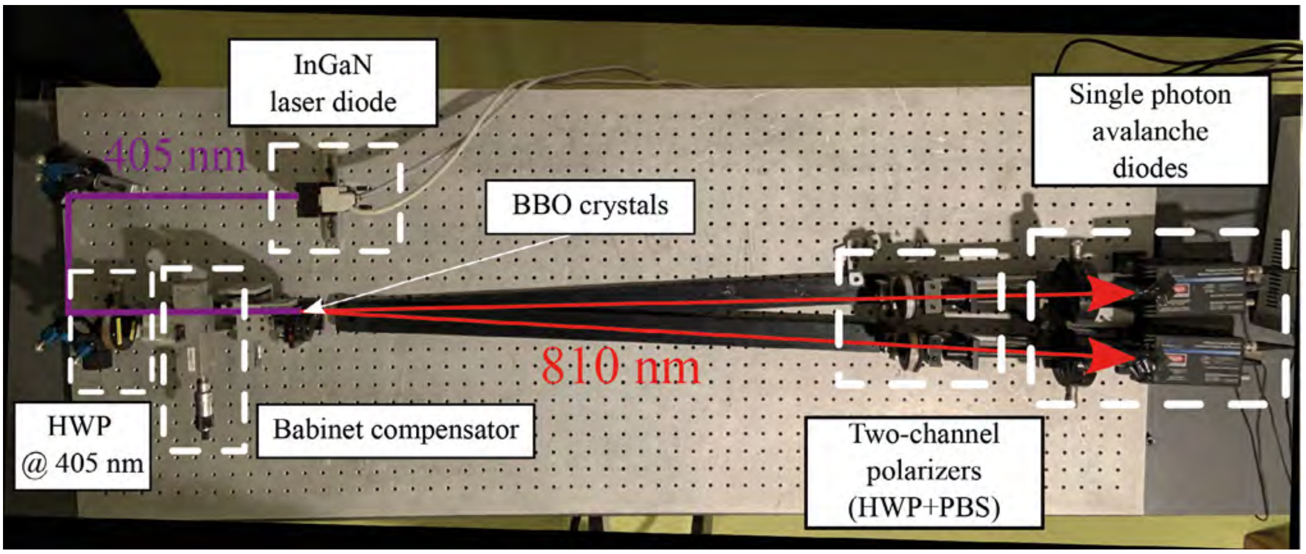

Figure 2. Experimental setup built in the LEnsE in 2005

> It seems that Niels Bohr was deeply troubled by the EPR argument relying precisely on quantum formalism itself to show its incompleteness. He was convinced that if the "EPR" reasoning on reality and locality was correct, all of quantum physics would collapse.

physics description failed at giving an appropriate understanding of the process. Einstein and his partners however believed that another theory, compatible with local reality (so called hidden variable theory or HVT), could explain the correlations of entangled states as predicted by quantum mechanics. This theory was yet to establish. The general idea behind local hidden variable theories is the following. It is assumed that the photon pairs have a new kind of physical property: for instance here, an identical "polarization property", shared by both photons and attributed to them via the pair-generation process, and labeled, say, by θ. Since θ is the same for both photons, it would explain why both photons of any pair are measured along the same direction whatever this direction is. And since it is established *at the source*, it is *local*: the photons carry θ with them at all time. The result of the measurement performed on each channel depends on the value of θ for the photon itself, and not on what happens to the other photon. θ is called a *hidden variable*, in the sense that it does not appear explicitly in the expression of the state, $|\psi_{2ph}\rangle$, in the quantum formalism. This tends to show that the wavefunction somehow "lacks" some of the information on the system. This is why it is said that the EPR paper and the hidden variable theories contradict the completeness of the quantum theory.

It seems that Niels Bohr was deeply troubled by the EPR argument relying precisely on quantum formalism itself to show its incompleteness. He was convinced that if the "EPR" reasoning on reality and locality was correct, the whole quantum physics theory would collapse. Bohr defended the formalism of quantum mechanics by asserting that, for these entangled quantum states of several particles, one could not speak of the individual properties of each of the particles: thus, there are no hidden variables. Entangled particles definitely behave as a single object regardless of their separation distance.

The debate between Bohr and Einstein lasted for more than twenty years until they both died. In fact, Einstein never contested the correctness of quantum physics predictions, but how quantum physics explained these predictions.

Bell's theorem and parameter

But in 1965, surprising breakthrough, the Irish physicist John Bell showed that this debate could be settled experimentally [5]. He showed that if we measure the Bell's parameter, S_{Bell}, as defined before, assuming any local hidden variable hypothesis, its value is less than two.

$$-2 < S_{\text{Bell}} < 2$$

These are the so-called Bell's inequalities. In parallel, quantum physics predicts value of $S_{\text{Bell}} > 2$ for specific choices of α, α', β and β', with a maximal value of $S_{\text{Bell}} = 2\sqrt{2}$. Entangled states are said to violate Bell's inequalities.

Since the two formalisms are not compatible, then who is right? Einstein or Bohr? An experimental test of Bell's inequalities is thus to choose a conflictual set of measurements and to measure what is the value of Bell's parameter, and see if it is compatible or not with a local hidden variable theory.

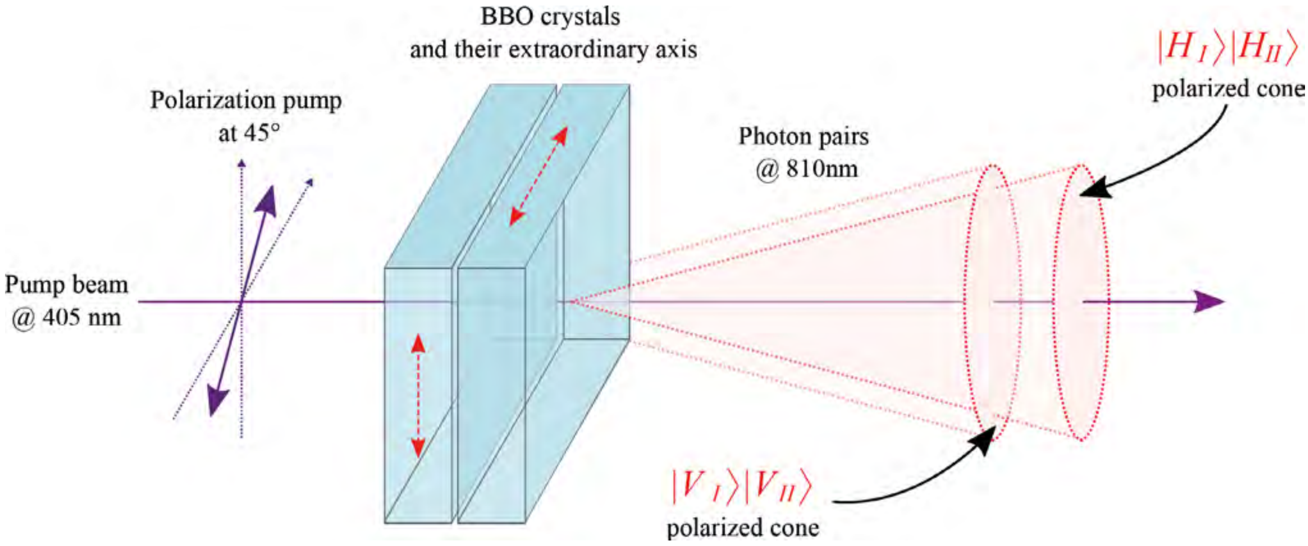

Figure 3. Two-crystal downconversion source: The crystals are 0.5 mm thick and in contact face-to-face, while the pump beam is approximately 1 mm in diameter.

An overview of the labwork setup

This experimental setup was proposed in the early 2000's [2,5]. What limited many experiments a few decades ago was the difficulty to create a bright source of photon pairs. A convenient way to proceed is to use a type I phase matching spontaneous parametric downconversion process in nonlinear crystals, see figures 2 and 3. The pump, a 60mW at 405nm blue InGaN laser diode, gives 810nm entangled photons. We will come back later to the detailed description of the Bell's state preparation. Downconverted photons are collected by two lenses (focal length: 75mm, diameter: 12.5mm) at about one meter from the crystals and focused on single photon counting avalanche photodiodes. Filters at 810nm, 10nm width, are placed just in front of each lens. Polarization is analysed by rotating the half wave plates in front of the polarization beam splitter cubes.

Black plastic tubes prevent from stray light and protect single photon counting modules. For each detected single photon, these modules give a 25ns TTL pulse which is sent to a coincidence detector to ensure that the coincidences are measured between photons of the same downconverted pair. In our experiment, for single detection rates of about 23000 on each side, we detect a coincidence rate of about 1600 (that is 1600 pairs of photons persecond).

Bell state preparation

The key of the setup is the preparation of a pure entangled state, one that will make sure that we can discriminate between hidden variable theories and quantum mechanics. We shall create photon pairs through a process that will indistinguishably generate either $|H_I\rangle|H_{II}\rangle$ or $|V_I\rangle|V_{II}\rangle$ in a superposition state (and not in a statistical mixture).

To produce polarization entangled pairs of photons, we use two identical thin crystals, rotated by 90° from each other about the pump beam direction (see figure 3). For a vertically polarized pump, the down-conversion process generates pairs of horizontally polarized photons in the first crystal; the second crystal has no more effect. For a horizontally polarized pump, the first crystal has no effect; the down-conversion process generates pairs of vertically polarized photons in the second crystal.

$$|V_{pump}\rangle \rightarrow e^{i\varphi H}|H_I\rangle|H_{II}\rangle$$
$$\text{and } |H_{pump}\rangle \rightarrow e^{i\varphi V}|V_I\rangle|V_{II}\rangle$$

For a rectilinearly polarised pump at 45°, the pump photons state is written as:

$$|\psi_{pump}\rangle = \frac{1}{\sqrt{2}}\left(|V_{pump}\rangle + |H_{pump}\rangle\right)$$

In this configuration, 45° polarized pump photons can down-convert in either crystal. **But it is absolutely impossible to know in which crystal the photon pairs were created!** By erasing this "which crystal information", we ensure that the photon pairs are in the superposition state:

$$|\psi_{2ph}\rangle = \frac{1}{\sqrt{2}}\left(|V_I\rangle|V_{II}\rangle + e^{i\varphi_0}|H_I\rangle|H_{II}\rangle\right)$$

Where φ_0 is a phase which depends on many different parameters (wavelengths of pump and down-converted photons, for example), and is a direct consequence of the birefringence of the crystals.

In practice, to get a pure Bell's state, we pre-compensate this phase by placing a Babinet compensator in front of the pair of crystals. The role of the Babinet compensator is to introduce a relative phase between $|H_{pump}\rangle$ and $|V_{pump}\rangle$:

$$|\psi^{Babinet}_{Pump}\rangle = \frac{1}{\sqrt{2}}\left(|V_{pump}\rangle - e^{-i\varphi_0}|H_{pump}\rangle\right),$$

The measurement of a Bell parameter is now routinely used with various quantum systems, in order to evaluate their performances in the context of quantum technologies.

leading to a pure Bell's state :

$$|\psi_{EPR}\rangle = \frac{1}{\sqrt{2}}\left(|V_I\rangle|V_{II}\rangle + |H_I\rangle|H_{II}\rangle\right),$$

For this state, the joint probability of detection in the $\langle V_I^{45°}|\langle V_{II}^{45°}|$ configuration reaches a maximum. The Babinet compensator is adjusted while monitoring the coincidence rate until it reaches an optimum for $\alpha = \beta = 45°$.

Results

The Bell parameter is measured by using a configuration of the four measurement basis that maximizes the deviation between local hidden variable theories and quantum mechanics. It is given by the angles $\alpha = 0°$, $\beta = 22.5°$, $\alpha' = 45°$, $\beta' = 45°$.
In our experiment, we obtain $S_{bell}(\alpha, \alpha', \beta, \beta') = 2.48$ with a standard deviation $\sigma = 3.10^{-3}$. The result shows that we do not reach an ideal entanglement quality ($S_{bell} = 2\sqrt{2}$), but it clearly and unambiguously disagrees with any hidden variable local theory.

Conclusion

Since the eighties, the EPR paradox is no longer a "Gedankenexperiment". Now, it has become a very exciting labwork for students. It also has recently taken another dimension: the measurement of a Bell parameter is now routinely used with various quantum systems, in order to evaluate their performances in the context of quantum technologies.
This labwork therefore now echoes with other ambitions aiming at building more advanced experimental training platforms for the second quantum revolution. Talking about indistinguishability, the Lense has been proposing for now more than 8 years a labwork dedicated to the Hong-Ou-Mandel effect, a two-particle interference experiment allowing to quantify the indistinguishability of photons generated by a similar downconversion process. Another setup under construction will be dedicated to the study of nitrogen vacancy centres in diamond, and their behaviour as single photon sources.

REFERENCES

[1] A. Aspect, "Bell's Theorem: The Naive View of an Experimentalist," Quantum [Un] speakables, 119–153 (2002). https://doi.org/10.1007/978-3-662-05032-3_9.

[2] D. Dehlinger, M. W. Mitchell, Am. J. Phys. **70**, 903–910 (2002). https://doi.org/10.1119/1.1498860.

[3] C. Fabre, Photoniques **107**, 55-58 (2021) https://doi.org/10.1051/photon/202010755

[4] A. Einstein, B. Podolsky, N. Rosen, Phys. Rev. **47**, 777–780 (1935). https://doi.org/10.1103/PhysRev.47.777.

[5] J. S. Bell, Phys. Phys. Fiz. **1**, 195–200 (1964). https://doi.org/10.1103/PhysicsPhysiqueFizika.1.195.

[6] D. Dehlinger, M. Mitchell, Am. J. Phys. **70**, 898–902 (2002). https://doi.org/10.1119/1.1498859.

SURFACE PLASMON PROPAGATION IMAGING BY A PHOTON SCANNING TUNNELING MICROSCOPE

F. DE FORNEL[1,*], P. DAWSON[2], L. SALOMON[1], B. CLUZEL[1]
[1] Laboratoire Interdisciplinaire Carnot de Bourgogne, Université de Bourgogne, 9 Avenue Alain Savary, 21078 Dijon, France
[2] Centre for Nanostructured Media, School of Mathematics and Physics, Queen's University, Belfast, BT7 1NN, UK
***ffornel@u-bourgogne.fr**

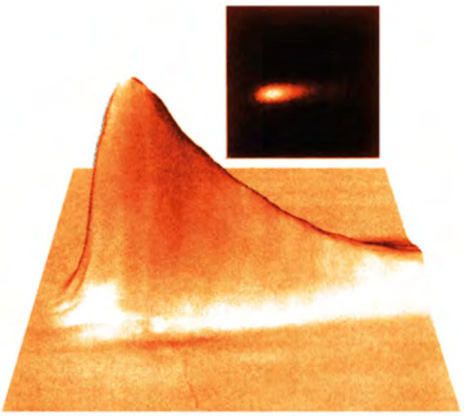

This paper describes the first direct observation of surface plasmon propagation on a metallic thin film deposited on a glass slide, thus facilitating the first direct measurement of the propagation length. This was achieved using photon scanning tunneling microscopy (PSTM). Subsequently, near-field observations of the surface plasmon buried at the metal-glass interface, generated from a discontinuity in the metallic thin film, were reported.

https://doi.org/10.1051/photon/202111332

In the 1990's, near-field optical microscopies took off promising to become a unique tool for exploring optical phenomena at the nanoscale. At that time, the photon scanning tunneling microscope (PSTM) [1,2] which was the analog for photons of the electronic scanning tunneling microscope (STM) demonstrated these capabilities. Using this technique, it became possible to measure the optical near field in the vicinity of subwavelength structures illuminated under various conditions. Among them, the PSTM has proven to be a powerful tool for the study and the analysis of surface plasmons which are resonant electromagnetic modes associated with the collective oscillation of an electron plasma at the interface between a metal and a dielectric [3]. Indeed, for a thin film of silver deposited on glass, the metal-air surface plasmon excited in Kretschmann configuration [4] has an extension in air of a few hundred nanometers in the visible range, making it an ideal candidate for optical near-field measurement with a PSTM. In the seminal paper of Dawson et al [5], the propagation of a surface plasmon was shown for the first time and its damping was directly quantified by viewing its propagation length. These results were further completed by the demonstration of the contribution of a buried metal-glass plasmon in the near- field pictures thanks to successive improvement in near-field measurement techniques.

DIRECT OBSERVATION OF THE METAL-AIR SURFACE PLASMON

Figure 1 shows the schematic of the seminal experiment performed at the University of Bourgogne. A 50 nm thin silver film was illuminated by two Helium:Neon lasers in oblique incidence. A first, green one at λ_1=543,5nm was unfocussed to yield a spot size on mm^2 scale on the silver film while the second one at λ_2 = 632.8 nm was tightly focused into a ~10 µm diameter spot at the silver film. The angle of incidence of the red beam was chosen so that it excited the silver-air surface plasmon by phase matching the parallel (to the sample interface) component of wavevector of the incident light to that of the surface plasmon. In plasmonics this phase matching technique is well known as the Kretschmann configuration [4]. The angle of incidence of the green laser was likewise chosen to excite ● ● ●

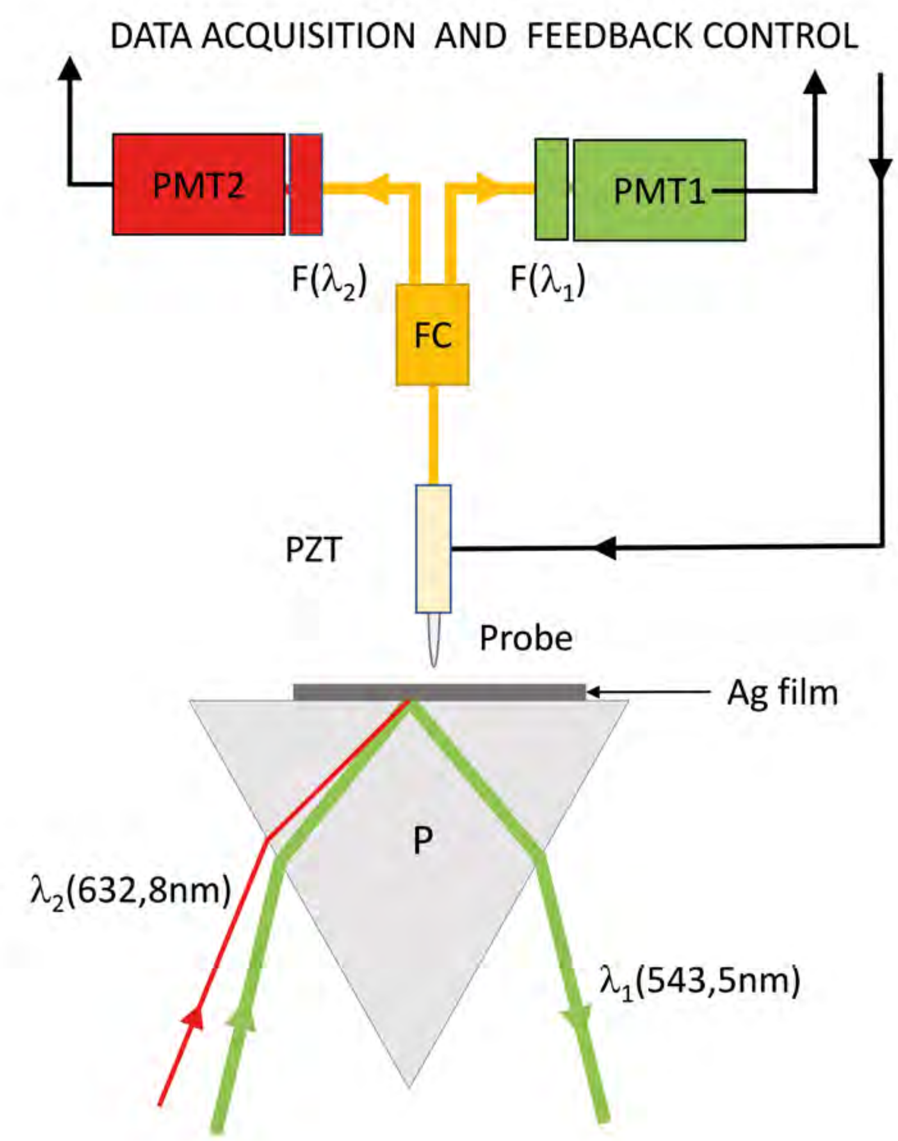

Figure 1. Schematic of the experiment: a silver film evaporated on a glass prism was illuminated by two lasers. The green one acts as a pilot for scanning a tapered optical fiber in the near-field of the silver film while the red one excites the silver-air surface plasmon in Kretschmann configuration.

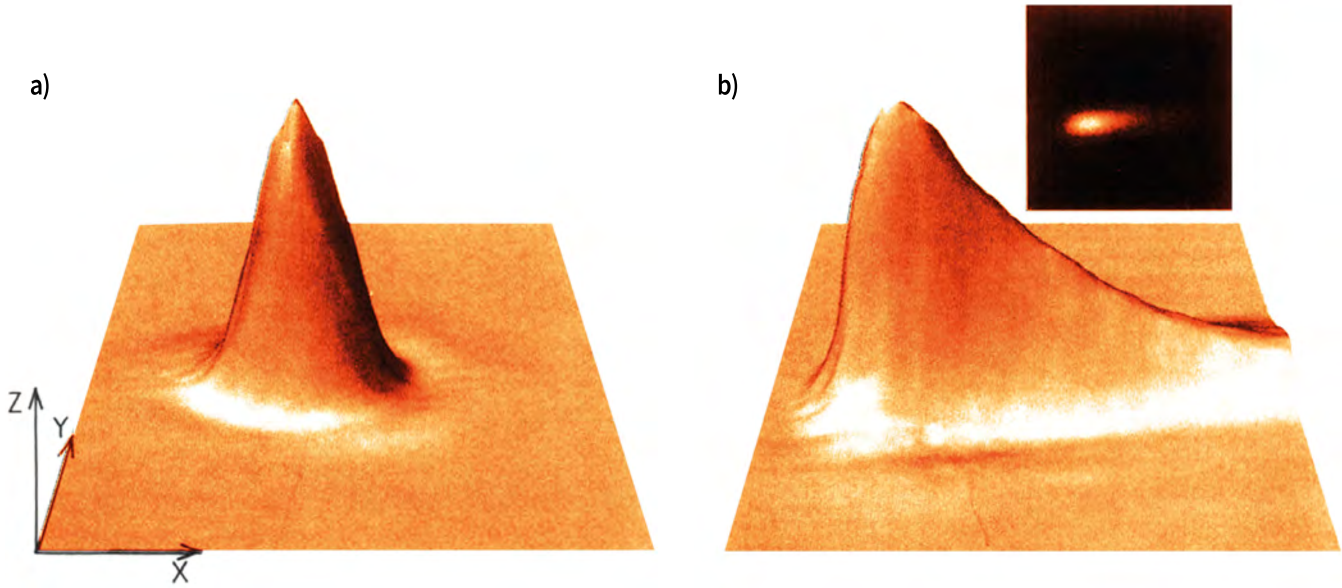

Figure 2. a) PSTM image of the optical near field intensity of the incident beam, λ_1 = 543.5 nm, on a simple prism illuminated under total internal reflection. b) PSTM image recorded at λ_2 = 632.8 nm at the surface plasmon excitation angle for red light on a section of the same prism covered by a 50nm thin silver film. The right side of the image displays a clear exponentially decaying tail explicitly demonstrating the propagation and damping of the surface plasmon. All images are 40 µm x 40 µm.

surface plasmons at the silver-air interface at that wavelength. An optical probe, obtained by tapering an optical fiber, was brought into the optical near field of the metal film in order to 'collect the surface waves' (i.e. by scattering the surface-bound optical field of the surface plasmons to photons travelling up the tapered optical fiber) while scanning the metal film with help of a home-made stack of piezoelectric tubes.

In this configuration, the near-field probe simultaneously detects signals coming from the two lasers at 632.8 nm and 543.5 nm. A fiber optic coupler then separates the signal in two arms. On one arm, a spectral filter selected the green laser which acts as a pilot for driving a feed-back loop allowing the probe to scan the surface without touching it. For this reason, the green laser spot is large (mm scale) in order to generate a surface intensity distribution on the topside of the silver film that is (near-) constant on the ~10µm scale of the surface plasmon propagation length. The green signal is used as the input signal for the feedback loop of the piezoelectric scanners to allow for scanning the silver film at a constant height. On the second arm, the red laser exciting the surface plasmon is filtered out and then sent to a photomultiplier while the

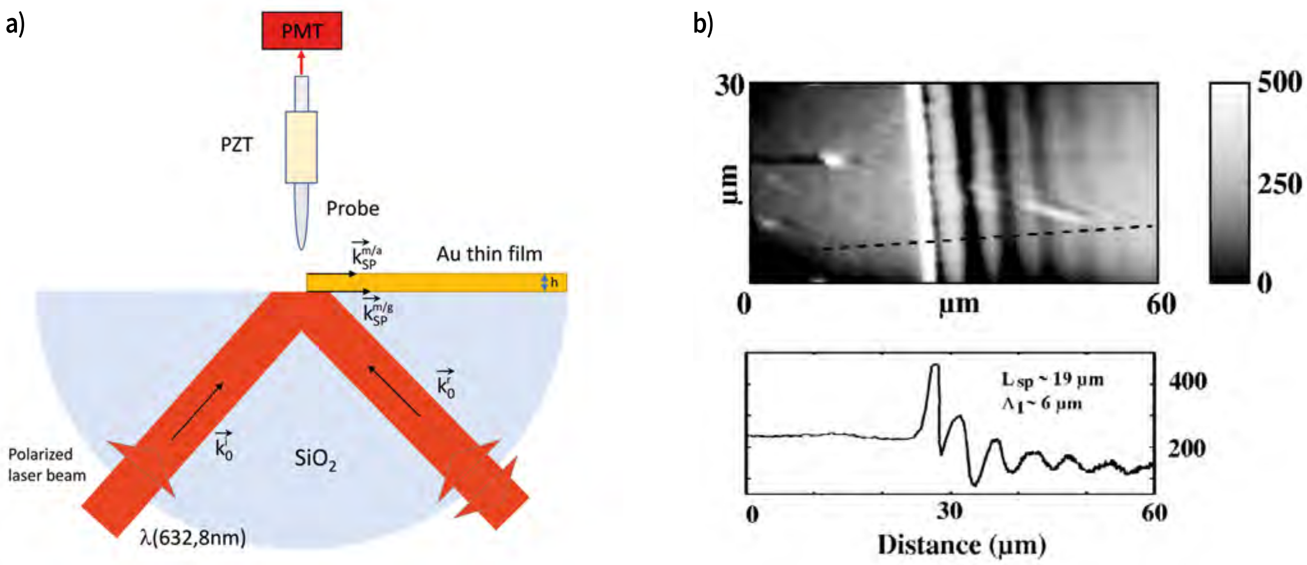

Figure 3. a) Scheme of the experiment. A semi-infinite thin gold film of thickness h=55 nm is vacuum deposited onto a glass prism. The illumination is carried out at various incident angles θ, by a collimated laser beam preliminary linearly polarized. The optical signal is collected via the probe and a photomultiplier tube (PMT). b) PSTM image operating in a constant intensity mode for an angle of incidence of 52°

This was the first direct observation of the propagation of a surface plasmon on top of a metal film by near- field imaging paving the way to many other achievements and realizations in this field and development of commercial near-field microscopes for studying the optical near-field at nanoscale.

probe is scanning the surface. At 632.8 nm, the typical images reported in [5] are displayed in Fig. 2. It shows the original near-field pictures obtained in the same conditions on a section of the glass slide without the silver film (Fig.2a) and with the silver film (Fig.2b). Without the silver film, the measured laser spot is approximately circular with a ~ 10 µm diameter, while with the silver film the right side of the imaged spot appears elongated with an exponential decay directly mapping the surface plasmon excitation, propagation and attenuation.

From the image of Fig. 2b) the propagation length was measured to be 13.6µm, which is less than that predicted for a thin silver film of this thickness. The difference was attributed to re-radiation of the surface plasmon back into the prism as it propagates, contamination of the silver surface with a thin, optically ●●●

SURFACE PLASMON POLARITON

A surface plasmon polariton (SPP) is an electromagnetic excitation that propagates in a wave like fashion along the planar interface between a metal and a dielectric medium. Thus, a SPP is a surface electromagnetic wave, whose electromagnetic field is confined to the near vicinity and whose amplitude decays exponentially with increasing distance into each medium from the interface of the dielectric–metal interface. For a film deposited on glass, plasmons at each interface can exist.

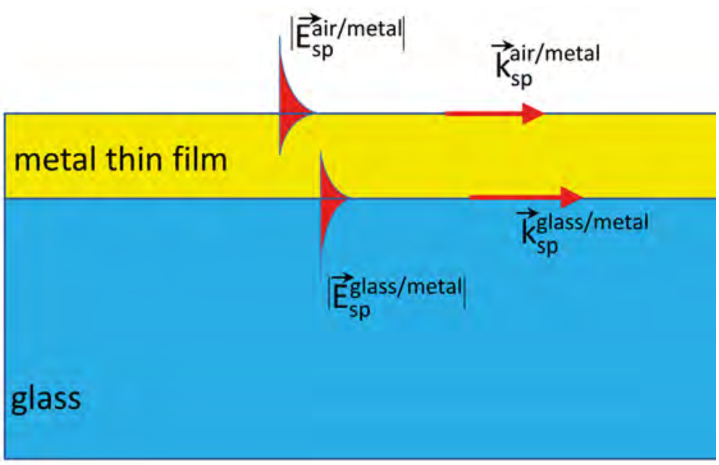

dissipative silver sulphide layer and a possible angular shift between the theoretical and actual angle of incidence. This was the first direct observation of the propagation of a surface plasmon on top of a metal film by near- field imaging paving the way to many other achievements and realizations in this field and the development of commercial near-field microscopes for studying the optical near-field at nanoscale.

However a metallic thin film has two interfaces and further studies were then conducted to explore the surface plasmon buried at the metal-glass interface, which is not excited in Kretschmann configuration.

BURIED SURFACE PLASMON OBSERVATION

In this second experiment, a semi-infinite metallic film was deposited on glass prism as shown in Fig. 3. It is noteworthy that here, gold was preferred to silver to avoid sulfurization. Under collimated illumination, the edge of the metal film scatters the incident laser and generates both the metal-air and the metal-glass surface plasmons.

First measurements in this configuration were reported in [6] which was employing the same laser for exciting surface plasmons as well as for driving the piezoelectronic scanners through a feedback loop. In this configuration, the height of the probe during the scan was modulated by the detected light intensity. Recorded near-field images showed both an exponential decay related to the propagation and damping of the gold:air surface plasmon and but also the presence of oscillations whose period corresponds to an interference between the incident light and the gold:air plasmon. These results were in very good agreement with numerical simulations. However, these latter also predicted that interferences between the glass-to-metal plasmon and the incident beam should also be visible in the measurements but was not observed experimentally. This was finally achieved by Brissinger *et al.* [7] many years after, benefiting from a shear-force feedback for driving the near-field probe with an improved reliability.

At that point, the angle of incidence was tuned from 30° to 60° and both surface plasmons were finally visible in the near-field images. Interferences were in very good agreement with numerical predictions. It should be noted that the wavector of the buried surface plasmon, that of the metal: glass interface, was recovered experimentally (1.63±0.08) ω/c quantitatively compared to its theoretical value of 1.59ω/c.

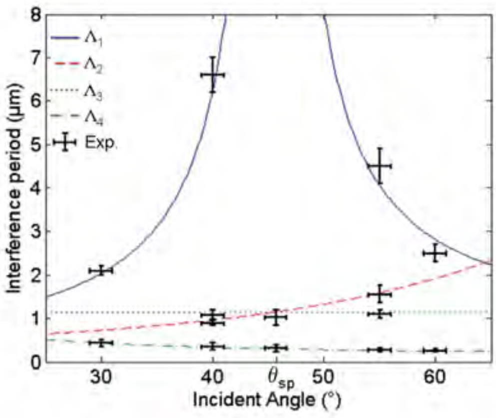

Figure 4. IInterference periods Λ_i in near-field images obtained in the experiment described in Fig.3a by varying the angle of incidence. Λ_1 and Λ_2 are associated with the interferences of the incident wave and the plasmonic waves, respectively at the m/a and the m/g interfaces. Λ_3 is associated with the interferences between both surface plasmon waves and Λ_4 between the incident wave and the back reflection at the prism/air interface. The solid and dotted lines are the values from the numerical simulations and the crosses are recovered from the near-field optical images.

If the photon scanning tunneling microscope in constant optical intensity mode is no longer used, it has nevertheless allowed the direct and first imaging of the surface plasmon excited at oblique incidence in Kretschmann configuration.

CONCLUSION

If the photon scanning tunneling microscope in constant optical intensity mode is no longer used, it has nevertheless allowed the direct and first imaging of the surface plasmon excited at oblique incidence in Kretschmann configuration As such these experiments have paved the way to the emergence of plasmonics as an entire field of research which has enabled applications in optoelectronics, medicine, chemistry, or sensing to cite just a few. In addition, current improvements in the stability of feedback loops, piezoelectric scanners, nanotechnologies used for shaping near-field probes, as well as recent developments in laser technologies have allowed the near-field microscope to move beyond the walls of the laboratory and to become a standard imaging tool for materials science.

REFERENCES

[1] R.C. Reddic, R.J. Warmack, T.Ferrel, Phys. Rev. B **39**,767-770 (1989)

[2] D. Courjon., K. Saraeyeddine ., M. Spajer, Opt. Commun. **71**, 23 (1989)

[3] A. Zayats, I. Smolyaninov , A. Maradudin, Phys. Rep. **408**, 131 – 314 (2005)

[4] E. Krestschman, H. Rather, Z. Naturforsch, **A23**, 2135 (1968)

[5] P. Dawson et al, Phys. Rev. Lett. **72**, 2927 (1994)

[6] L. Salomon et al., Phys. Rev B **65**, 125409 (2002)

[7] D. Brissinger et al, Opt. Express **19**, 17750 (2011)

COMPLETE SOLUTIONS FOR QUANTUM APPLICATIONS

Menlo Systems' optical frequency combs and ultra-stable lasers enable the second quantum revolution

Quantum technology lets us exploit the laws of quantum mechanics for tasks like communication, computation, simulation, or sensing and metrology. As the second quantum revolution is ongoing, we expect to see the first novel quantum devices replace classical devices due to their superior performance.

There is a strong impetus to transform quantum technologies from fundamental research into a broadly accessible standard. Quantum communication promises a future with absolute security through quantum key distribution; quantum simulators and computers can perform calculations in seconds where the world's most powerful supercomputers would require decades; quantum technologies enable advanced medical imaging techniques. Further applications will likely arise that we cannot anticipate yet. The global market has realized the huge potential of quantum technologies. Menlo Systems, a pioneer in the field, provides commercial solutions for these novel challenges.

The link between photonics and quantum physics is obvious. Quantum simulation and computation use cold atoms and ions as qubits, labs worldwide use optical frequency combs and ultra-stable lasers in these types of experiments. Quantum communication often relies on single photons, which are generated with precisely synchronized femtosecond laser pulses in the near-infrared (-IR) spectral range. Quantum sensing and metrology require the highest stability and accuracy in frequency comb and laser technology. And – an application worth highlighting – optical atomic clocks are under way to replace the current definition of the second in the International System of Units (SI).

The transition frequency in optical clocks is on the order of hundreds of terahertz, corresponding to the visible or the ultraviolet region of the electromagnetic spectrum. Counting these optical frequencies is only possible using a frequency comb [1], a mode-locked laser with evenly spaced frequency modes within its optical spectrum. When referenced to a CW laser which is stabilized to a high-finesse optical cavity, the bandwidth of the comb lines narrows down to below 1 Hertz [2], corresponding to a stability of 10^{-15} or better. The newest generation of optical atomic clocks enabled by this technology reach an accuracy of 10^{-18} [3], two orders of magnitude higher than the best cesium atomic clock.

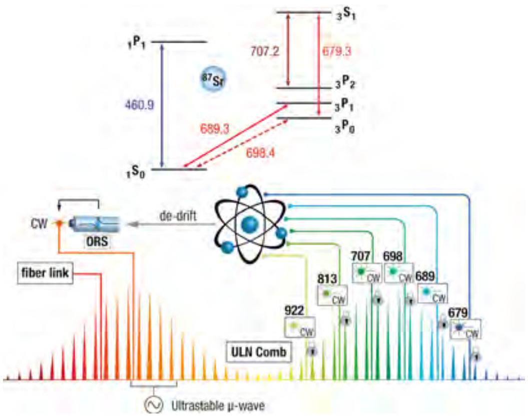

Figure: The hyperfine transitions in strontium (Sr) atoms with the ultra-narrow clock transition at 698.4 nm (upper part). A commercial FC1500-Quantum system for optical clock applications contains an ultra-stable laser transferring its spectral purity onto an optical frequency comb and all other lasers which are also locked to the comb (lower part).

Menlo Systems' FC1500-Quantum is a complete CW laser system with an ultra-stable frequency comb. It provides several CW lasers for atom cooling, repumping, and addressing the sub-Hertz linewidth clock transition in atoms or ions used in optical clocks (see figure). The low phase noise obtained on the comb-disciplined CW lasers is essential for coherent gate manipulation in many atom optical quantum computing schemes and for fast and high-fidelity gate operations. The laser light is delivered *via* optical fiber to the "physics package" consisting of vacuum chamber with all the necessary optics and electronics components and the atoms. Labs no longer need to undergo the time consuming process of designing and building their own ultra-stable lasers. Eventually, the comb itself has two purposes: It acts as reference for all the lasers to maintain their narrow linewidth, and it is the clockwork that transfers the optical frequency's spectral purity to the microwave region, or to a different optical frequency [4].

CONTACT:

Menlo Systems GmbH
Bunsenstraße 5
82152 Martinsried, Germany
Phone: +49 89 189166 0
Fax: +49 89 189166 111
sales@menlosystems.com
www.menlosystems.com

REFERENCES

[1] J. Reichert *et al.*, Opt. Commun. **172**, 59 (1999)

[2] R. W. P. Drever *et al.*, Appl. Phys. B. **31**, 97 (1983)

[3] E. Oelker *et al.*, Nat. Photonics **13**, 714 (2019)

[4] M. Giunta *et al.*, Nat. Photonics **14**, 44 (2020)

INTERFEROMETRY WITH OPTICAL FREQUENCY COMBS

Nathalie PICQUÉ[1,*], Theodor W. HÄNSCH[1,2]
[1]Max-Planck Institute of Quantum Optics, Garching, Germany
[2]Ludwig-Maximilian University of Munich, Faculty of Physics, Munich, Germany
***nathalie.picque@mpq.mpg.de**

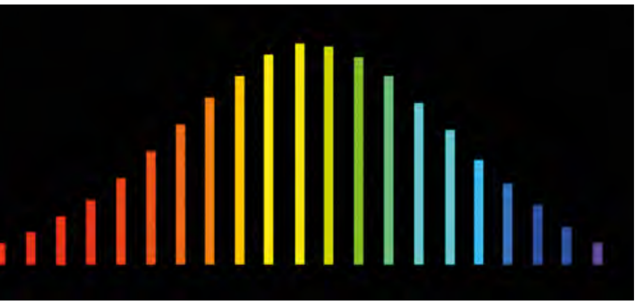

https://doi.org/10.1051/photon/202111338

A frequency comb, a spectrum of equidistant phase-coherent laser lines, can be harnessed for new approaches to interferometry. The dual-comb interferometer exploits the time-domain interference between two combs of slightly different line spacing. The instrument, which performs direct frequency measurements over a broad spectral bandwidth, opens up new perspectives in applications such as spectroscopy, distance metrology or holography.

A frequency comb [1] is a spectrum of narrow evenly spaced laser lines, whose absolute frequency can be known within the accuracy of an atomic clock (Insert 1). Initially invented for precision frequency metrology in the simple hydrogen atom, frequency combs have become key to a variety of applications, from the generation of attosecond pulses to the calibration of astronomical spectrographs. They are enabling ground-breaking approaches to interferometry with applications as diverse as spectroscopy [2], distance metrology [3], or holography [4]. This short article recounts the principle and applications of frequency comb interferometry.

FREQUENCY COMBS AND INTERFEROMETRY

Early on, frequency combs have been coupled to known interferometers. For example, if a frequency comb is used as a light source before a scanning Michelson interferometer, Fourier transform spectroscopy sees its measurement speed, sensitivity precision and accuracy dramatically improved. Distance measurements using a spectrally-dispersed static Michelson interferometer -or a scanning Michelson interferometer- benefits from the many comb lines for improved precision and large ambiguity range. A comb of narrow line spacing can be frequency filtered in a Fabry interferometer, of matching but larger free spectral range, to generate a comb of large repetition frequency, suited to the calibration of astronomical spectrographs. The Fabry-Pérot resonator can also be used as an enhancement cavity, for extreme-ultraviolet high-harmonic generation or for absorption spectroscopy with long absorption paths.

DUAL-COMB INTERFEROMETERS

More interestingly, frequency combs have enabled a new class of interferometers, called dual-comb interferometers. Two frequency comb generators emit trains of pulses at slightly different repetition frequencies, f_{rep} and $f_{rep}+\Delta f_{rep}$, respectively. The two beams of the two combs are combined on a beam splitter and their interference is measured on a fast photodetector as a function of time. In the time domain (Fig.1a), the pulses from one laser walk through the pulses from the second laser, with a time separation that automatically increments from pulse pair to pulse pair by an amount $\Delta f_{rep}/ f_{rep}^2$ (e.g. 10^{-14} s). This way, optical delays from 0 to $1/f_{rep}$ are repetitively scanned without moving parts. Akin to a sampling oscilloscope, the periodic optical waveforms are stretched in time by a factor $f_{rep}/\Delta f_{rep}$ (e.g. 10^6), and they can be electronically recorded and digitally processed. In the frequency domain (Fig.1b), pairs of optical comb lines, one from each comb, produce radio-frequency beat notes on the detector, forming a frequency comb of line spacing Δf_{rep} in the radio frequency domain. Optical frequencies $nf_{rep}+f_0$ are thus down-converted into radio frequencies $n\Delta f_{rep}+\Delta f_0$.

The principle of dual-comb interferometry may be reminiscent of that of asynchronous optical sampling. A significant difference, though, is that mutual coherence between the two combs is required for an interferometric measurement. As a rule of thumb, many applications require a relative stability on the order of λ/100 to achieve high fringe contrast. At a wavelength of 1 µm, this means that the timing jitter between pairs of pulses must be kept smaller than 30 as. Learning how to control and minimize the relative timing and phase fluctuations between two frequency comb generators has been at the center of significant efforts in the early days of dual-comb interferometry. A number of solutions, of various complexity and performance, now enable to experimentally maintain mutual coherence and/or to compensate for the (residual) fluctuations through analog or digital processing. Experimentally, coherent averaging over more than half an hour has become feasible, illustrating the degree of control achieved for a dual-comb system.

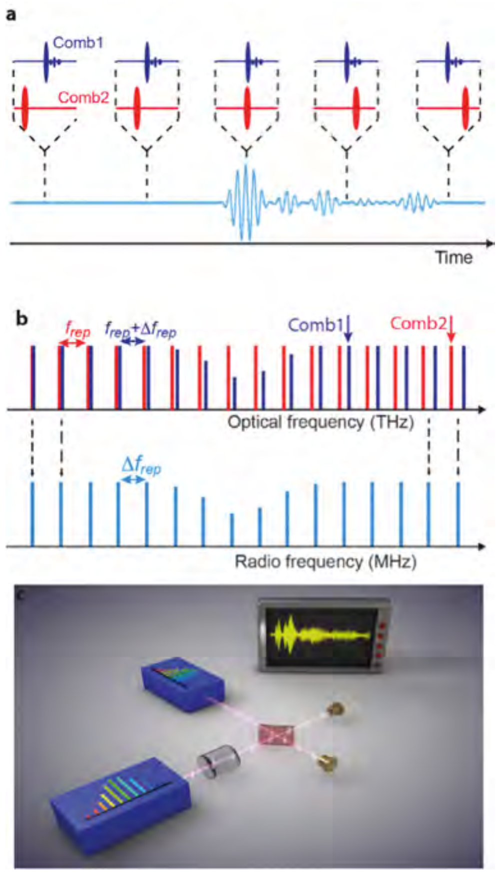

Figure 1. a. Time-domain principle of dual-comb interferometry (in the situation where an absorbing sample is in the beam path of comb 1). **b.** Frequency-domain principle **c.** Sketch of a typical dual-comb spectrometer. **c.**: Adapted from "Mid-IR Spectroscopic Sensing," Optics & Photonics News **30(6)**, 26-33 (2019). https://doi.org/10.1364/OPN.30.6.000026

FREQUENCY COMB

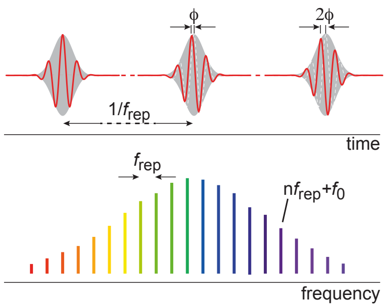

A frequency comb, a spectrum of equidistant phase-coherent spectral lines, is commonly generated by a mode-locked laser. Such a laser emits a periodic train of pulses at a frequency f_{rep}. The periodicity applies not only to the pulse envelopes, but to the whole electric field of the pulses, including their optical phase, apart from a reproducible slip ϕ of the phase of the electromagnetic carrier-wave relative to the pulse envelope from pulse to pulse. Such phase slips occur in a laser owing to dispersion in the cavity. As a consequence, the frequency f_n of a comb line writes: $f_n = n\, f_{rep} + f_0$ where n is an integer and $f_0 = f_{rep}\,\phi / 2\pi$ is the carrier-envelope offset frequency. Both f_{rep} and f_0 can be measured and controlled against an atomic clock. Therefore, frequency combs act like rulers in frequency space that can for instance be used to measure a large separation between two different optical frequencies in terms of the countable signal of the pulse repetition frequency. Frequency combs can conveniently link optical and microwave frequencies and enable absolute measurements of any frequency. Frequency combs have revolutionized the way the frequency of light is measured and are now common equipment in all frequency metrology-oriented laboratories. They have paved the way for the creation of all-optical clocks with a precision that approaches the 10^{-18} level.

Owing to the absence of moving parts, one of the first features of dual-comb interferometers that attracted interest has been the ability to perform fast measurements. Moreover, the sensitivity is further enhanced. is further enhanced by the use of coherent light sources. Remarkably, a dual-comb interferometer can simulate a mirror moving at 10 km.s^{-1}, the escape velocity from earth. The beat notes between pairs of comb lines are mapped in the radio-frequency domain where the 1/f noise in the detector signal can be greatly reduced, and a million-fold improvement in the acquisition speed of a spectrum has been demonstrated. Furthermore, all the spectral elements are simultaneously measured on a single photodetector, like in other interferential spectrometers. This multiplexed recording grants excellent overall consistency of the spectral measurements and applicability in any spectral regions. As research progressed, other distinguishing assets have been highlighted, offering interferometry a unique and novel host of powerful features, which are summarized below for the key applications.

DUAL-COMB SPECTROSCOPY

The main application of dual-comb interferometers has been spectroscopy over broad spectral bandwidths, in particular of molecules [2]. Dual-comb spectroscopy is a new form of Fourier transform spectroscopy, which has been over the past 50 years the overriding tool in molecular spectroscopy and analytical chemistry. If a sample is present on the beam path of one of the combs (Fig.1c), the interference signal will record the signature of the absorption and dispersion experienced by the sample. The dual-comb spectrometer mimics a scanning Michelson interferometer by sampling the free-induction of the molecules over the range of optical delays. One uses then a harmonic-analysis tool, the Fourier transformation, to get the spectrum. In a single recording, the spectrum is sampled by the discrete comb lines and therefore the spectral resolution is limited to the comb line spacing f_{rep}. As most combs can be precisely controlled, it is however possible to measure a sequence of spectra with different comb-line positions and to interleave the spectra a posteriori to reach a resolution ultimately limited by the width of the optical comb lines. Initially developed in the near-infrared spectral region, where frequency comb generators are conveniently available, dual-comb spectroscopy is now efficient in the mid-infrared spectral region at wavelengths as long as 5 µm (Fig. 2). It is emerging at longer wavelengths in the mid-infrared and THz ranges and at shorter wavelengths in the visible range. The ultraviolet domain is still mostly unexplored, due to outstanding instrumental challenges for generating low-noise frequency combs of a broad span and implementing ultra-stable interferometers at short-wavelengths.

To broadband spectroscopy, dual-comb interferometers add the remarkable features of the interrogation of the sample by laser lines of narrow width which provides a negligible contribution of the instrumental line-shape, as well as the calibration of the frequency scale within the accuracy of an atomic clock. These features are not available from any dual-comb interferometers though. They derive from the use of frequency combs of narrow and stable optical lines, referenced to a radio-frequency clock or to an ultra-stable optical frequency standard. Initially, it was not clear which light sources should be used and a variety of comb generators have been tested, from the metrology-grade fiber mode-locked lasers stabilized to accurate optical references to simple electro-optic modulators or quantum cascade lasers that are free-running. Over the years, the fiber-laser technology has considerably evolved towards ease of use, compactness, low noise and ultra-high stability. Fiber laser have become the most suited tools for realizing the potential of dual-comb interferometry. Free-running frequency combs do not enable to benefit from the above-mentioned advantages, although they might still be valuable tools in some niche applications.

Although linear absorption spectroscopy has been predominantly explored, frequency combs synthesizers based on mode-locked lasers involve intense ultrashort pulses that can generate nonlinear phenomena at the sample. Using this, various schemes of nonlinear Raman spectroscopy and imaging and of Doppler-free two-photon excitation spectroscopy [5] have open up new opportunities for nonlinear spectroscopy over broad spans. One can expect that this line of research will develop further in the near future, owing to the progress in high-power laser amplifiers at high repetition frequency. Finally, the system is not limited to two frequency combs and recent proof-of-principle demonstrations explore the intriguing potential of using three combs for multidimensional spectroscopy, such as photon echoes [6].

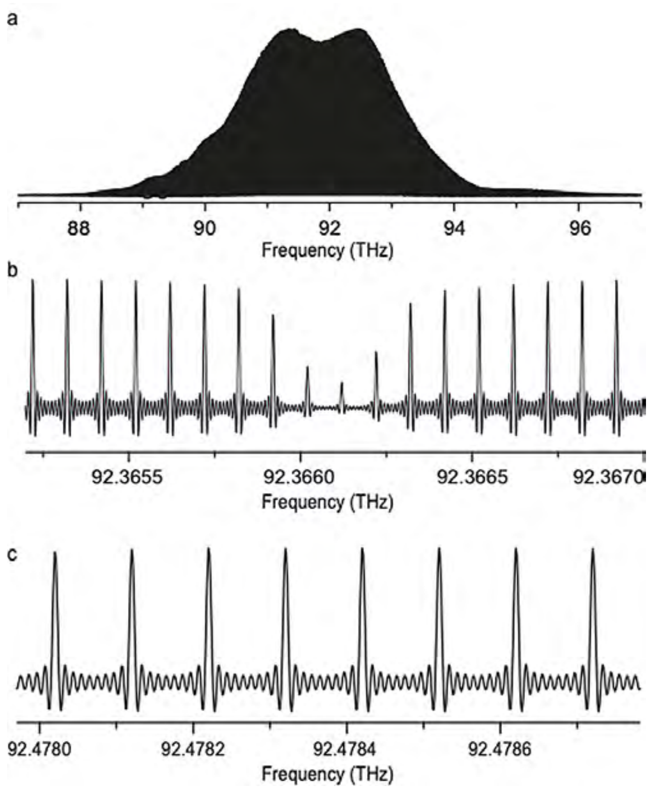

Figure 2. Mid-infrared experimental dual-comb spectrum, shown with different magnifications. **(a.-c.)** 82000 comb lines spaced by 100 MHz, centered at 92 THz (3.2 µm), were measured within 29 minutes. In **b**. an absorption transition of ethylene attenuates the comb lines. Reproduced from "Mid-infrared feed-forward dual-comb spectroscopy," Proc. Natl. Acad. Sci. USA **116**, 34549 (2019). https://doi.org/10.1073/pnas.1819082116

DUAL-COMB RANGING AND HOLOGRAPHY

Another successful application of dual-comb interferometers involves distance measurements and ranging [3]. The dual-comb scheme combines the time-of-flight and interferometric approaches to deliver absolute distance measurements over an extended ambiguity range.

One of the most exciting recent trends, though, has been to replace the single photodetector by a camera sensor. As many spectra as there are detector pixels can be simultaneously measured. Dual-comb interferometers move digital holography • • •

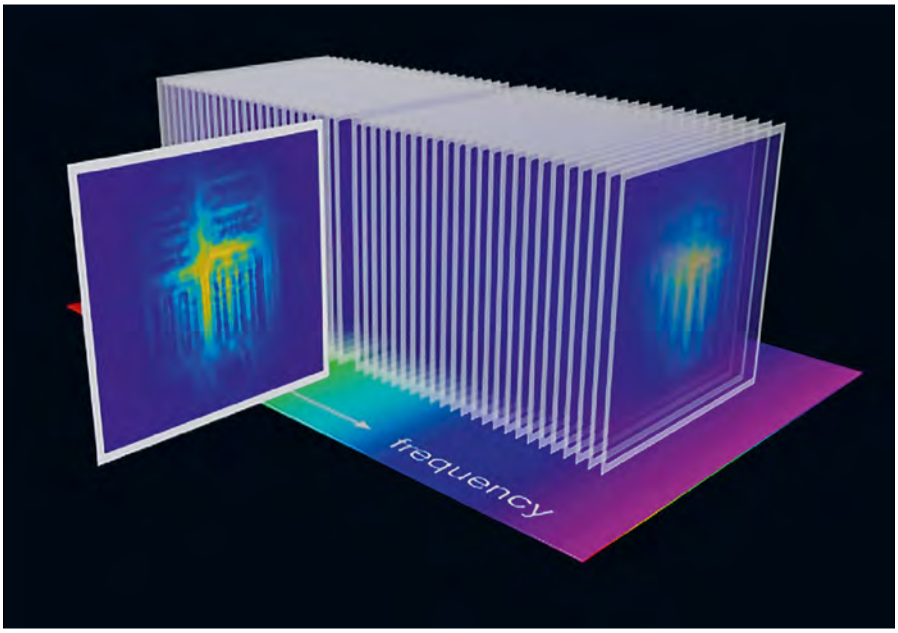

Figure 3: In dual-comb holography, as many holograms as there are comb lines are generated.

forward by recording simultaneously thousands of holograms [4], one per comb line (Fig.3), and they show an intriguing potential for reaching new frontiers in scan-free wavefront reconstruction. By digital processing, each hologram provides a 3-dimensional image of the scene, where the focusing distance can be chosen at will. Combining all these holograms renders the geometrical shape of the 3-dimensional object with very high precision and without ambiguity. At the same time, other diagnostics can be performed by the frequency combs: in the first proof of concept, molecule-selective imaging of a cloud of ammonia vapor was simultaneously demonstrated.

CONCLUSION

Dual-comb interferometry has been developed over the past 15 years and now involves a vibrant research community of more than 200 research groups. The dual-comb interferometer provides a unique combination of broad-spectral-bandwidth, long temporal coherence, absence of moving parts and multi-heterodyne read-out which offers interferometry a revolutionary host of features – frequency multiplexing, resolution, accuracy, precision, speed. Other emerging applications include analog-to-digital conversion, two-way time and frequency transfer, vibrometry, etc.

Excitingly, the technique is still far from realizing its full potential. A remarkable difference with respect to other types of interferometers is that the dual-comb interferometer performs direct time/frequency measurements. With a dispersive or interferential instrument, the resolving power is the ratio of the maximum path difference to the wavelength, hence the bulky instruments for high resolution. With a dual-comb interferometer, it becomes the ratio of the maximum optical retardation to the period of the optical wave. Dual-comb spectroscopy is therefore the only technique that can, for any spans and any spacing, potentially reach a resolution equal to the comb line spacing, freed from geometric limitations and aberrations. This apparently simple but fundamental distinction, first pointed out in [2], has not been exploited yet in experiments that would go significantly beyond the state of the art. On an applied touch, the path is open to integrated chip-scale ultra-miniaturized devices that combine high resolution and broad spectral bandwidth. Using III-V-on-silicon mode-locked lasers in the telecommunication region, an on-chip spectroscopy laboratory for gas sensing is already underway using battery-operated devices of a footprint smaller than 1 mm^2 [7]. The most exciting prospect is nevertheless that of merging frequency metrology and broadband spectroscopy: with Doppler-free dual-comb spectroscopy, the envisioned improvement in accuracy is expected similar to that achieved in the 1990s when going from optical wavelength metrology to frequency measurements. As the technique is able to measure very faint signals, down to the single-photon level, single atoms and molecules may become observable over a broad span with an unmatched precision, opening up new strategies for tests of fundamental physics. ●

REFERENCES

[1] T. Udem, R. Holzwarth, T.W. Hänsch, Nature **416**, 233 (2002)

[2] N. Picqué, T.W. Hänsch, Nat. Photon. **13**, 146 (2019)

[3] I. Coddington, W.C. Swann, L. Nenadovic *et al.* Nat. Photon. **3**, 351 (2009)

[4] E. Vicentini, Z. Wang, K. Van Gasse *et al.* Nat. Photon. **15**, 890 (2021)

[5] S.A. Meek, A. Hipke, G. Guelachvili *et al.* Opt. Lett. **43**, 162 (2018)

[6] J.W. Kim, J. Jeon, T.H. Yoon *et al.*, J. Opt. Soc. Am. B **39**, 934 (2022)

[7] K. Van Gasse, Z. Chen, E. Vicentini, *et al.* preprint at arXiv:2006.15113 (2020)

OPTICAL FREQUENCY COMBS FOR ATOMIC CLOCKS AND CONTINENTAL FREQUENCY DISSEMINATION

Rodolphe LE TARGAT*, Paul-Eric POTTIE, Yann LE COQ
LNE-SYRTE, Observatoire de Paris, Université PSL, CNRS, Sorbonne Université,
61 Avenue de l'Observatoire, F-75014, Paris, France
***Rodolphe.LeTargat@obspm.fr**

https://doi.org/10.1051/photon/202111343

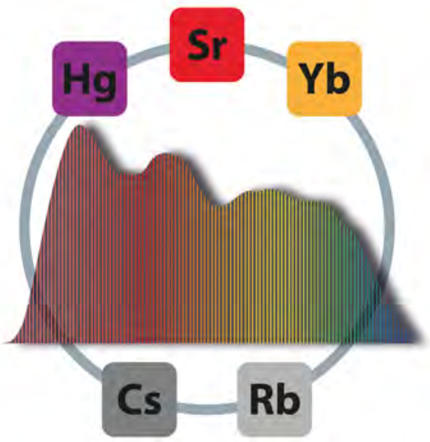

Nearly 25 years ago, Optical Frequency Combs (OFCs) have revolutionized practically from one day to the next the metrology of optical frequencies. Before that, only a few labs in the world could connect the optical (~10^{15} Hz) and the microwave (~10^{10} Hz) domains, at the price of the complex operation of a chain of multiple non-linear frequency conversions. In contrast, OFCs provided a table-top instrument, compact, reliable and operable by a single scientist. Unmistakeable sign: only a few years had passed before pioneering inventors of OFCs Theodor Hänsch and John Hall were awarded the 2005 Nobel prize in Physics, together with Roy Glauber.

The principle of operation relies on a femtosecond pulsed laser, featuring a spectrum of typically ~100 000 phase-locked modes contributing simultaneously. The field can therefore be defined as:

$$E_{\text{comb}}(t) = \sum_{n} E_{n}\, e^{i\phi_n(t)}$$

The average value of each phase $\phi_n(t)$ can be described by $2\pi(nf_{rep} + f_0)t + \phi_n(0)$, where f_{rep} is the repetition rate, f_0 the offset frequency, n an integer number and $\phi_n(0)$ a mode-dependent offset . The Fourier transform of this field shows that a comb is strictly equivalent to a ruler in the frequency space: while f_0 is the offset of the first tooth of the ruler, f_{rep} is the difference between adjacent teeth. Very importantly, the coherence is preserved throughout the whole spectrum, which makes it a unique tool to connect reliably very different spectral domains. Beatnotes between an oscillator at ν_{osc} and the comb feature a frequency at $f_{osc} = \nu_{osc} - n_{osc} f_{rep} - f_0$, which leads to a complete determination of ν_{osc} provided parameters f_{osc}, n_{osc}, f_{rep} and f_0 are measured accurately.

The advent of OFCs renewed considerably the interest of the Time and Frequency community in the metrology of optical atomic transitions. Even though the definition of the SI second had been based on the hyperfine transition of Cs since 1967, researchers early realized that the use of atomic transitions in the optical domain would dwarf radically most of possible systematic shifts affecting clock frequencies. Nevertheless, if single ion clocks had been under development since the early 80's, the very cumbersome connection to the SI second was considerably hindering the perspective of a new definition. OFCs changed completely this perspective, and it is about at the same time, in 2003, that a researcher from the University of Tokyo, Hidetoshi Katori, proposed a scheme allowing the trapping and high resolution spectroscopy of many neutral atoms simultaneously. The race between optical clocks based either on single ions or neutral atoms had started and is still ongoing today: with published uncertainties down to 1×10^{-18} or below, instruments operated notably with Sr, Yb, Hg, Yb^+, Al^+ or Sr^+ have outperformed even state-of-the-art Cs clocks by more than 2 orders of magnitude. OFCs are used to compare optical clocks either to the SI second or directly one with another: the span of the comb spectrum is so large that it allows comparing clocks that are hundreds of nanometers apart. In the perspective of the roadmap for a new definition the second, aiming at 2026, possible contenders to new primary and secondary representations of the SI second are thus compared frequently and reliably in order to progressively refine, year after year, the knowledge of their frequency ratios.

Progressively, the technology supporting OFCs improved and industrial devices became available. If the original mode-locked sources were Titanium-Sapphire lasers, they often missed the reliability necessary to measurements bound to last days, if not months. The alternative offered by fiber lasers in the near infrared region soon released this constraint: erbium-doped fiber laser based OFCs notably offer a mode-lock so reliable that a year of continuous operation is not an issue. More recently, research on compact combs based on micro-resonators or semiconductor systems has raised a strong interest in the community. Despite their low power and high repetition rate, making notably the measurement of f_0 challenging, the potential of devices that could be easily installed in a large range of academic or industrial applications is very appealing. Generally, the technical progress opened the door to contributions to a large variety of scientific and technical fields, way beyond frequency metrology, as detailed in reference [1]. Striking applications were for example published in molecular spectroscopy (dual-comb spectroscopy, analysis of gas sample to track pollution, analysis of human breath), astronomy (calibration of spectrograph), or distance measurements (laser ranging).

At SYRTE (Systèmes de Référence Temps-Espace), the French National Metrology Institute for Time and Frequency, OFCs are used on the one hand for accurate and high resolution frequency metrology and on the other hand for the transfer of spectral purity from one frequency domain to another. In the following sections, we describe how this is applied to atomic clocks comparisons, to the construction of very low noise sources in the optical and microwave domains and to the dissemination of frequency standards on national and even international distances.

ACCURATE AND HIGH RESOLUTION ATOMIC CLOCK COMPARISONS

In the last 30 years, the SYRTE teams have developed and improved an ensemble of seven atomic

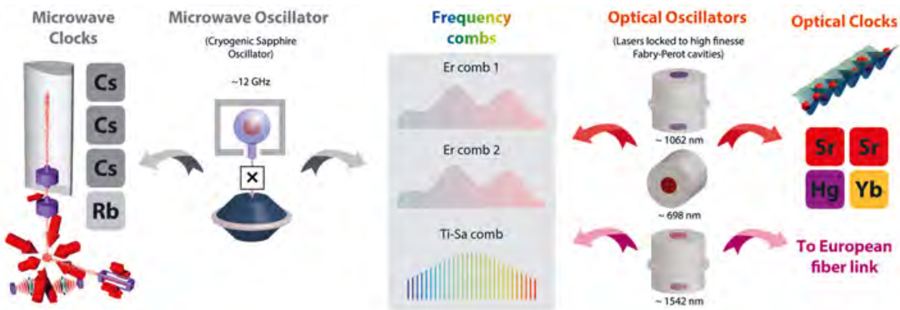

Figure 1. Architecture of atomic clocks, oscillators and frequency combs at SYRTE. The three operational OFCs act as a bridge between microwave and optical oscillators, probing respectively the SYRTE microwave fountains and optical lattice clocks.

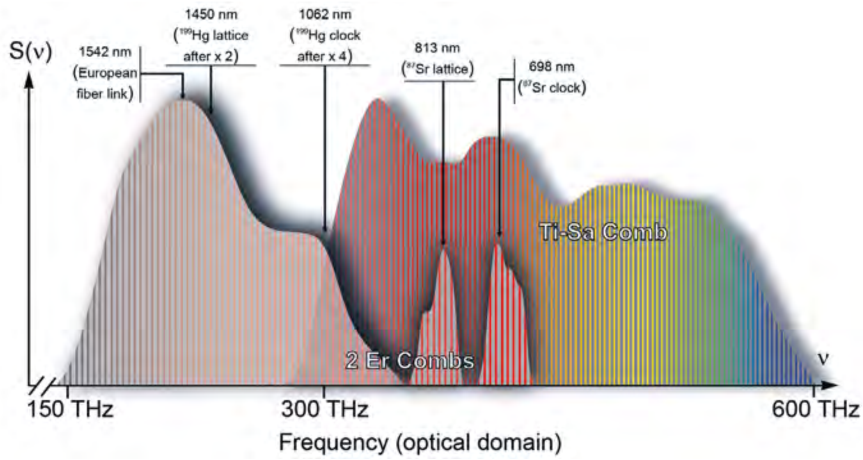

Figure 2. Spectral coverage of the SYRTE combs architecture. All the relevant laser sources can be counted by at least two of the three OFCs. The connection to the 1542 nm laser is essential for the referencing of the two Er combs and of the REFIMEVE network.

clocks strongly contributing to the accuracy of international timescales UTC (Coordinated Universal Time) and TAI (Temps Atomique International), and to the SI second monthly calculated by the BIPM (Bureau International des Poids et Mesures). This clock ensemble includes four microwave fountains, three based on cesium and one on rubidium, all featuring an accuracy of a few 10^{-16} and regularly contributing to the steering of TAI. In addition, we are developing three optical lattice clocks operated with strontium or mercury that reach an uncertainty of a few 10^{-17} and already provided calibrations reports to the BIPM. This is one of the most complete sets of clocks existing in the world, and in order to compare frequently all these instruments, we have developed an ensemble of three operational OFCs. The goal of this redundancy is twofold: ensure the accuracy of the measurements, and evaluate the stability of the comparisons (figure 1)

Our architecture relies on two Erbium doped fiber laser based OFCs (Menlo Systems, FC1500) featuring a spectrum in the near infrared, spanning from 1 µm to 2 µm after broadening. This allows a straightforward connection to the telecommunication bands around 1.5 µm, but does not permit to address directly all optical clock transitions (typically between 200 and 800 nm). Modules doubling the frequency of the combs in specific spectral windows are therefore necessary, for instance to generate teeth at 698 nm and 813 nm to connect respectively the strontium clock and lattice lasers (figures 2 and 3). This is complemented by a former generation titanium-sapphire laser based OFC, with a spectrum after broadening (500 nm to 1.1 µm) enabling the direct comparison of all SYRTE optical clocks. We chose to phase-lock all our frequency combs to a cw ultrastable laser (frequency instability below 10^{-15} between 0.1 and 1000 s timescales) in order to reach the so-called narrow linewidth regime: this ultrastability is transferred to each tooth of the comb, which leads to beatnotes with external oscillators that can be filtered in a narrow band. After mixing out f_0 from all the beatnotes f_{osc} , we effectively generate a virtual comb at $f_0 = 0$ after isolating the RF single tone at $\nu_{osc} - n_{osc} f_{rep}$, thus rendering every following measurement insensitive to f_0. From this point, phase-locking a single beatnote between the comb and an ultrastable laser by applying feedback to the optical length of the femtosecond laser cavity, so as to keep $f_{osc} - n_{osc} f_{rep}$ constant, is sufficient to 'freeze' entirely f_{rep} and therefore the position of the comb in frequency domain. Comparing the frequency of the resulting f_{rep} signal (in the RF or microwave domain and easily obtained by photodetection of the pulse train emitted by the femtosecond laser) with signals referenced to microwave frequency standards •••

(atomic fountain clocks in particular) and to the SI second produces a high-precision measurement of the absolute frequency of optical clocks. Furthermore, by appropriate arithmetic combination of the various signals involved, it is even possible to extract directly the frequency ratio between two optical clocks without involvement of microwave standards and even independent of the residual noise of the OFC itself! [2]

REFIMEVE FIBER NETWORK AND DISSEMINATION OF AN ACCURATE 1542 NM REFERENCE

The research infrastructure REFIMEVE[1] is a network of optical fibers dedicated to the ultra-low noise dissemination of an ultrastable carrier at 1542 nm throughout the French territory. It provides sustainably and reliably (uptime > 85%) this infrared reference to many academic institutions and other research infrastructures, state agencies and industrials. The source of the disseminated signal is a SYRTE 1542 nm ultrastable laser, which defines the stability and the accuracy received by the end users. Both operational Erbium combs are phase locked to this laser, which in turns allows us to lock its frequency to a hydrogen maser on long (>100 s) timescales, while benefiting from the stability of a high finesse Fabry-Perot cavity on shorter timescales. The active compensation of the propagation noise in the network yields a signal at the disposal of the users featuring a stability below 2×10^{-15} at any timescale, and an accuracy of 1×10^{-14} on the fly, that can be pushed down to $< 1 \times 10^{-15}$ on demand.

International connections to similar networks have enabled comparisons on a continental scale between SYRTE and PTB (Germany, since 2015), NPL (UK, since 2016), INRIM (Italy, since 2020) and soon CERN (Switzerland). All together, this is an ensemble of ~12 optical clocks that are interfaced with this European 1542 nm reference by OFCs. These instruments are frequently compared one to the others, in order to ascertain the reproducibility of frequency ratios between the various contenders to a new definition of the second. The long term monitoring of these ratios also contributes to tests of fundamental Physics, such as the search for a possible drift of fundamental constants. Finally, in the last years, the field of Earth Sciences has expressed a growing interest in optical clocks: as their frequency is sensitive to the local gravitational potential, this allows them to contribute to the refined mapping of the geopotential and to an improved determination of the geoid (equipotential approximating the mean sea level). It is in this spirit that SYRTE started recently the development of a transportable ytterbium optical lattice clock, that will be moved in the future along the REFIMEVE[1] network and remotely compared to the stationary European clocks. This new device will be equipped with a transportable OFC in order to measure the frequency of the clock versus the 1542 nm carrier, thus opening the possibility to exploit the ~60 outputs of the network over the metropolitan territory.

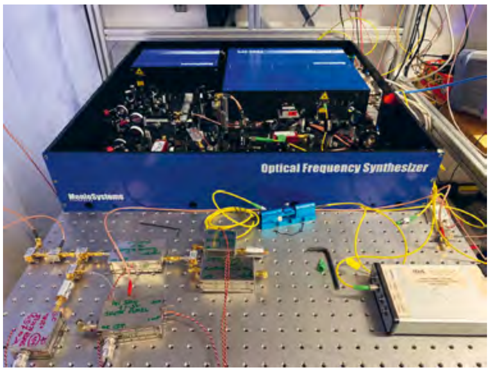

Figure 3. Operational OFC 'Er2' at SYRTE. The comb is equipped with optical setups to form ultrastable optical beatnotes with various lasers. At the forefront, an electronic setup is being set up to generate operational low-noise microwave to replace the cryogenic sapphire oscillator in the long run.

[1] Network under supervision of Université Sorbonne Paris Nord, Observatoire de Paris-PSL and CNRS

TRANSFER OF SPECTRAL PURITY

Beyond their measurement capacity, OFCs can also be utilized for novel applications where the excellent spectral purity of a state-of-the-art optical oscillator (cw laser) serves as a reference to create an ultra-pure radiation in an entirely different part of the electromagnetic spectrum, where high purity sources are difficult or even impossible to realize by any other technique. The idea is simply that when appropriately phase-locked to a high spectral purity source (in the optical or near-infrared domain), each tooth of the comb reproduces this spectral purity, and can be used to generate and/or phase-lock other sources in different spectral domain. Provided the phase comparison/phase-locking processes are set up with extreme care and expertise to be sufficiently low noise, the final radiation will reproduce the spectral purity of the initial state-of-the-art reference, but transferred to a different spectral domain.

At SYRTE, we have first demonstrated the use of this technique to transfer the spectral purity from an ultra-stable laser in the near-infrared domain (1542 nm) to an other laser in the same domain but at a significantly different wavelength (1062 nm) [3]. We showed how, with extreme precautions, this could be realized with a minute added noise corresponding to a few 10^{-18} at a 1s timescale, well below the residual frequency fluctuations of any existing ultra-stable laser. In this case, the idea is simply to directly phase-lock the 1062 nm laser onto an existing tooth of the comb close to it in frequency. Significant care must, however, be taken to minimize or cancel the noise resulting from the propagation of the laser radiations in fibered or free-space optics where even minute fluctuations arising - for example - from temperature changes or air flow currents may degrade the final performance.

In collaboration with our colleagues from LPL (Laboratoire de Physique des Lasers, CNRS/Université Sorbonne Paris Nord), we have also demonstrated a transfer of spectral purity from a 1542 nm wavelength laser to a ~10 µm wavelength radiation emitted by a Quantum Cascade Laser (QCL) [4]. In this case, an extra level of difficulty arose from the physical separations between SYRTE (hosting the 1542 nm laser) and LPL (where the QCL, the OFC, the equipment to phase lock it and characterize its spectral purity, was residing). This difficulty was solved by the use of the REFIMEVE network which connects the two laboratories. In this case, the 10 µm wavelength spectral range is not directly accessible by existing OFCs, and we utilized non-linear optics (difference frequency generation) to generate a comparison signal between the near-infrared OFC and the 10 µm QCL. This technique demonstrated not only the most spectrally pure QCL-laser emission ever produced, but also provided absolute and SI-traceable referencing of its frequency.

Last, in collaboration with our industrial partners from MenloSystems GmBH and Discovery Semiconductor Inc., we have demonstrated how realizing the transfer of spectral purity from a near-infrared laser (1542 nm) to the microwave domain (12 GHz) was able to produce the lowest phase-noise microwave signal ever demonstrated by any existing technique [5]. This is of large interest – in particular – for radar applications where the quest for low-phase noise carrier is one of the sources of resolution improvement. In this case, the microwave signal is simply produced by photo-detecting the train of pulses emitted by the OFC. Mathematically speaking, if the spectral purity transfer is perfect, since the emitted microwave signal is phase-coherent with the comb and the near-infrared reference laser, its phase fluctuations are imposed by those of the reference laser at 1542 nm, but with a very large division factor (of the order of 17000... the ratio between the optical and the microwave frequency). In order to be as close as possible to this mathematical ideal, an ultra-low-noise OFC was developed for this purpose by MenloSystems, and a very high linearity photo-diode was developed by Discovery Semiconductor. This is paramount for extreme performance, in particular because amplitude-fluctuations will generate phase fluctuations in the photo-detection process (even though we use special "magic point" conditions in the vicinity of which this effect is strongly reduced), and because high optical power needs to be used for photodetection in order to minimize the effect of thermal and quantum noise. We demonstrated an absolute phase noise of -173 dBc/Hz at 10 kHz and -106 dBc/Hz at 1 Hz from a 12 GHz carrier.

CONCLUSION

We have presented how optical frequency combs, both utilized as measurement tools and as mean for transferring spectral purity between various spectral domains, can achieve an extremely high level of metrological performance and be put to use in the most demanding high-precision measurements apparatus. Extreme care must however be taken in order to achieve the best result, but as commercially available systems are constantly improving, such performances will progressively become available for non specialists in turn-key systems.

REFERENCES

[1] T. Fortier and E. Baumann, Commun. Phys. **2**, 153 (2019)

[2] H. R. Telle, B. Lipphardt, and J. Stenger, Appl. Phys. B **74**, 1–6 (2002)

[3] D. Nicolodi *et al.*, Nat. Photonics **8**, 219 (2014)

[4] B. Argence *et al.*, Nat. Photonics **9**, 456 (2015)

[5] X. Xie *et al.*, Nat. Photonics **11**, 44 (2017)

KERR FREQUENCY COMBS: A MILLION WAYS TO FIT LIGHT PULSES INTO TINY RINGS

Aurélien COILLET[1]*, Shuangyou ZHANG[2], Pascal DEL'HAYE[2,3]
[1] Laboratoire Interdisciplinaire Carnot de Bourgogne, 21000, Dijon, France
[2] Max Planck Institute for the Science of Light, 91058, Erlangen, Germany
[3] Department of Physics, Friedrich Alexander University Erlangen-Nuremberg, 91058, Erlangen, Germany
*** aurelien.coillet@u-bourgogne.fr**

Frequency combs can be generated in millimeter-sized optical resonators thanks to their ability to store extremely high light intensities and the nonlinearity of their materials. New frequencies are generated through a cascaded parametric amplification process which can result in various optical waveforms, from ultrastable pulse patterns to optical chaos. These Kerr frequency combs have been studied extensively, with a wealth of fascinating nonlinear dynamics reported, and myriads of applications being developed, ranging from precision spectroscopy and Lidars to telecom channel generators.

https://doi.org/10.1051/photon/202111348

Kerr frequency combs are a novel way to generate frequency combs based on the nonlinear interaction between a single wavelength light source and a dielectric material [1]. Since such interactions are quite weak, a resonator which forces light to recirculate in the material is used, accumulating sufficient optical power until new frequencies are generated through a nonlinear process called four-wave mixing (FWM, see insert). Depending on the parameters of both the resonator and pump light used, a variety of optical patterns can be generated and used for different applications ranging from time-and-frequency metrology to building blocks for integrated photonic circuits. The temporal dynamics of the combs generation in microresonators can be described by the Lugiato-Lefever equation (a nonlinear Schrödinger equation), which predicts exceptionally well the dynamics of these systems.

RECIPE FOR A KERR FREQUENCY COMB

The first and most important ingredient for Kerr comb generation is undoubtedly the resonator itself. It needs to have a relatively large

Depending on its exact frequency compared to the resonance, the pump laser light will be more or less enhanced, and all of the newly generated frequencies will interact differently with the resonances of the resonator, leading to a wide variety of circulating soliton pulse patterns.

Kerr nonlinearity, but most importantly, extremely low losses, so that light can remain trapped for a long time. Typically, its quality factor Q — which is proportional to the lifetime of a photon in the cavity — has to be larger than 10^6 to cross the threshold for parametric oscillations at reasonably low optical power. The next step consists in coupling as much monochromatic light as possible into the resonator using the evanescent field of a microfiber, cleaved fiber, waveguide or a prism, and scan the input frequency to excite one resonance. When the pump light within the resonator exceeds the threshold for comb generation, new frequencies are generated. The generated comb (corresponding to solitons in the time domain) is coupled out of the resonator for further analysis or for use in applications. Depending on its exact frequency compared to the resonance, the pump laser light will be more or less enhanced, and all of the newly generated frequencies will interact differently with the resonances of the resonator, leading to a wide variety of circulating soliton pulse patterns.

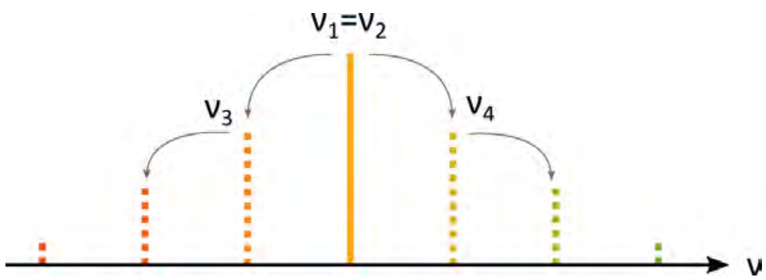

Four-wave mixing is one of the effects of the third-order Kerr optical nonlinearity: assuming two optical waves with different frequencies ν_1 and ν_2 are co-propagating inside a Kerr material, a modulation occurs which leads to the creation of two new frequencies ν_3 and ν_4 such that energy is preserved, that is $\nu_1 + \nu_2 = \nu_3 + \nu_4$. One can also use one single pump wavelength, as is the case for Kerr frequency comb generation, and such process is then called degenerate four-wave mixing. Once new frequencies have been generated though, a cascading effect can occur and all the spectral lines can interact through four-wave mixing. Since the Kerr effect is rather low in most materials, a high power is required for this conversion to be efficient. In the case of Kerr frequency comb generation, such high power is reached thanks to the cavity enhancement of the optical field at resonance. Like most Kerr effects, four-wave mixing is phase-sensitive, hence leading to inherently phase-locked frequency lines.

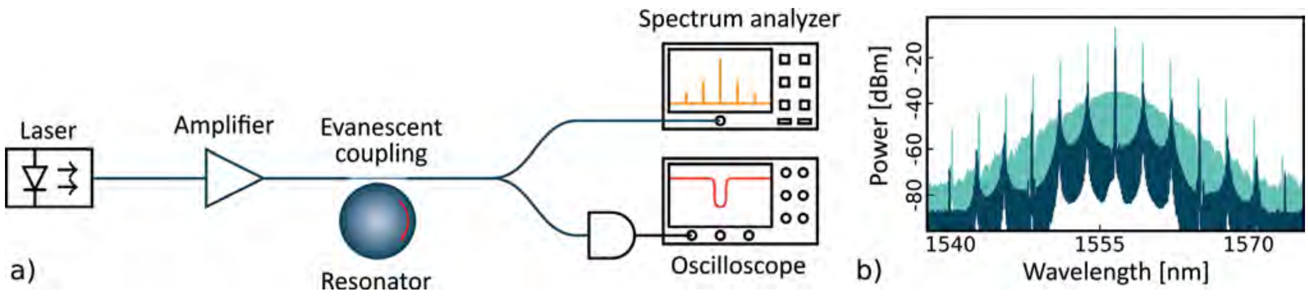

Figure 1. a) Simplest experimental scheme for Kerr comb generation with an amplified, single-wavelength laser source coupled to a resonator using a microfiber in this case. The output signal can directly be monitored through the same coupling microfiber. b) Examples of different Kerr combs (light and dark blue) generated in the same resonance, at the same power, but for a slightly different detuning between the cavity resonance and the pump frequency.

THE LUGIATO-LEFEVER EQUATION

The initial observation of various types of Kerr combs led to the search for an appropriate theoretical model that could describe the experimental observations. One can understand Kerr comb generation either by looking at it as a collection of spectral modes that interact through four-wave mixing [2], or rather like the propagation of light in a closed-loop, with a continuous pump wave constantly pouring energy into the system [3]. In both of these approaches, one finds that the optical field in the cavity follows the following normalized equation:

$$\frac{\partial\psi}{\partial\tau}=-(1+i\alpha)\psi+i|\psi|^2\psi-i\frac{\beta}{2}\frac{\partial^2\psi}{\partial\theta^2}+F$$

The evolution of the field is hence governed by the interactions between losses, the frequency detuning between the pump and the resonance α, the normalized nonlinearity, the second order dispersion of the resonator β and the pump field amplitude F. With these notations, the field ψ depends both on the long timescale time τ and the angle θ which marks the position within the resonator. This equation is a modified version of a nonlinear Schrödinger equation, with both losses and driving included, and is known as the Lugiato-Lefever equation. This equation was introduced in 1987 by Luigi Lugiato and René Lefever [4] in order to model the spontaneous formation of patterns in 2D resonant Kerr media, and a large corpus of theoretical analyses is already available. In particular, the analysis of the stability of the flat solution, that is when no other frequencies or combs are generated, predicts in which region of the parameter space interesting structures can be formed [5]. For our purpose, a

Figure 2. a) Bifurcation diagram of the 1D Lugiato-Lefever equation in the anomalous dispersion regime ($\beta < 0$) with the regime of Kerr comb one can expect in each region of the parameter space. The detuning α is the difference between the laser and resonance frequency normalized by the resonance bandwidth. b) Numerical simulations of the intracavity intensity for the most notable regimes of Kerr comb. Turing rolls and soliton are stable structures, while breather and chaotic regimes vary with time. c) Comparison between experiments and the LLE model for the spectra of the generated Kerr combs, while varying the detuning along the green line in a).

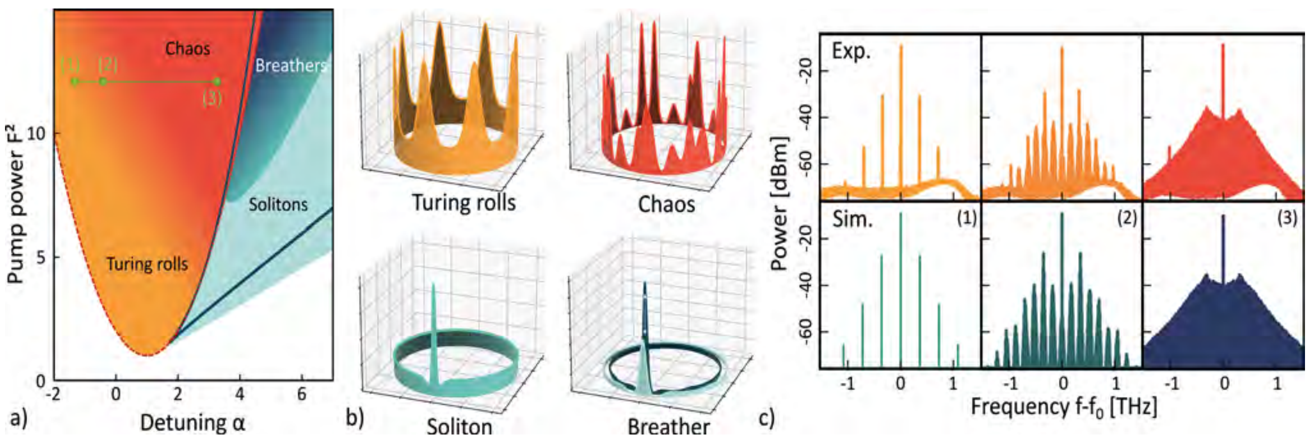

resonator has its dispersion fixed during the manufacturing process, and the only 2 parameters that remain accessible to the experimentalist are the detuning of the laser with respect to the resonance frequency α and the pump power F^2. In the anomalous dispersion regime, a wealth of comb states can be achieved: Turing rolls appear spontaneously above a given threshold, and correspond to sine-like oscillation of the intensity. A soliton is obtained when the laser frequency is slightly higher than the resonance frequency (positive detuning), but requires a seed pulse or significant fluctuations to be generated, as this part of the parameter space is multi-stable; multiple excitations can therefore lead to multiple solitons. Increasing the pump power can lead to instability, with breathers and chaotic pulsed regimes taking place. Despite its mathematical simplicity, the Lugiato-Lefever has been able to model the experimental results obtained with various resonators with an impressive precision, as can be seen in figure 2 c). The evolution from a stable comb to chaos is reproduced with high accuracy over several orders of magnitude of intracavity power. Such an accuracy stems from the very simple processes at play, and particularly the parametric gain: the Kerr effect is indeed quasi-instantaneous, with a very large spectral bandwidth, such that its modelling is very easy.

BEYOND THE LUGIATO-LEFEVER EQUATION

Rich cavity soliton states have been predicted by Lugiato-Lefever equation and experimentally observed in different dispersion regimes and with different pumping schemes. As shown in Fig. 3, with a single frequency pumping and anomalous dispersion, bright soliton pulses (intensity peaks on a dark background) can be generated through a well-defined balance between the Kerr nonlinearity, group velocity dispersion, cavity loss and gain [6]. Crystallized soliton structures with crystallographic defects have also been observed in this regime. These correspond to fixed patterns of solitons that are stable within the resonator and repeat after each round-trip. In contrast, the normal dispersion regime leads to dark pulses (intensity dips embedded in a high-intensity background) that arise through the interlocking of switching waves connecting the homogeneous steady states of the bi-stable cavity solutions (middle panel in the right of Fig. 3) [7]. Distinct soliton structures in the zero-dispersion regime have also been reported with asymmetrical behaviour both in the frequency domain and time domain. The zero-dispersion regime is of particular interest because it allows to investigate how higher-order dispersion affects the soliton formation dynamics. The soliton (bright or dark) formation in this regime is associated with the interlocking of abrupt changes of •••

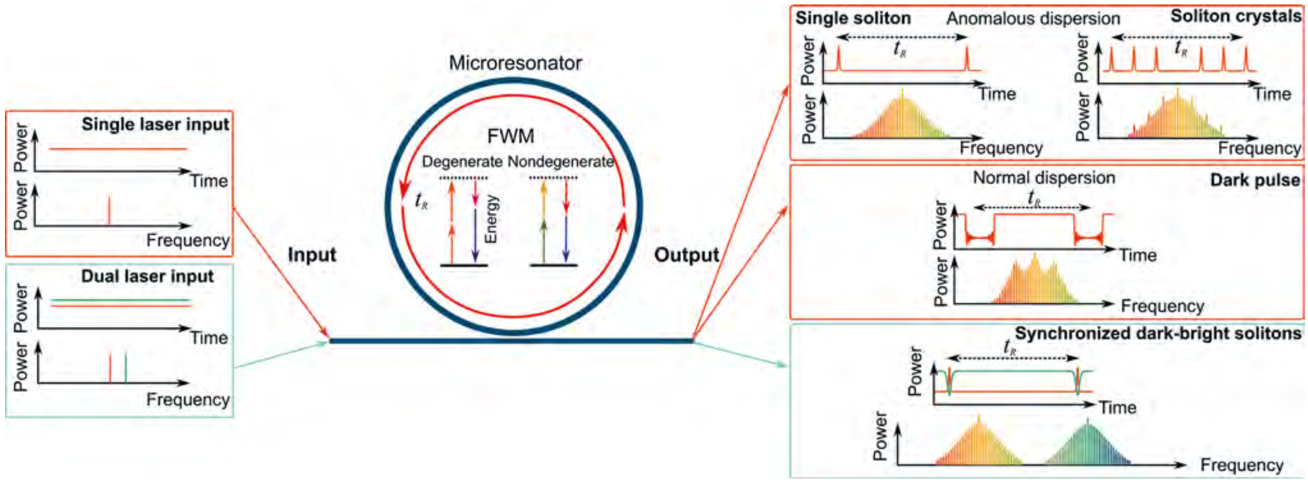

Figure 3. Different light pulses emitted from the resonators. With single frequency driving of a resonator (marked with red boxes), bright solitons and soliton crystals can be generated in anomalous dispersion regime, while dark pulses can be observed by driving at normal dispersion. Seeding with two colors of lights, dark-bright soliton bound states can be emitted from a resonator with a mutually trapped dark-bright soliton pair.

power in a resonator, so-called switching waves. Most importantly, zero or small dispersion is very desirable to obtain spectrally broadband frequency combs. In addition, the coexistence and mutual locking of dark and bright pulses in the regime of normal, zero, and anomalous dispersion has been predicted by the Lugiato-Lefever equation when considering higher-order dispersion effects. Recent research revealed bound states of dark-bright solitons in a resonator through seeding two modes with opposite dispersion via two colors of light (lower panel in the right of Fig. 3) [8]. These mutually trapped dark-bright pulses lead to a light state with constant output power in the time domain but spectrally resembling frequency combs.

In addition to the generation by a CW laser source, cavity solitons can be generated with even higher efficiency by synchronously pulsed-driving. The corresponding soliton dynamics are also well modelled by the Lugiato-Lefever equation. An additional way for the generation of Kerr solitons is the use of active media as part of an external cavity, which has been studied with increasing attention in the last years. This concept has the advantage of not requiring a narrowband tuneable laser source for the soliton generation.

CONCLUSION

Frequency combs generated through four-wave mixing in high quality factor resonators constitute a very promising alternative to mode-locked lasers for many applications where compacity is required. In the past 15 years, research on this topic went from early demonstration of frequency generation to theoretical understanding and prediction, and to applications, including optical frequency synthesis, ultrastable microwave generation, calibration for astronomy spectroscopy, and ranging. Most of these applications make use of a single pulse revolving inside the cavity – a unique soliton – yet a myriad of other exotic and physic-rich regimes can be obtained. The Lugiato-Lefever equation and its refinements have been used to accurately predict the generation of these original states, such as soliton crystals and locked switching waves. The full extent of the possibility offered by Kerr frequency combs and their variants – pulse-driven, dual-pump, with gain medium, ... – remains to be explored, both for fundamental study in nonlinear dynamics and for demanding applications.

REFERENCES

[1] P. Del'Haye, A. Schliesser, O. Arcizet, T. Wilken, R. Holzwarth & T. J. Kippenberg, Nature **450**, 1214-1217 (2007)

[2] Y.K. Chembo, & C. R. Menyuk, Phys. Rev. A **87**, 053852 (2013)

[3] S. Coen, H. G. Randle, T. Sylvestre, & M. Erkintalo, Opt. Lett. **38**, 37-39 (2013)

[4] L.A. Lugiato, & R. Lefever, Phys. Rev. Lett. **58**, 2209 (1987)

[5] C. Godey, I. V. Balakireva, A. Coillet, & Y. K. Chembo, Phys. Rev. A **89**, 063814 (2014)

[6] T. Herr, V. Brasch, J. D. Jost *et al.*, Nature Photon. **8**, 145–152 (2014)

[7] X. Xue, Y. Xuan, Y. Liu *et al.*, Nature Photon. **9**, 594–600 (2015)

[8] S. Zhang, T. Bi, G. N. Ghalanos, N. P. Moroney, L. Del Bino, & P. Del'Haye, Phys. Rev. Lett. **128**, 033901 (2022)

THE OPTICAL HELICITY
IN A MORE ALGEBRAIC APPROACH TO ELECTROMAGNETISM

Ivan FERNANDEZ-CORBATON*
Institute of Nanotechnology, Karlsruhe Institute of Technology, 76021 Karlsruhe, Germany
***ivan.fernandez-corbaton@kit.edu**

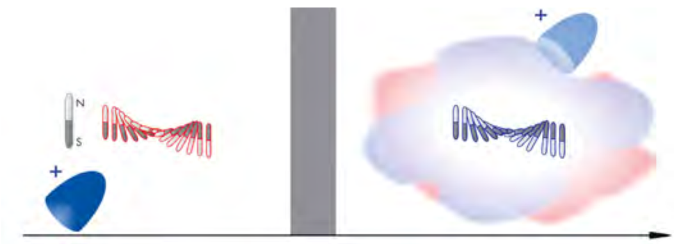

https://doi.org/10.1051/photon/202111354

The constant miniaturization trend in nanophotonics challenges some of the theoretical tools at our disposal: Analytical shortcuts such as the dipolar and paraxial approximation become unapplicable, and the computational cost of fully numerical studies often renders them impractical. A basic electromagnetic property, the optical helicity, and the use of more abstract tools inspired by it, are rising to meet the challenge.

The optical helicity, also known as electromagnetic helicity, represents the handedness of Maxwell fields, and is the conserved quantity connected to the electromagnetic duality symmetry. This connection allows to consider the polarization of the field within the powerful framework of symmetries and conservation laws. Such framework is formalized in electromagnetic Hilbert spaces thanks to the existence of an appropriate scalar product for Maxwell fields [1]. While these ideas may seem of purely theoretical interest, the abstraction and generality that they afford facilitate both the understanding and the design of specific light-matter interaction effects. The algebraic treatment of helicity and its eigenstates [2] is also a valuable tool for extending the theory, as exemplified by the recently established new connection between optics and magnetism [3].

FUNDAMENTALS AND APPLICATIONS

Helicity is the projection of the angular momentum vector **J** onto the direction of the linear momentum vector **P**,

$$\Lambda = \frac{\mathbf{J} \cdot \mathbf{P}}{|\mathbf{P}|}. \qquad (1)$$

Equation 1 is the most general form of the helicity operator, which is valid for many particles and fields, such as electrons and gravitational waves. For Maxwell fields, helicity describes the sense of screw in light: The circular polarization handedness.

Helicity is a pseudoscalar: Its sign flips under any spatial inversion operation such as parity or mirror reflections. Figure 1 illustrates some transformation properties of helicity comparing them with the transformation properties of angular momentum. Helicity and angular momentum are two different properties of the field. A very basic difference is that, while a two dimensional plane is enough to define a rotation (angular momentum), three spatial dimensions are required to define a sense of screw (helicity). The systematic consideration of how helicity and angular momentum transform allows the identification of the symmetry reasons for particular light-matter interaction effects, which can then be used for the analysis and prediction of experimental measurements. For example, the optical vortices seen in focusing by or scattering off cylindrically symmetric systems are readily shown to be due to the breaking of a different

In its most general illumination-independent embodiment, helicity preservation is achieved by objects exhibiting electromagnetic duality symmetry, a fundamental continuous symmetry in electromagnetism.

symmetry in each case (see Chap. 3 [4]): Translational symmetry in focusing, and electromagnetic duality symmetry (see below) in scattering. For the directional coupling of emitters onto waveguides, it is readily shown that the polarization handedness of the emission cannot be responsible for the directionality, which is controlled by angular momentum [5], see Fig. 3.

For transverse Maxwell fields, helicity has two possible eigenvalues, $\lambda = +1$ and $\lambda = -1$, whose corresponding eigenstates for $(\mathbf{r},t)$ -dependent Maxwell fields are (SI units assumed):

$$\mathbf{F}_\lambda(\mathbf{r},t) = \sqrt{\frac{\epsilon_0}{2}}[\mathbf{E}(\mathbf{r},t) + i\lambda c_0\mathbf{B}(\mathbf{r},t)],\ \Lambda\mathbf{F}_\lambda(\mathbf{r},t) = \lambda\mathbf{F}_\lambda(\mathbf{r},t). \qquad (2)$$

The $\mathbf{F}_\lambda(\mathbf{r},t)$ can be built as the following sum of plane waves:

$$\mathbf{F}_\lambda(\mathbf{r},t) = \int_{\mathbb{R}^3-\{0\}} \frac{d\mathbf{k}}{\sqrt{(2\pi)^3}}\mathbf{F}_\lambda(\mathbf{k})\exp(i\mathbf{k}\cdot\mathbf{r} - ic_0|\mathbf{k}|t), \qquad (3)$$

where $\mathbf{k}\cdot\mathbf{F}_\lambda(\mathbf{k}) = 0$, $i\hat{\mathbf{k}} \times \mathbf{F}_\lambda(\mathbf{k}) = \lambda\mathbf{F}_\lambda(\mathbf{k})$ since $\Lambda \equiv i\hat{\mathbf{k}}\times$ in this representation and, importantly, the frequency is restricted to positive values $\omega = c_0|\mathbf{k}| > 0$. The $\mathbf{F}_\lambda(\mathbf{r},t)$ are the positive frequency restriction of the Riemann-Silberstein vectors • • •

Figure 1. Transformations of helicity, represented by the helices, and of angular momentum, represented by the 2D turns. The initial objects in a) are transformed by a rotation by 180 degrees along the y axis in b), by the parity operation in c), by a mirror reflection across the YZ plane in d), and by a mirror reflection across the XY plane in e). Spatial inversion transformations always flip the screw sense of the helix, while rotations never do. The chosen angular momentum changes sign (the sense of the turn is inverted) upon the rotation in b) and the reflection in e), and stays invariant upon parity and the reflection in d).

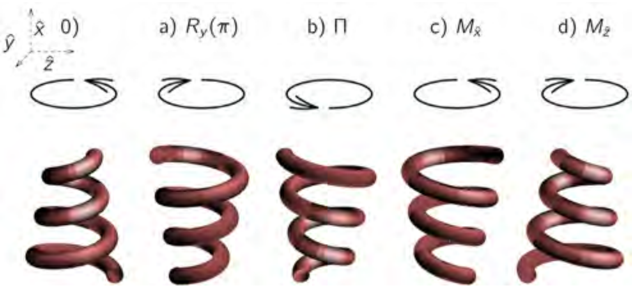

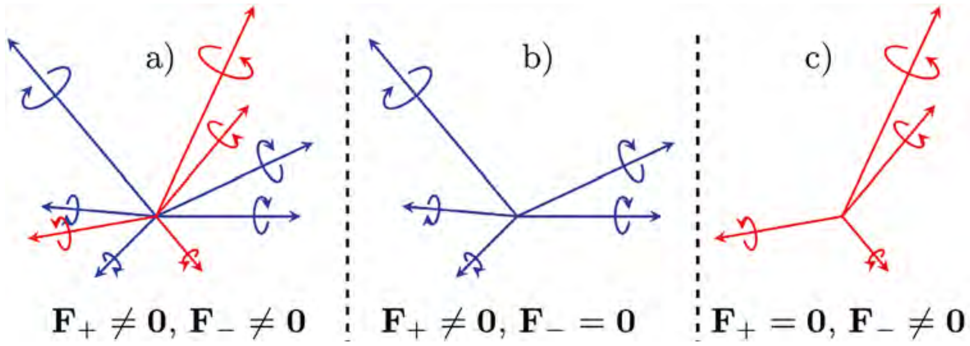

Figure 2. $F_\pm$ split a general electromagnetic field such as the arbitrary multi-frequency combination of circularly polarized plane waves in a) into its two helicity components, left-handed (blue) in b), and right-handed (red) in c).

[2], and its monochromatic components are also known as Beltrami fields [6]. As illustrated in Fig. 2, the $\mathbf{F}_\lambda(\mathbf{r}, t)$ split the electromagnetic field into its left and right circular polarization handedness, for λ = +1 and λ = -1, respectively. The restriction to positive frequencies makes $\mathbf{E}(\mathbf{r}, t)$ and $\mathbf{B}(\mathbf{r}, t)$ necessarily complex valued, and is crucial for achieving the handedness splitting: If $\mathbf{E}(\mathbf{r}\ t)$and $\mathbf{B}(\mathbf{r}, t)$ are real-valued, then $|\mathbf{F}_+(\mathbf{r}, t)| = |\mathbf{F}_-(\mathbf{r}, t)|$follows from Eq. 2, negating the handedness separation.

The splitting allows to analyze the handedness of near fields around illuminated nanostructures, such as the silicon disk in Fig.4, which is illuminated on axis by a single plane wave of positive helicity. Figures 4a) and 4b) correspond to illumination with two different frequencies. Each sub-figure is divided into two areas where the false color scale shows point-wise intensities: $|\mathbf{F}_+(\mathbf{r},|\mathbf{k}|)|^2$ on the left, and $|\mathbf{F}_-(\mathbf{r},|\mathbf{k}|)|^2$ on the right. The monochromatic $\mathbf{F}_\lambda(\mathbf{r},|\mathbf{k}|)$ are obtained as in Eq. 2, but using single frequency complex electric and magnetic fields. To a good approximation, and in contrast with what Fig. 4b) shows, Fig. 4a) shows that the disk does not couple the two helicities upon light-matter interaction: It preserves the incident helicity. In its most general illumination-independent embodiment, helicity preservation is achieved by objects exhibiting electromagnetic duality symmetry, a fundamental continuous symmetry in electromagnetism, whose action is:

$$\begin{aligned} \mathbf{E}(\mathbf{r},t) &\to \mathbf{E}^\theta(\mathbf{r},t) = \mathbf{E}(\mathbf{r},t)\cos\theta - c_0\mathbf{B}(\mathbf{r},t)\sin\theta, \\ c_0\mathbf{B}(\mathbf{r},t) &\to c_0\mathbf{B}^\theta(\mathbf{r},t) = \mathbf{E}(\mathbf{r},t)\sin\theta + c_0\mathbf{B}(\mathbf{r},t)\cos\theta, \end{aligned} \tag{4}$$

for a real angle θ, and its action on the helical fields

$$\mathbf{F}_\lambda(\mathbf{r},t) \to \mathbf{F}^\theta_\lambda(\mathbf{r},t) = \mathbf{F}_\lambda(\mathbf{r},t)\exp(-\lambda i\theta) \tag{5}$$

reveals that, in the same way that rotations are generated by angular momentum operators, *e.g.* $R_z(\theta) = \exp(-i\theta J_z)$, duality is generated by the helicity operator $D_\theta = \exp(-i\theta\Lambda)$. The polarization of the field can then be treated within the powerful framework of symmetries and conservation laws. Such

Figure 3. Emitters (circles) on top of waveguides (gray boxes) emit light with a definite angular momentum along the z-axis (yellow-brown arrows), and a definite helicity (blue/red circles), which couples asymmetrically to the waveguide modes, with more power going towards the +x direction than to the -x direction, or vice versa (purple arrows). The initial situations [panels a) and e)] are transformed by mirror reflections which are symmetries of the waveguide and leave the position of the emitter unchanged: Mx [panels b) and f)], Mz [panels c) and g)], and the composition MxMz [panels d) and h)], respectively, where *α* indicates a reflection across the plane perpendicular to the *α* direction. In each panel, the origin of coordinates is at the position of the emitter, and the coordinate axes are oriented as shown in the central part of the figure. The transformation properties of helicity allow us to conclude that it cannot be responsible for the directional coupling: For example, e) and h) show the same helicity producing the opposite directionality. Such contradictions do not arise for angular momentum, which is indeed the property of light which controls directionality [5].

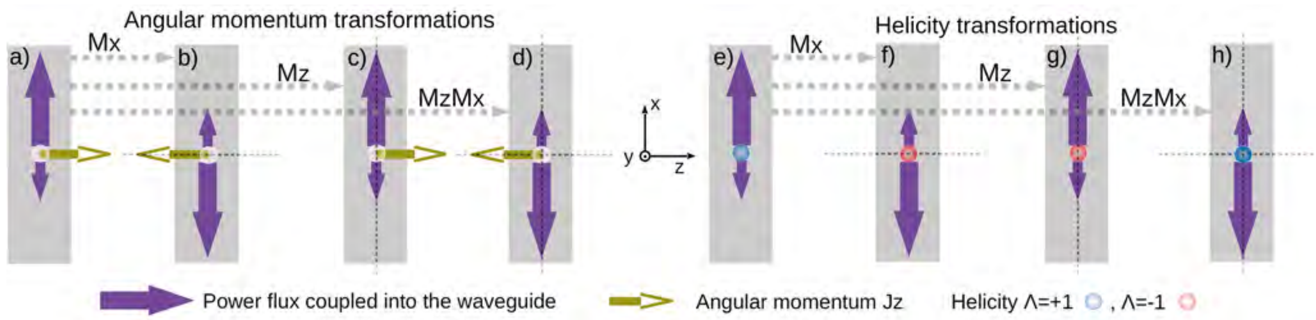

framework facilitates the identification of design guidelines for achieving specific effects, such as zero back-scattering (anti-reflection) (see Chap. 4 in [4]), and enhanced near-field interaction with chiral molecules (see Chap.5.3 in [4], [7]). Helicity preservation is one of the guidelines in these two particular cases. Unfortunately, dual-symmetric systems are hard to fabricate. The theoretically most straightforward way to design a dual system is by using materials with equal relative electric permittivity and magnetic permeability: a very demanding requirement. Fortunately, the essential idea in duality symmetry, balanced electric and magnetic responses, allows to design non-magnetic systems that preserve helicity, at least for particular frequencies and illumination directions. For example, the aspect ratio of the silicon disk in Fig. 4 was optimized [7] for hosting equal electric and magnetic dipole moments upon on-axis illumination at f = 125 THz.

A SCALAR PRODUCT PROVIDES MORE TOOLS

The appropriate scalar product for Maxwell fields is [1]:

$$\langle F|G\rangle = \int_{\mathbb{R}^3 - \{0\}} \frac{d\mathbf{k}}{\hbar c_0|\mathbf{k}|}[\mathbf{F}_+(\mathbf{k})^\dagger \mathbf{G}_+(\mathbf{k}) + \mathbf{F}_-(\mathbf{k})^\dagger \mathbf{G}_-(\mathbf{k})] \qquad (6)$$

where $|F\rangle$ and $|G\rangle$ are two different sets of Maxwell fields, specified by their corresponding $\mathbf{F}_\lambda(\mathbf{k})$, and $\mathbf{G}_\lambda(\mathbf{k})$. Equation 6 is conformally invariant: Its numerical value is identical to the scalar product between $X|F\rangle$ and $X|G\rangle$, for any transformation X in the conformal group, the 15 parameter group which is the largest group of invariance of Maxwell equations [8].

Equation 6 is defined for free Maxwell fields which do not interact with matter. Nevertheless, in a light-matter interaction sequence such as the one depicted in Fig.5a), Eq. 6 can be applied to the pre- and post-interaction fields, only excluding the grayed out period where the interaction is ongoing.

The scalar product for Maxwell fields allows to use the tools of Hilbert spaces in electromagnetism, and to leverage ● ● ●

Figure 4. Helical decomposition of the scattered field around a silicon disk illuminated on axis with two different frequencies (adapted from [7]).

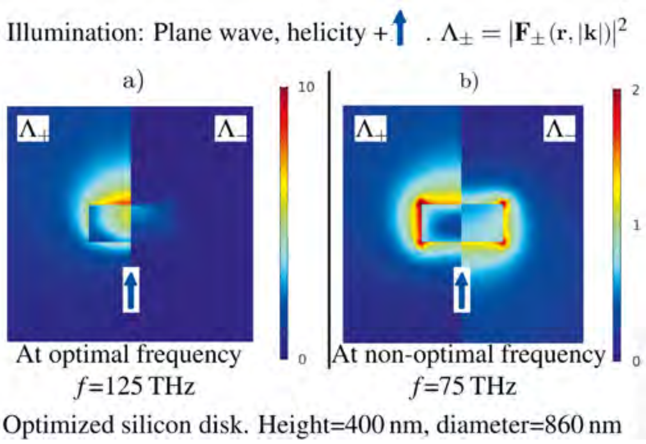

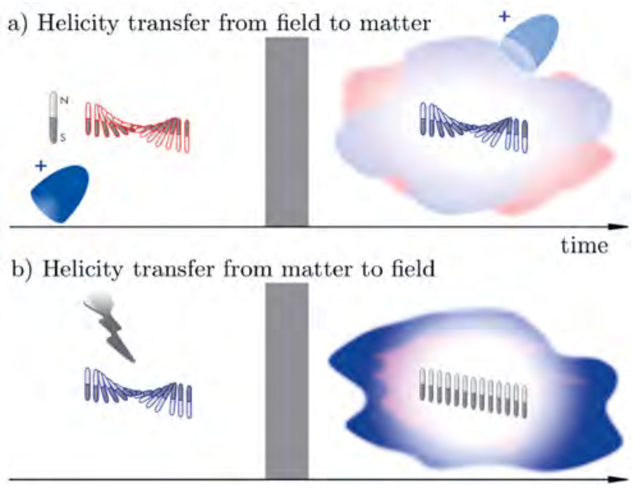

Figure 5. Helicity exchange between electromagnetic fields and material magnetization. In a) a beam of positive helicity interacts with a magnetization of the opposite helicity and flips its handedness. In b), an initially chiral magnetization is turned into an achiral one by achiral and non-necessarily optical forces. In this process, the material radiates an electromagnetic field which contains (part of) the helicity lost by the material.

some of the methods from quantum mechanics. Given an electromagnetic field $|F\rangle$, the average of its linear momenta, angular momenta, energy, and any other quantity represented by a hermitian operator Γ is $\langle F|\Gamma|F\rangle$, which can be readily written down as a k-space integral [2] using Eq.6.

Recently, the k-space integral expression of the average electromagnetic helicity, $\langle F|\Lambda|F\rangle$, has lead to the definition of material helicity [3]. Matter in static equilibrium is electromagnetically represented by its electric charge density $\rho(\mathrm{r})$, and its magnetization density $\mathbf{M}(\mathrm{r})$, which are bijectively connected to the static fields that they generate at $\omega = 0$. It is then possible to define the total helicity, $\langle\Lambda\rangle$, as the sum of two terms: The electromagnetic helicity, $\langle F|\Lambda|F\rangle = \langle\Lambda_{\omega>0}\rangle$ that measures the difference between the number of left-handed and right-handed photons of the free field, and a static term, $\langle\Lambda_{\omega=0}\rangle$, that measures the screwiness of the static magnetization density in matter:

$$\langle\Lambda\rangle = \langle\Lambda_{\omega>0}\rangle + \langle\Lambda_{\omega=0}\rangle, \text{ where}$$

$$\langle\Lambda_{\omega>0}\rangle = \int_{\mathbb{R}^3 - \{0\}} \frac{d\mathbf{k}}{\hbar c_0|\mathbf{k}|} |\mathbf{F}_+(c_0|\mathbf{k}|, \mathbf{k})|^2 - |\mathbf{F}_-(c_0|\mathbf{k}|, \mathbf{k})|^2,$$

$$\langle\Lambda_{\omega=0}\rangle = \int_{\mathbb{R}^3 - \{0\}} \frac{d\mathbf{k}}{\hbar c_0|\mathbf{k}|} \frac{|\mathbf{M}_+(0, \mathbf{k})|^2 - |\mathbf{M}_-(0, \mathbf{k})|^2}{2/\mu_0} \qquad (6)$$

The $\mathbf{F}_\pm$ $(c_0|\mathbf{k}|, \mathbf{k})$ are the $\mathbf{F}_\lambda(\mathbf{k})$ of Eq.3, and $\mathbf{M}_\lambda(0, \mathbf{k})$ are the $\lambda = \pm 1$ helicity components of the 3D Fourier transform $\mathbf{M}(0, \mathbf{k})$ of the static magnetization density $\mathbf{M}(\mathbf{r})$: $2\mathbf{M}_\lambda(0,\mathbf{k}) = (I + \lambda i\hat{\mathbf{k}}\times)(i\hat{\mathbf{k}}\times)^2\mathbf{M}(0,\mathbf{k})$. The charge density $\rho(\mathrm{r})$ does not host any material helicity because the electric field that it produces is longitudinal (parallel to $\mathbf{k}$), and is hence annihilated by the action of the helicity operator $\Lambda \equiv i\hat{\mathbf{k}}\times$. Importantly, $\langle\Lambda_{\omega=0}\rangle$ can be readily shown to be $1/2\sqrt{\epsilon_0/\mu_0}$ times the magnetic helicity. The electromagnetic helicity of the dynamic Maxwell fields and the static magnetic helicity [9] are unified as two different embodiments of the same physical quantity, establishing the theoretical basis for studying the conversion between the two embodiments of total helicity upon light-matter interaction [3], as illustrated in Fig.5.

OUTLOOK

The design of helicity preserving systems is an area of research with technological implications. While approximations such as the geometric optimization illustrated in Fig.4 can already be of some use, recent advances in molecular science prompt the question of whether a truly dual symmetric material, albeit likely with a narrow operational frequency band, can be achieved through molecular design.

Finally, the transfer of helicity from the field into a magnetic material is a mechanism for affecting the chirality of matter in static equilibrium, that is, in its ground state. This points to possible applications in magnetization control by optical means. The potential role of the effect in the all-optical helicity-dependent magnetization switching [10] is an exciting research question.

ACKNOWLEDGMENTS

Partially funded by the Deutsche Forschungsgemeinschaft (DFG, German Research Foundation) --Project-ID 258734477 -- SFB 1173.

REFERENCES

[1] L. Gross, J. Math. Phys. **5**, 687 (1964).

[2] I. Bialynicki-Birula, Prog. Optics **36**, 245 (1996).

[3] I. Fernandez-Corbaton, Phys. Rev. B **103**, 054406 (2021).

[4] I. Fernandez-Corbaton, Helicity and duality symmetry in light matter interactions: Theory and applications, Ph.D. thesis, Macquarie University (2014), arXiv: 1407.4432.

[5] A. G. Lamprianidis, X. Zambrana-Puyalto, C. Rockstuhl, and I. Fernandez-Corbaton, Laser & PhotonicsReviews **16**, 2000516 (2022).

[6] Lakhtakia A., Beltrami fields in chiral media (World Scientific, 1994).

[7] F. Graf, J. Feis, X. Garcia-Santiago, M. Wegener,C. Rockstuhl, and I. Fernandez-Corbaton, ACS Photonics **6**, 482 (2019).

[8] H. Bateman, Proceedings of the London Mathematical Society s**2-7**, 70 (1909).

[9] M. A. Berger, Plasma Physics and Controlled Fusion **41**, B167 (1999).

[10] C. D. Stanciu, F. Hansteen, A. V. Kimel, A. Kirilyuk, A. Tsukamoto, A. Itoh, and T. Rasing, Phys. Rev. Lett. **99**, 047601 (2007).

HOW TO SELECT A NANOPOSITIONER SOLUTION?

Emmanuel Pascal[1,*], Scott Jordan[2]
[1] PI FRANCE, 380 avenue Archimède, bât D, 13100 Aix en Provence, France
[2] PI USA, Head Office, 16 Albert Street, Auburn, MA 01501, USA
***e.pascal@pi.ws**

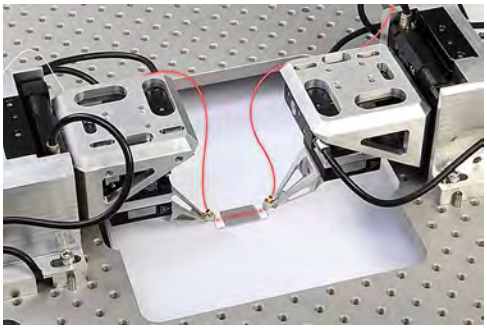

https://doi.org/10.1051/photon/202211360

Many recent innovations have been enabled by high precision positioning devices operating at a nanometer level or below. Developments in this field have been very fast over the last years supported by applications in material sciences, genomics, photonics, defense, biophysics, and semiconductors creating challenges for the scientists and engineers in need of precise and yet robust positioning systems. The critical point is: how should you select your nano positioning solution?

NANOPOSITIONING SYSTEM: A NEW DEFINITION?

By its original definition, a nanopositioning device is a mechanism capable of repeatedly delivering motion in increments as small as one nanometer. Lately, demands from industry and research have pushed requirements to the picometer range. While electroceramics such as piezo materials with flexure guides remain the gold standard for breaking the resolution nanometer barrier, there are several other solutions available today providing repeatable single-digit nanometer step resolution including linear motors, voice-coil drives, and frictionless guides such as air bearings and magnetic bearings. Dynamic issues dominate many applications and can be addressed by novel approaches that benefit real-time/high-dynamic applications. They present new opportunities for optimizing process economics.

Rapid testing and packaging of the latest silicon photonics (SiPh) devices — starting at the wafer level — is the perfect example. In these applications, optical elements and probes must be brought into perfect coupling with devices in various stages of manufacture from wafer to final package. With thousands of optical elements on a single wafer, coupling time becomes the most critical cost factor in testing. The same applies to all further process steps up to assembly and packaging, where active and passive optical elements (e.g., LEDs, laser diodes, photodiodes and optical fibers and waveguides) must be precisely positioned

Emmanuel Pascal: Country Director, PI France
Scott Jordan: Head of Photonics Market Segment, PI Group

Figure 1. A double-sided test and alignment system for silicon photonics wafers based on hexapods and piezo nanopositioning stages to combine the fastest alignment speeds with the highest flexibility.

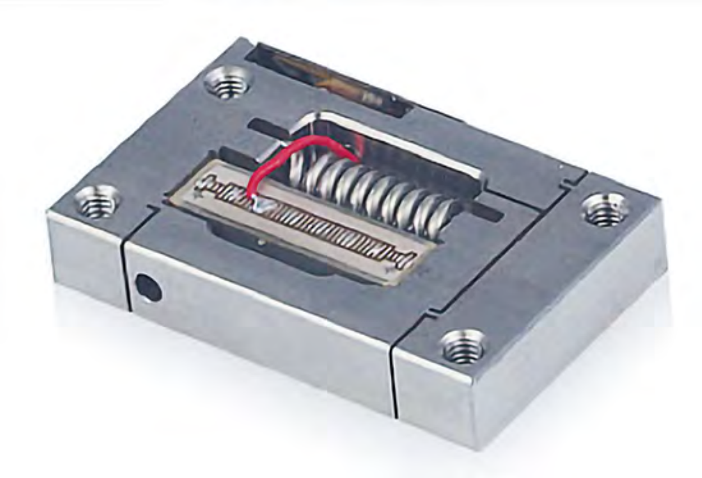

Figure 2. A motion amplified, flexure-guided actuator based on a multilayer piezo stack. Piezo flexure drives can last 100 billion cycles!

relative to each other, typically with accuracies in the sub micrometer range. Here, too, the time required for coupling optimization is decisive for cost-effectiveness. What makes these applications even more challenging is the frequent requirement to optimize positioning in up to all six degrees of freedom. This requires intelligent, precisely coordinated motion control in order not to destroy the result once achieved in one axis by movements in another axis. Complex algorithms that enable parallel, *i.e.*, simultaneous, optimization in multiple degrees of freedom are the solution here. This creates a new paradigm for the definition of a nanopositioning system. We are not talking anymore about a single piezo flexure stage but sophisticated and yet robust systems, built application specific, that can work from lab to fab environment.

NANO POSITIONING: NO FRICTION PLEASE

As a rule of thumb, the lower the mechanical friction in a motion system, the higher the positioning performance. Three frictionless guiding technologies are often used in nanopositioning applications: flexures, air bearings, and magnetic bearings.

Flexures guides are highly stable and stiff, but with travels limited to the millimeter region. For motion ranges from a few to hundreds of millimeters, air bearings offer a solution. An air-bearing stage is a linear or rotary positioner constrained on a cushion of air, using preload mechanisms, virtually eliminating mechanical contact and thus wear, friction, bearing noise, and hysteresis effects. Air-bearing nano-positioning stages are used in numerous high precision motion applications, such ● ● ●

PIEZO ACTUATORS ON MARS!

All-ceramic-encapsulated, cofired piezo actuators were introduced many years ago pushing performance and reliability to new limits to respond to the industrial requirements.

These actuators improve greatly the reliability of devices based on this technology, especially when used in challenging environments.

In fact, NASA/JPL engineers ran these actuators through harsh life tests including 100 billion expansion/contraction cycles before selecting them for the Mars Rover's science lab!

as metrology, flat panel display inspection, large-area photonics test etc. The non-contact design also makes these stages work well in cleanroom applications.

SHORT TRAVEL PIEZO POSITIONERS

When talking about nanopositioning actuators with precision in the nm range and travel ranges of up to a few millimeters, piezo actuators combined with flexure designs are the historical solution. Flexure guides are frictionless and can be extremely small and robust at relatively low cost.

Piezoelectric technologies play a foundational role in positioning applications with nanometer resolution requirements. The benefits of piezo-based devices include:

- Unlimited resolution: positioning increments well below 1nm are possible and fit applications ranging from semiconductor to super resolution microscopy
- Fast response (microsecond time constants)
- Maintenance-free, solid-state construction that reduces wear and tear
- High efficiency: energy is absorbed only to perform movement
- Inherent vacuum-compatibility
- Non-magnetic and magnetic-insensitive construction
- High throughput and dynamic accuracy

Figure 3. Example of Voice Coil Miniature Linear Stage with Air Bearings.

LONG-TRAVEL PIEZO TECHNOLOGIES

By combining lateral actuation and longitudinal actuation of piezo actuators, it is possible to create the basic element of a **piezo walking drive**. A digital controller sequences their operation, providing high-force, long travel step-mode actuation plus picometer resolution fine high-bandwidth actuation. Forces can be generated to 800N and resolution down to 50pm are achievable. This unique combination of class-leading characteristics is proving to be an enabling technology for a wide variety of applications.

Figure 4. High-load walking drives combine piezo clamping and shear actuators in order to move a rod.

Another use of piezo ceramics technology is in **ultrasonic piezo motors**. These are composed of monolithic slabs of piezo ceramics; standing waves are driven in the substrate at frequencies of tens to hundreds of kilohertz. A hardened contact-point attached at a resonant node-point is thereby made to oscillate in a quasi-elliptical fashion; when preloaded against a runner, this confers linear or rotary motion. These piezo motors achieve up to 500mm/sec or 720 degrees/sec over virtually unlimited travel ranges while providing high precision and fast start/stop dynamics. A key benefit of this class of motor is the in-position stability.

CLOSED LOOP OPERATION: SELECTING THE RIGHT SENSOR/ CONTROLLER SOLUTION

Achieving nanometer precision requires further technologies. The stage's internal metrology system must also be capable of measuring motion at the nanometer scale. The characteristics to consider when selecting a stage metrology system are linearity, resolution, stability and bandwidth. Other factors include the ability to measure the moving platform directly and contact *vs.* noncontact measurements. Three types of sensors are mostly used in nanopositioning applications: linear encoders (for longer travels), and capacitive and strain sensors (for short travels).

Linear encoders are familiar devices for measuring long displacements up to hundreds of millimeters. While resolution in the nanometer range is common, accuracy is typically limited to 1 µm per 100 mm. However, this can be improved significantly with modern controllers. Incremental encoders measure changes in position and must be initially referenced to a home switch on power up; absolute encoders do not require this step but tend to be costlier. For short travel nanopositioning devices, cost-effective strain gauges (incl. piezoresistive sensors) use elements whose electrical characteristics

While resolution in the nanometer range is common, accuracy is typically limited to 1 µm per 100 mm. However, this can be improved significantly with modern controllers.

change with strain. These devices are usually attached to the piezo ceramics itself or to a structural element of the stage. Special care must be taken when designing them into a mechanism. If there are elastic or frictional elements in the path between the point of motion and the point of measurement, errors will result. Physically small sensors (such as piezoresistive sensors) measure a highly spatially localized strain, from which the overall mechanism position can be inferred. And these sensors cannot be configured to compensate for orthogonal (parasitic) errors in multi-axis configurations – only parallel metrology of the actual moving platform can provide this valuable capability. Capacitive sensors have emerged as the preferred solution for the most demanding nanopositioning applications requiring short travel ranges. They are absolute, extremely accurate and ultrahigh-resolution devices for determining absolute position over ranges of hundreds of microns or even millimeters. The device's positioning motions vary the distance between two nano-machined capacitor plates, providing a sensitive and drift-free positional feedback signal.

ACTIVE OPTIC MOUNTS: TRAVELLING IN SPACE

Beyond linear single or multi-axes configurations, piezoelectric devices are very suitable to create tip/tilt platforms. With the integration of actuators with resolutions well below 1nm, these systems routinely offer angular resolutions surpassing 1/100 arcsec. Compact piezo- and voice-coil-actuated active optic mounts are available with multiple degrees of optical deflection. Two-axis, parallel-kinematic piezo mounts offer advantageous gimbal-style actuation with coplanar rotational axes. Compared to galvos and voice-coil systems, piezo-driven active optic mounts are typically more compact, fieldless, faster, inherently stiffer, and more predictable when power is cut. They are of great interest in the innovative field of Free Space Optical Communications (FSOC), where thousands of satellites form a high-speed, low-latency global information network. For these applications, robustness, long life and environmental insensitivity are prized.

INTERFACING

A wide variety of interfaces is available today, RS-232 to Ethernet, SPI, and USB, plus a host of specialty interfaces are among them. The choice depends on your environment, and all have pros and cons. Since motion controllers communicate via short messages, latency is often much more important to overall throughput than bulk transfer speed. USB and Ethernet are very common, with the latter supporting remote and distributed communications at the cost of variable latencies when the common TCP/IP communications protocol •••

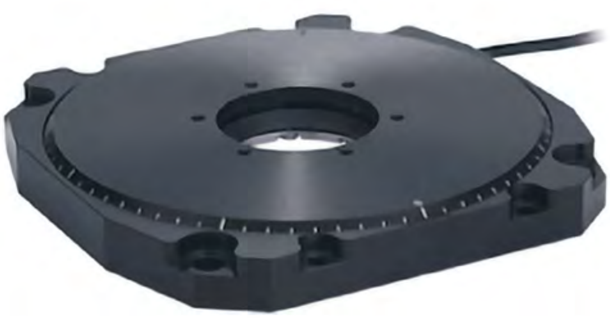

Figure 5. Example of Voice Coil Miniature Linear Stage with Air Bearings.

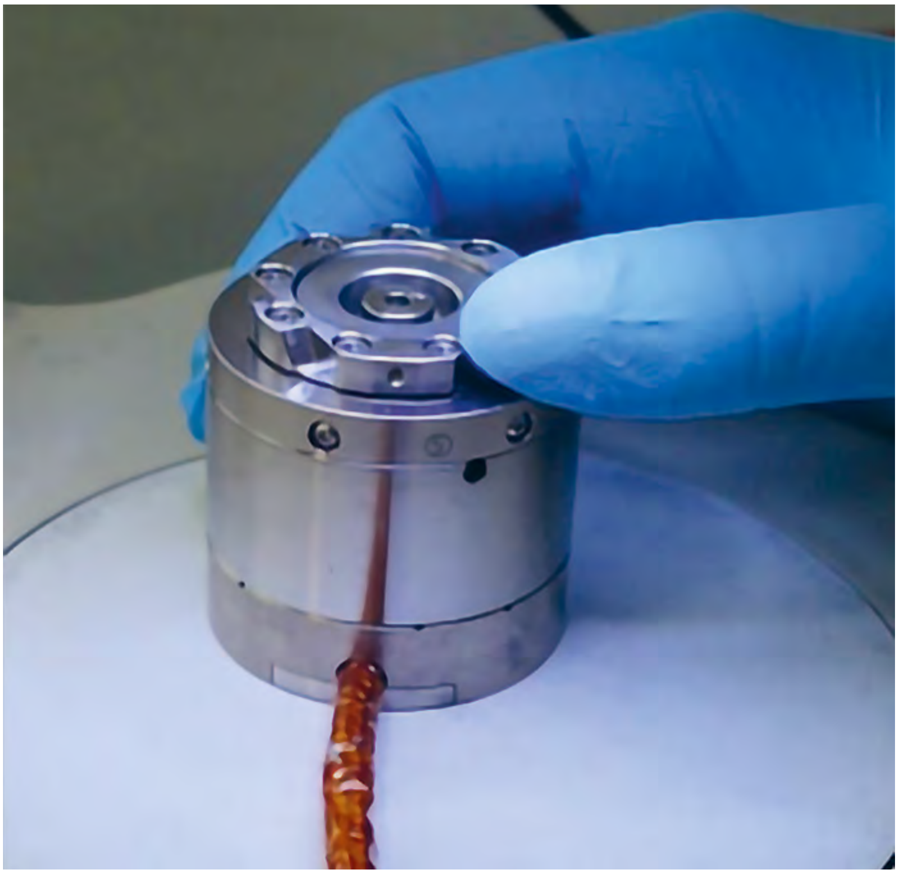

Figure 6. A tip/tilt beam steering platform, used in the Solar Orbiter space probe. In principle various sizes of mirror can be installed and optical deflections to several degrees are achievable.

is used. By comparison, EtherCAT is a deterministic, open protocol that leverages the ubiquity and speed of Ethernet hardware, allowing flexible construction of sophisticated and scalable systems. Although analog interfacing may sound obsolete, it has essentially zero latency and infinite speed and is easily coordinated with data acquisition, triggering and other real-time processes. Good implementations of a digital interface with a precision DAC generally add internal waveform generation and synchronization capabilities; the highest-performance implementations are of course fully fledged DSP architectures which eliminate the analog servo-circuitry entirely. A particularly common application of nanopositioners to photonics is in automated alignment. Recent advanced controllers for piezo nanopositioners, hexapods and stage stacks embed automated alignment routines including parallel gradient search methods for the most rapid optical alignments. Advanced controllers for sophisticated automation tasks in industrial environments are now available on the market with nanoscale capabilities. They can drive linear or brushless motors, are based on a real time architecture and serve applications such as laser material processing, photolithography, fine inspection or any application where tight synchronization is required. They can generate controlled trajectories—for example from a 3D CAD file—and offer advanced correction capabilities to achieve the best results.

CONCLUSION

It is nowadays possible to build advanced instrumentation with nanoscale performances with various technologies. Beyond the fundamentals of product capability, quality, global support, and applications savvy, choosing a vendor represents a choice of partners. There are tangible benefits of working with a supplier whose experience crosses many fields and many drive technologies. Such a supplier is able to share best-practices from other arenas. This multicompetences ability can help you drive innovation in your application, delivering a competitive advantage through a holistic approach.

VENDORS IN EUROPE	WEBSITE
Aerotech	https://www.aerotech.com/
Attocube	https://www.attocube.com/en
Cedrat Technologies	https://www.cedrat-technologies.com/en/
Leuwen Air Bearings (LAV)	https://www.labmotionsystems.com/
Mad City Lab (MCL)	http://www.madcitylabs.eu/
MKS Newport	https://www.mksinst.com/b/newport
nPoint	https://npoint.com/
Physik Instrumente (PI)	https://www.physikinstrumente.com/en/
Piezo Motor	https://piezomotor.com/
Piezo System Jena	https://www.piezosystem.com/
Piezoconcept	https://piezoconcept-store.squarespace.com/
Pro-lite	https://www.pro-lite.fr/
Smaract	https://www.smaract.com/index-en
Tekceleo	https://www.tekceleo.fr/
Thorlabs	https://www.thorlabs.com/

Optical frequency comb synthesizer

Menlo Systems introduces the FC1500-LN^{nova}, its latest optical frequency comb synthesizer model. The enhanced design of the laser oscillator results in significantly improved robustness against acoustical distortion and thermal drift. The major benefit of this novel design is a reduced free running linewidth of only 15 kHz. Owing to this leap in linewidth reduction, the FC1500-ULN^{nova} has proven to support a frequency stability on the 10^{-19} level within 1 s averaging time.

www.menlosystems.com/products/optical-frequency-combs/fc1500-250-uln/

SWEPT LASER

The Quantifi Photonics Laser 2000 Series is a laboratory-grade O-band or C-band swept, tunable laser that can be operated as both a step-tuned or swept-wavelength laser source. With 0.01 dB power stability, 400 nm/s high-speed scan rate, and built-in synchronization trigger inputs and outputs, users can synchronize the laser sweep with other measurement tools such as optical power meters, spectrum analyzers, oscilloscopes, and more.

www.quantifiphotonics.com/products/lasers-amplifiers/matriq-swept-laser/

Dual Color Stimulated Raman Scattering

The new deltaEmerald allows simultaneous Stimulated Raman Scattering (SRS) imaging of two vibrational bands with its dual color SRS (DC-SRS) scheme. Two Stokes pulses, separated by 85 cm^{-1} and modulated at different frequencies are overlapped with the tunable Pump pulse. Fully automated tuning, power control and temporal and spatial overlap of all three beams are given. Additionally a ~100 fs output at 1030 nm is provided for efficient SHG and two-photon imaging.

www.ape-berlin.de/en/dc-srs/

LASER BEAM PROFILE ANALYZER

The SLED 1000 Ophir® SP932U is a compact device designed and developed for analyzing the profile of laser beams in the UV, VIS, NIR and Nd:YAG wavelength ranges. It offers a wide dynamic range, high sensitivity and linearity, and high resolution. The SP932U profile analyzer offers a resolution of 2048 × 1536 pixels, a pixel spacing of 3.45 µm and a repetition rate of 24 Hz at full resolution.

www.ophiropt.com/laser--measurement/beam-profilers/

High-Speed LCOS Spatial Light Modulator

SLM-210 is the high speed model of SANTEC. SLM-210 features a significantly improved response speed. It is a high performance product which uses its second generation LCOS technology. Its response time of less than 10 ms is expected to contribute to the improvement of performances in optical applications such as wavefront correction, optical beam shaping for laser processing, biosensing and quantum computing.

www.santec.com/en/products/components/slm/slm-210/